21st International Workshop on Physical Processes in Natural Waters

Program and Abstracts

PPNW

20–24 Aug 2018

Solothurn, Switzerland

UNIVERSITÉ DE GENÈVE
FACULTÉ DES SCIENCES

DEPT. F.-A. FOREL
AQUATIC PHYSICS

eawag
aquatic research

Program Overview

Mon, 20 August 2018

18:00 – 20:00	Rockland Scientific Turbulence Mixer and Registration at conference venue: ***Altes Spital*** (*Oberer Winkel 2, Solothurn*)

Tue, 21 August 2018 – Lake Response to Climate Change and Other Anthropogenic Impacts

07:00 – 08:00	Registration and Poster Set-Up
08:00 – 08:30	Opening Remarks and Introduction to Solothurn City
08:30 – 09:15	***Keynote Lecture: Rita Adrian***
09:15 – 12:45	6 Talks and *Coffee Break (10:15-10:45)*
12:45 – 14:15	Lunch
14:15 – 14:30	Sponsor Introductions
14:30 – 17:00	4 Talks and *Coffee Break (15:30-16:00)*
17:00 – 17:30	1 minute Poster Teasers
17:30 – 20:00	Apéro and Poster Session

Wed, 22 August 2018 – Running Waters, Gas Exchange, and Bubbles

08:15 – 09:00	***Keynote Lecture: Amber Ulseth***
09:00 – 10:30	2 Talks and *Coffee Break (10:00-10:30)*
10:30 – 11:15	***Keynote Lecture: Werner Eugster***
11:15 – 12:45	3 Talks
12:45 – 14:15	Lunch
14:15 – 16:45	4 Talks and *Coffee Break (15:15-15:45)*
16:45 – 17:30	Free Time
17:30 – 18:30	Öufi Walking Tour of Solothurn City
18:30 – 19:00	Free Time
19:00 – 24:00	Conference Dinner at ***Palais Benseval***

Thu, 23 August 2018 – Small to Large-Scale Mixing: role of internal waves and convection

08:15 – 09:00	***Keynote Lecture: Ali Mashayek***
09:00 – 12:30	6 Talks and *Coffee Break (10:30-11:00)*
12:30 – 14:00	Lunch
14:00 – 15:00	2 Talks
15:00 – 15:30	Free Time
15:30 – 18:30	Boat Cruise on the Aare River

Fri, 24 August 2018 – Interactions Between Hydrodynamics and Biology

08:15 – 09:00	***Keynote Lecture: Roman Stocker***
09:00 – 12:00	5 Talks and *Coffee Break (10:30-11:00)*

Detailed Program

Tuesday, 21 August 2018

Lake Response to Climate Change and Other Anthropogenic Impacts

07:00 – 08:00	Registration and Poster Set-Up
08:00 – 08:15	Dan McGinnis & Damien Bouffard: Opening Remarks
08:15 – 08:30	Solothurn City Services: Introduction to Solothurn City
08:30 – 09:15	***Keynote Lecture: Rita Adrian*** ***Long-term change of lake ecosystems: Lessons learned from linking theory with empirical data*** (p. 11-13)
09:15 – 09:45	M. Toffolon, S. Piccolroaz *When lakes warm the most: Considerations on the use of average indices for climate-change studies* (p. 14-15)
09:45 – 10:15	L. Råman Vinnå, A. Wüest, M. Schmid, D. Bouffard *Climate reaction of lakes affected by global and local anthropogenic influences* (p. 16)
10:15 – 10:45	Coffee Break
10:45 – 11:15	G. López Moreira, M. Toffolon, F. Hölker *The impact of euthrophication and brownification on lake thermal dynamics: When should hydrodynamic modellers care?* (p. 17-18)
11:15 – 11:45	A. Wüest, T. Steinsberger, B. Müller, R. Schwefel *Why is deepwater oxygen depletion not decreasing despite reoligotrophication?* (p. 19-20)
11:45 – 12:15	S. Piccolroaz, M. Amadori, H. Dijkstra, M. Toffolon *Wind forcing and planetary rotation as key drivers of ventilation in deep elongated lakes: evidence from Lake Garda* (p. 21-22)
12:15 – 12:45	M. Genseberger, A. Bijlsma, P. Boderie, M. Borsboom, C. Chrzanowski, M. Dionisio Pires, C. Eijsberg-Bak, M. Eleveld, A. Fujisaki, V. Harezlak, T. van Kessel, N. Kramer, R. Noordhuis, S. Loos, J. Morris, A. Nolte, S. de Rijk, A. Smale, B. Stengs, C. Thiange, T. Troost, M. Zagonjolli *Towards an integrated hydrodynamic, water quality, and ecological modelling approach for Lake IJssel and Lake Marken* (p. 23-24)
12:45 – 14:15	Lunch

Tuesday, 21 August 2018 (cont.)

Lake Response to Climate Change and Other Anthropogenic Impacts

14:15 – 14:30	Sponsor Introductions
14:30 – 15:00	U.G. Kobler, M. Schmid, A. Wüest *Will climate change enhance the effects of pumped-storage on the thermal properties of the connected waterbodies?* (p. 25-26)
15:00 – 15:30	C.L. Ramón, F.J. Rueda, M. Priet-Mahéo, H.Ó. Andradóttir *Human-induced changes in lake forcing: the impact of the Kárahnjúkar hydroelectric scheme in the hydrodynamics of Lake Lagarfljót* (p. 27-28)
15:30 – 16:00	Coffee Break
16:00 – 16:30	D.M. Robb, R. Pieters, G.A. Lawrence *Effects of hydropower operation on turbidity in a glacially-fed reservoir* (p. 29-30)
16:30 – 17:00	T. Liblik, F. Buschmann, G. Väli, I. Suhhova, M-J. Lilover, U. Lips, J. Laanemets *Impact of different dredging scenarios on circulation and environmental parameters in Lake Viljandi* (p. 31-32)
17:00 – 17:30	1 minute Poster Teasers
17:30 – 20:00	Apéro and Poster Session (p. 84-138)

Tuesday, 21 August 2018 - Poster Presentations

A.I. Ayala, D.C. Pierson

Simulation of the effects of climate change on Lake Erken thermal structure (p. 84-86)

F. Bärenbold, M. Brennwald, R. Britt, R. Kipfer, M. Plüss, M. Schmid

On-site analysis of gas concentrations in Lake Kivu, Central Africa (p. 87-88)

S. Bogdanov, S. Volkov, A. Terzhevik, G. Zdorovennova, R. Zdorovennov, N. Palshin, T. Efremova, G. Kirillin

Turbulence parameters estimations via inter-beams ADCP correlations (p. 89-90)

L. Cimoli, A. Mashayek, H. Johnson, D. Marshall, C. Whalen, M. Alford, J. McKinnon, A. Naveira-Garabato

Diapycnal leakage in the Atlantic Meridional Overturning Circulation (p. 91)

D. Deepwell, M. Stastna, A. Coutino

Multi-scale processes of rotation modified mode-2 internal waves (p. 92-93)

N. Deering, B. Gibbes, A. Grinham, S. Albert, C. Lemckert, B. Boehrer

Stability of a tropical crater lake as a sentinel for climate change (p. 94-95)

T. DelSontro, H-P. Grossart, D.F. McGinnis, Y.T. Prairie, M. Koschorreck, R. McClure, J. Beaulieu

GLEON MetOx project: Methane in oxic surface waters (p. 96-97)

G.S. Diakonov, R.A. Ibrayev

Impact of the global climate shift of 1976-1978 on the Caspian Sea thermohaline circulation (p. 98-100)

T. Doda, H.N. Ulloa, A. Wüest, D. Bouffard

Buoyancy-driven cross-shore flows in lakes induced by night-time cooling: field observations (p. 101-102)

A. Forrest, H. Ulloa, B. Laval

Diurnal cycling of convective plume formation (p. 103)

J. Gros, S. Sommer, A. Dale, M. Schmidt

Simulating Panarea's offshore CO2 seeps as a natural proxy for potential leakage from sub-seabed CO2 storage (p. 104)

J. Jansen, B. Thornton, M. Wik, P. Crill

Interactions between physical and biogeochemical controls on lake carbon gas emissions in spring (p. 105)

J.P. Mesmen, S. Goyette, J. Kasparian, B.W. Ibelings

Physical, chemical, and biological effects of changing stratification in deep lakes. Can mixing regimes qualify as alternative stable states? (p. 106-109)

T. Moore, K. Bolding, J. Bruggeman, R-M. Couture, M. Dillane, M. Estroti, E. de Eyto, G. Gal, J-L. Guerrero, E. Jennings, E. Jeppesen, A. Nielsen, D. Trolle, D. Pierson

Assessing the optimal input data frequency for the GOTM Lake Physical Model (p. 110-111)

S. Moras, A. Ayala-Zamora, D. Pierson

Evaluation of historical patterns of thermal structure ofLake Erken using hydrodynamic model (p. 112)

J. Olsthoorn, E. Tedford, G. Lawrence

Convection near the temperature of maximum density (p. 113-114)

C. Ordóñez, T. Langenegger, T. DelSontro, S. Flury, K.W. Tang, D.F. McGinnis

Multi-lake Swiss Survey: hydrodynamic response to climate forcing (p. 115)

A. Irani Rahaghi, U. Lemmin, D.A. Barry

Effect of meso-scale surface water temperature heterogeneity on surface cooling estimates of a large lake: Airborne remote sensing results from Lake Geneva (p. 116-117)

R.S. Reiß, U. Lemmin, D.A. Barry

Differential cooling and near-shore density currents in a large lake (Lake Geneva) (p. 118-119)

V. Rostovtseva, I. Goncharenko

Optica characteristics of Aral Sea waters obtained by above water measurements with passive optical complex EMMA (p. 120)

T. Serra, J. Colomer, M. Soler, X. Casamitjana, C. Oldham

Local hydrodynamics in fragmented seagrass canopies (p. 121)

S. Simoncelli, D.J. Wain, S.J. Thackeray

Effect of temperature on zooplankton vertical migration (p. 122-123)

F. Soulignac, U. Lemmin, D.A. Barry

Hydrodynamics and sediment transport in the near-field region of the Rhône plume in Lake Geneva (France/Switzerland): Measurements and 3D modelling (p. 124-125)

U. Spank, M. Hehn, P.S. Keller, M. Koschorreck, C. Bernhofer

Micrometeorological and hydro-chemical measurements of mass and energy exchange between atmosphere and water surfaces using a floating platform (p. 126-128)

M. Tiessen, A. Umutoni, G. Sakindi, D. Bouffard, R. Uittenbogaard, R. de Graaff

Lake Kivu: Development of a 3D model to study stratification, methane entrapment and deep currents in a volcanic lake in the Great Rift Valley (p. 129-130)

H.N. Ulloa, K.A. Davis, S.G. Monismith, G. Pawlak

Temporal variability in thermally-driven cross-shore exchange: The role of the M2 tide (p. 131)

Z. Yang, B. Cheng, Y. Xu, D. Liu, J. Ma, D. Ji

Stable isotopes in water indicate sources of nutrients that drive algal blooms in the tributary bay of a subtropical reservoir (p. 132-135)

X. Zhang, B. Boehrer, K. Wang

Simulation of Lake Surface Temperature and Ice Cover with 1-D model (p. 136)

M. Zimmermann, M.J. Mayr, D. Bouffard, W. Eugster, B. Wehrli, H. Bèrgmann, A. Brand

Methane emissions during lake overturn: a tug-of-war between physical mixing and methanotrophs (p. 137-138)

Wednesday, 22 August 2018

Running Waters, Gas Exchange, and Bubbles

08:15 – 09:00	***Keynote Lecture: Amber Ulseth*** ***Two-state gas-exchange in streams and the implications of bubbles on scaling CO_2 fluxes*** (p. 33-35)
09:00 – 09:30	M. Klaus, E. Geibrink, E.R. Hotchkiss, J. Karlsson *Listening to air-water gas exchange in running waters* (p. 36-37)
09:30 – 10:00	A. Lorke, C. Anlanger, U. Risse-Buhl, M. Weitere, C. Noss *Spatial and temporal scales of flow and morphological diversity in gravel bed streams* (p. 38)
10:00 – 10:30	Coffee Break
10:30 – 11:15	***Keynote Lecture: Werner Eugster*** ***Direct gas flux measurements from surface waters*** (p. 39-41)
11:15 – 11:45	A. Verlet-Bandide, A. Rutgersson, E. Sahlée *Physical process impacting methane emissions from Swedish lakes* (p. 42-44)
11:45 – 12:15	M. Hofmann, R. Winkler *(Semi-) Continuous measurements of dissolved greenhouse gases with Cavity Ring-Down Spectrometers* (p. 45)
12:15 – 12:45	M. Provenzale, A. Ojala, J. Heiskanen, K-M. Erkkilä, I. Mammarella, P. Hari, T. Vesala *High-frequency productivity estimates for a lake from free-water CO_2 concentration measurements* (p. 46-47)
12:45 – 14:15	Lunch

Wednesday, 22 August 2018 (cont.)

Running Waters, Gas Exchange, and Bubbles

14:15 – 14:45	E. Tedford, S. Change, K. Zhao, J. Olsthoorn, R. Pieters, G. Lawrence *Methane bubbles under ice in Base Mine Lake* (p. 48-49)
14:45 – 15:15	L. Liu, K. Sotiri, Y. Dück, S. Hilgert, I. Ostrovsky, E. Uzhansky, R. Katsman, B. Katsnelson, R. Bookman, J. Wilkinson, A. Lorke *The control of surface sediment gas accumulation on spatial distribution of ebullition in Lake Kinneret* (p. 50-51)
15:15 – 15:45	Coffee Break
15:45 – 16:15	T. Langenegger, D. Vachon, D. Donis, D.F. McGinnis *What the CH_4 bubble knows: CH_4 fluxes revealed by sediment bubble gas composition* (p. 52)
16:15 – 16:45	B. Boehrer, I. Hentschel, M. Koschorreck *Oxygen ebullition from lakes* (p. 53-54)
16:45 – 17:30	Break
17:30 – 18:30	Öufi Walking Tour of Solothurn City: *Meet at Altes Spital at 17:25*
18:30 – 19:00	Break
19:00 – 24:00	Conference Dinner at Palais Benseval (Kronengasse 1, north end of Kreuzackerbrücke – bridge)

Thursday, 23 August 2018

Small to Large-Scale Mixing: Role of Internal Waves and Convection

08:15 – 09:00	***Keynote Lecture: Ali Mashayek*** ***Turbulence induced by overturning breaking waves: from small scale mixing to large scale overturning circulation*** (p. 55-56)
09:00 – 09:30	A.V.S. Rodrigues, J. Carpenter, L. Merckelbach *Turbulence and restratification from glider measurements* (p. 57-58)
09:30 – 10:00	J.B.T. McInerney, A.L. Forrest, S.G. Schladow *Seasonality of internal wave action in a large alpine lake* (p. 59-60)
10:00 – 10:30	P.A. Davies, M. Carr, M. Stastna, K. van de Wal *Experiments on shoaling Mode-2 internal solitary-like waves* (p. 61-62)
10:30 – 11:00	Coffee Break
11:00 – 11:30	H.N. Ulloa, A. Wüest, D. Bouffard *Mechanical energy budget and mixing efficiency in an ice-covered and radiatively-forced freshwater basin* (p. 63-64)
11:30 – 12:00	G. Kirillin, L. Wen, T. Shatwell *Extraordinary mixing conditions in ice-covered lakes of Tibetan Plateau* (p. 65-66)
12:00 – 12:30	V. Stepanenko, I. Repina, A. Artamonov, G. Ganbat, G. Davaa *Numerical simulation of stratification and ice regime of saline lakes* (p. 67)
12:30 – 14:00	Lunch
14:00 – 14:30	S. Volkov, G. Zdorovennova, R. Zdorovennov, T. Efremova, N. Palshin, A. Terzheki, D. Bouffard, S. Bogdanov *Radiatively driven under-ice convection: the impact of lake depth* (p. 68-69)
14:30 – 15:00	J. Wang, J. Kessler, A. Fujisaki-Manome, P. Chu *Modeling seasonal and interannual variability of Great Lakes ice cover using FVCOM+ice model* (p. 70)
15:00 – 15:20	Break
15:20 – 18:30	Aare River boat cruise: *Meet at Altes Spital at 15:20*

Friday, 24 August 2018

Interactions Between Hydrodynamics and Biology

08:15 – 09:00	***Keynote Lecture: Roman Stocker*** ***Plankton in Flow*** (p. 71-72)
09:00 – 09:30	O. Sepúlveda Steiner, D. Bouffard, A. Wüest *Day and night bio-convection in Lake Cadagno* (p. 73-74)
09:30 – 10:00	E.L. Suarez, M.C. Tiffay, N. Kalinkina, T. Chekryzheva, A. Sharov, E. Tekanova, M. Syarki, R. E. Zdorovennov, E. Makarova, E. Mantzouki, P. Venail, B.W. Ibelings *Diurnal variation in the convection-driven vertical distribution of phytoplankton under ice and after ice-off in the large Lake Onego (Russia)* (p. 75-77)
10:00 – 10:30	B. Sherman *Phytoplankton response to hydrodynamically determined light and nutrient availability in a stratified reservoir* (p. 78)
10:30 – 11:00	Coffee Break
11:00 – 11:30	M. Soler, J. Colomer, A. Folkard, T. Serra *Effect of vegetated canopies in turbidity current deposits* (p. 79-80)
11:30 – 12:00	B. Rabe, A. Gallego, J. Hindson, J. Wolf *An applied physical oceanography study of Scottish coastal and fjordic waters with regard to sea lice dispersal between aquaculture farms* (p. 81-82)

Oral Presentation Abstracts

(The order of abstracts follows the order of oral presentations)

Keynote Speaker

Prof. Dr. Rita Adrian

Leibniz-Institue of Freshwater Ecology and Inland Fisheries (IGB)

Head of Department of Ecosystem Research

Address:	Müggelseedamm 301, D-12587 Berlin
Phone:	+49 (0)30 64181 680
Fax:	+49 (0)30 64181 682
Email:	Adrian@igb-berlin.de
Website :	http://www.igb-berlin.de/profile/rita-adrian

Research interests *Climate impact research on lakes, resilience and resistance of lakes towards disturbances, lake metabolisms, emergence and maintenance of biodiversity, role of temporal scales.*

University education *Biology, Freie Universität Berlin, Berlin Germany*

Recent publications

• *Adrian R, D O Hessen. Environmental Impacts. —Lake Ecosystems. 2016. In: The North Sea Region climate change assessment. Editors: M Quante, F Colijn. Chapter 10: 315-340.*

• *Özkundakci, D., Gsell, A.S., Hintze, T., Täuscher, H. & R. Adrian, 2016. Winter severity determines functional trait composition of phytoplankton in seasonally ice covered lakes. Global Change Biology, DOI: 10.1111/gcb.13085.*

• *Gsell, A.S., Dakos, V., Özkundakci, D., Scharfenberger, U., Hansson, L.-H., Nõges, P., Reid, P.C., Schindler, D.E., van Donk, E., Walters, A. & R. Adrian, 2016. Early-warning signals foreshadow regime shifts in natural aquatic ecosystems. PNAS;* www.pnas.org/cgi/doi/ *10.1073/pnas.1608242113.*

• Shatwell T., R.Adrian; G.Kirillin. 2016. Planktonic events may cause polymictic-domictic regime shifts in temperate lakes. Scientific Reports. - 6(2016) art.24361

• *Spears, BM, Martyn N. Futter, E Jeppesen, B Huser, S Ives, T A. Davidson, R Adrian, DG. Angeler, SJ. Burthe, L Carvalho, F Daunt, AS. Gsell, DO. Hessen, ABG. Janssen, EB. Mackay, L May, H Moorhouse, M Søndergaard, H Woods, SJ. Thackeray. 2016. Ecological Resilience in Lakes: A probability check using lakes as a model system. Nature Ecology and Evolution:1/Nov. 2017:1616-1624.doi.org/1038/s41559-017-0333-1.*

• Kraemer B.M., T.s Mehner, R. Adrian. 2017. Reconciling the opposing effects of warming on phytoplankton biomass in 188 large lakes. Scientific Reports. – 7 art. 10762.

• *Schmidt, S.R., D. Gerten, T. Hintze, G. Liescheid, D.M. Livingstone, R. Adrian. 2018. Temporal and spatial scales of water temperature variability as an indicator for mixing in a polymictic lake. Inland Waters.* *http://doi.org/10.1080/20442041.2018.1429067*.

Long-term change of lake ecosystems: Lessons learned from linking theory with empirical data

Rita Adrian
Leibniz-Institute of Freshwater Ecology and Inland Fisheries, Department of Ecosystem Research, Berlin, Germany

**Corresponding author, Adrian@igb-berlin.de*

KEYWORDS
Lakes; climate impact; extreme events; temporal scale, early warning, metabolism

Introduction

Long-term ecological research has become a cornerstone of the scientific endeavour to better understand lake ecosystems dynamics and complexity along with the responses to environmental change; particularly the nature of change - linear versus non-lineary responses, the resilience of ecosystems (Spears et al. 2017), threshold driven responses () and the predictability of abrupt changes (Gsell et al. 2016). Understanding of the mechanisms underlying these responses requires that records of ecological processes be not only sufficiently long, but also collected at an appropriate temporal resolution and/or during critical time windows within the year (Adrian et al. 2016, Spears et al. 2017). I base the arguments on studies of our prime case study site Lake Müggelsee in Berlin, Germany along with information from lakes of the North Temperate Zone and large scale experiments embedded in ecological theory. We consider response pattern in lakes towards long-term warming trends along with responses towards (short-term) extreme weather conditions. I will present a couple of case studies linking ecological theory (metabolic theory of biology, bifurcation theory) with empirical long-term and experimental data - touching the effects of global climate change and extreme events on plankton communities and lake metabolism, the role of critical thresholds along with the question whether we can foresee change by early warning indicators.

Materials and methods

We identify different processes and the associated time scales (hours- to decades) using data from one of the best-resolved north temperate lake dataset (Müggelsee, in Berlin Germany) along with high frequency data from GLEON lakes and temperature and chlorophyll a data derived from remote sensing images. With a statistical modelling framework we use regressing analyses -including wavelet coherence to partition the direction and strength of coherence of simultaneously occurring time series across different temporal scales. Our studies are embedded in ecological theory such as metabolic theory of ecology and ecosystem stability/resilience theory – bifurcation theory.

Results and discussion

We address the complexity of environmental change induced responses in lake ecosystems by linking ecological theory with large scale experiments and long-term data (empirical in situ data and data derived from remote sensing images). The three differ in their capability to extract causal understanding, capture the complexity of ecosystems and the level of control. Theoretical approaches are located at the end of highest control and immediate causal understanding, including the formulation of laws, concepts, but also process based models. Theoretical approaches are concerned with the direct formulation of causal relations based on first principles and current knowledge; often in the language of mathematics. In order to achieve this we need to abstract from the large complexity of ecosystems- this means theory or models do not capture the complexity. Opposed to theoretical approaches, long-term ecological research captures the development of an ecosystem under the full complexity of its abiotic and biotic interactions. Importantly, long-term research is unique in its capability to allow the detection of long-term trends. Other than in theory or experiments long-term ecological research requires detective skills to identify the 'experimental conditions' under which the observed pattern have developed. As the analysis of long-term empirical data is bound to correlational relationships only approximate causality can be identified. In between theory and long-term research the experiment is located which follows hypothesis testing on a varying degree of control and complexity of the system.

Two examples are documented in the following:

Metabolic theory of ecology: Based on the fundamentals of metabolic theory of ecology warming increases phytoplankton demands for resources to support higher metabolic rates at higher temperatures. As such warming should reduce algal mass as basal metabolic costs increase – if nutrient levels remain unchanged. This was, however, not necessarily the case for large lakes globally. In a recent study based on algal biomass estimated as *chla* and water temperatures derived from remote sensing data Kraemer et al. (2017) found that warm years tend to amplify trophic state in the worlds 188 largest lakes: phytoplankton-poor lakes get bluer while phytoplankton-rich lakes get greener.

Bifurcation theory: The existence of early warning indicators in time series from dynamics systems approaching a discontinuous regime-shift is predicted by bifurcation theory. Impending discontinuous regime-shifts might be difficult to predict, since the state variables of complex dynamic systems might show little systematic change prior to the regime-shift. EWI offer a potential way out, since they signal the increasing loss of system resilience which accompanies systems approaching a discontinuous regime-shift. Gsell et al. (2016) systematically assessed four commonly used EWI (autocorrelation, standard deviation, skewness, density ratio) based on long-term datasets of six lake ecosystems that have experienced a critical transition and for which the relevant ecological mechanisms and drivers are known; a prerequisite to apply the EWI concept. While EWI could be detected in the majority of state variables, often considerable time ahead, consistency among the four indicators was low. This study showed that EWI are not (yet) an irrefutable, consistent signal of impending critical transitions and they can only be applied if expert knowledge of the system is extensive.

REFERENCES

Adrian, R. and D.O. Hessen 2016. Environmental Impacts – Lake Ecosystems. In: M. Quante and F. Colijn (eds), North Sea Region Climate Change Assessment, Regional Climate Studies, DOI 10.1007/978-3-319-39745-0_10.

Gsell, A.S., Dakos, V., Özkundakci, D., Scharfenberger, U., Hansson, L.-H., Nõges, P., Reid, P.C., Schindler, D.E., van Donk, E., Walters, A. and R. Adrian, 2016. Early-warning signals foreshadow regime shifts in natural aquatic ecosystems. PNAS;

Kramer B, T. Mehner, and R. Adrian. 2017. Reconciling the opposing effects of warming on phytoplankton biomass in 188 large lakes. Scientific Reports, 7, *10762* |DOI:10.1038/s41598-017-11167-3.

Spears, BM, M. N. Futter, E. Jeppesen, B. Huser, S. Ives, T A. Davidson, R Adrian, D.G. Angeler, S.J. Burthe, L. Carvalho, F. Daunt, A.S. Gsell, D.O. Hessen, A.B.G. Janssen, E.B. Mackay, L. May, H. Moorhouse, S. Olsen, M. Søndergaard, H. Woods, S.J. Thackeray (2017), Ecological resilience in lakes and the conjunction fallacy. Nature Ecology and Evolution: doi:10.1038/s41559-017-0333-1.

When lakes warm the most: Considerations on the use of averaged indices for climate-change studies

M. Toffolon[1*] and S. Piccolroaz[2]

[1] Department of Civil, Environmental and Mechanical Engineering, University of Trento, Trento, Italy
[2] Institute for Marine and Atmospheric research Utrecht, Department of Physics, Utrecht University, Utrecht, The Netherlands

**Corresponding author, e-mail* marco.toffolon@unitn.it

KEYWORDS
Lakes; water temperature; climate change; averaged index; stratification

Introduction

Studying the thermal response of lakes to climate change, as any other large-scale and long-term analyses, requires averaged indices. In general, the choice of the averaging windows is not neutral. This is especially important when the thermal trends of lakes, the "sentinels of climate change" (Adrian et al., 2009), are used to gather insights on how inland water resources respond to evolving climate conditions.

Most studies on lake surface temperature (LST) assume air temperature (AT) as a simple proxy of climate change and rely on synthetic indexes to quantify the LST response typically focusing on three summer months: July, August and September (JAS; Schneider et al., 2009). We challenge the limits of these metrics, showing how their indiscriminate use may mystify the quantification of the thermal sensitivity of lakes to climate dynamics.

Results and discussion

In order to test the reliability of the dynamics detected through the JAS index, we performed a "natural experiment" (Jankowski et al., 2006) looking at a 20-year dataset of LST maps of the Laurentian Great Lakes (USA-Canada) and separating warm and cold years. We interpreted the difference among these years as a possible description of the effects of the future warming, looking at different lakes' regions in different periods of the year to understand the spatial and temporal variability (Fig. 1). The analysis confirmed Lake Superior as a hotspot for LST warming in JAS. However, a significant contribution to this warming depends on the AT warming in previous periods through the anticipated onset of summer stratification (Piccolroaz et al., 2015). This was detected by considering a longer period (e.g., March to August) for AT changes and JAS for LST: Lake Superior behaves similar to the other lakes, while the effect of warming appears more pronounced in Lake Ontario. Additional complexity is added by testing the MJJ-based (May, June, July) index, which describes an enhanced warming in other lakes (Ontario, in particular) and not only in Lake Superior.

Moreover, deep regions experience a stronger warming concentrated in early summer (see also Woolway and Merchant, 2017), mainly due to anticipated stratification, while shallow parts respond more uniformly throughout the year. The exercise shows that some lakes have larger reactions in summer, and others in late spring, so the exclusive use of the JAS metric might lead to erroneous conclusions (Winslow et al., 2017), especially if compared with concurrent AT. Should we be more careful when considering averaged indices of lakes' thermal response to climate change?

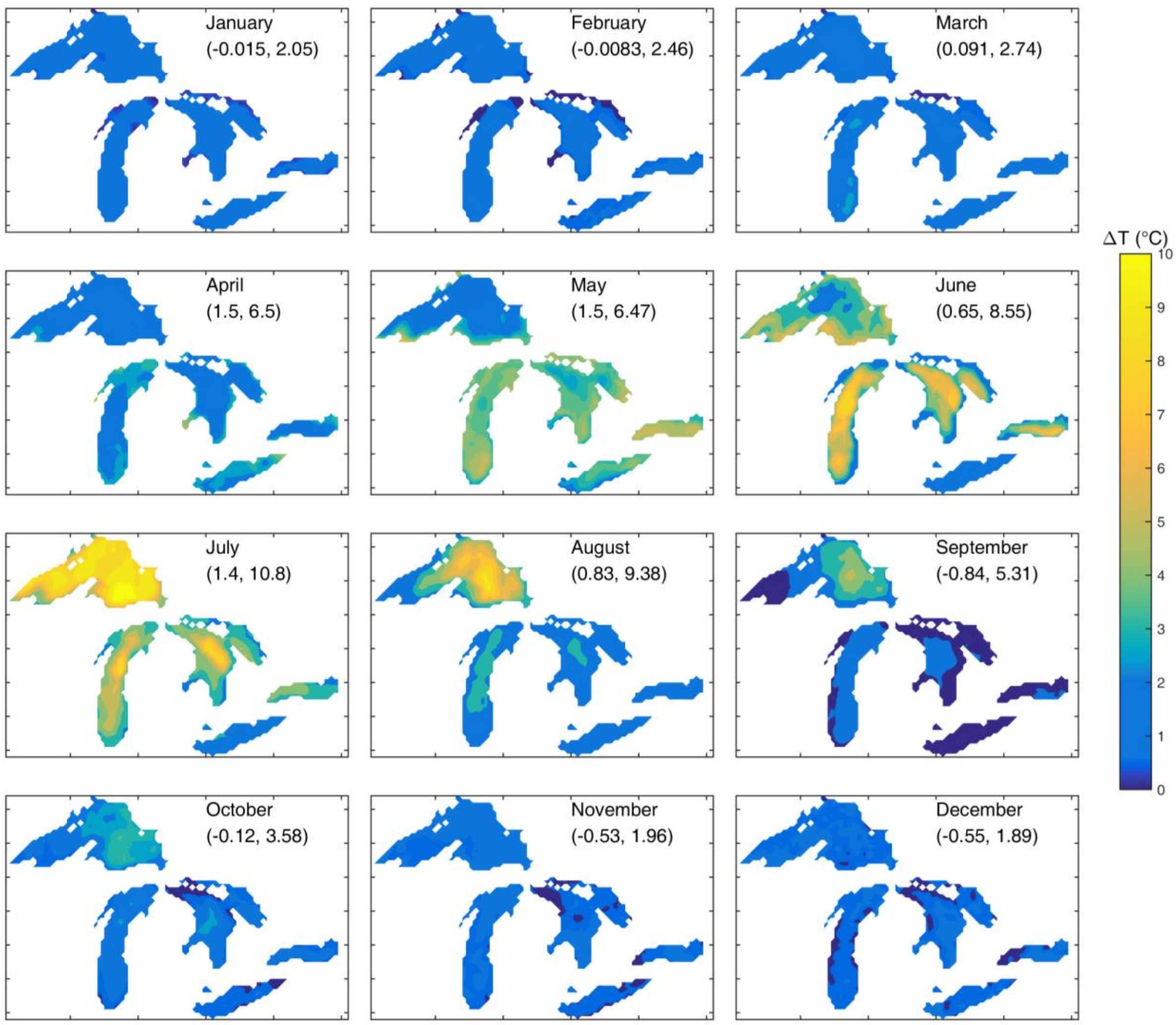

Fig. 1. Monthly averaged difference of temperature between the warm and cold climatological years. Colour bar is limited between 0 and 10°C, although a few larger and smaller values are obtained through the year. Minimum and maximum values (°C) are reported in parentheses in the subplots' titles. A nonlinear colour map is used to enhance the lower range of temperature difference.

REFERENCES

Adrian, R., C. M. O'Reilly, H. Zagarese, S. B. Baines, D. O. Hessen, W. Keller, D. M. Livingstone, R. Sommaruga, D. Straile, E. V. Donk, G. A. Weyhenmeyer, M. Winder (2009), Lakes as sentinels of climate change, *Limnol. Oceanogr., 54*, 2283–2297, doi:10.4319/lo.2009.54.6_part_2.2283.

Jankowski, T., D. M. Livingstone, H. Bührer, R. Forster, and P. Niederhauser (2006), Consequences of the 2003 european heat wave for lake temperature profiles, thermal stability, and hypolimnetic oxygen depletion: Implications for a warmer world, Limnol. Oceanogr., 51, 815–819.

Piccolroaz, S., M. Toffolon, B. Majone (2015), The role of stratification on lakes' thermal response: The case of Lake Superior, *Water Resour. Res.*, *51*, 7878–7894, doi:10.1002/2014WR016555.

Schneider, P., S. J. Hook, R. G. Radocinski, G. K. Corlett, G. C. Hulley, S. G. Schladow, T. E. Steissberg (2009), Satellite observations indicate rapid warming trend for lakes in California and Nevada, *Geophys. Res. Lett., 36*(22), doi:10.1029/2009GL040846.

Winslow, L. A., J. S. Read, G. J. A. Hansen, K. C. Rose, and D. M. Robertson (2017), Seasonality of change: Summer warming rates do not fully represent effects of climate change on lake temperatures, *Limnol. Oceanogr., 62*(5), 2168–2178, doi:10.1002/lno.10557.

Woolway, R. I., C. Merchant (2017), Amplified surface temperature response of cold, deep lakes to inter-annual air temperature variability, *Scientific Reports*, *7*(1), doi: 10.1038/s41598-017-04058-0.

Climate reaction of lakes affected by global and local anthropogenic influences

Love Råman Vinnå*, Alfred Wüest, Martin Schmid and Damien Bouffard
Eawag, Swiss Federal Institute of Aquatic Science and Technology, Surface Waters – Research and Management, Kastanienbaum, Switzerland

**Corresponding author, love.ramanvinna@eawag.ch*

Thermal responses of inland waters to climate change varies on global and regional scales. The extent of warming is determined by system-specific characteristics such as but not limited to fluvial input, morphology, transparency and ice cover. Additionally local anthropogenic emissions/withdrawals of heat into/from inland waters have the potential to affect water temperature and stratification. Local factors thus control both the reaction and the sensitivity of lakes to anthropogenic caused warming. Given the likely increased thermal stress on aquatic systems in the future by growing cooling/heating demands of riparian/costal infrastructures in combination with climate warming, the question arises of how to best monitor and manage these systems. Traditionally, predictions of inland waters reaction to climate change have focused on the effects associated with only increased air temperature, thereby neglecting probable changes of other important variables for the local heat budget between lakes and the atmosphere.

Here we investigate the future reaction of Swiss lakes to climate change under the influence of surrounding tributaries, known changes in anthropogenic heat emissions and the effect of diminished ice cover. Given the upcoming climate report CH2018 which enables precis regional predictions of changes not only in air temperature but also precipitation, radiation, wind and humidity, we put special focus on the difference between this new novel development and the more traditional air temperature focused method. We use simple and efficient deterministic models to predict future water temperatures, ice cover, river-borne suspended sediment concentration, lake stratification and river intrusion depth/volume. Climate-induced shifts in river discharge regimes, including seasonal flow variations, was found to act as positive/negative feedbacks in influencing both river and lake temperatures. The extent of this repressive effect on warming was found to be controlled by the hydraulic residence time.

The impact of eutrophication and brownification on lake thermal dynamics: When should hydrodynamic modellers care?

G. López Moreira[1,2,3]*, M. Toffolon[1] and F. Hölker[2,3]

[1] Department of Civil, Mechanical and Environmental Engineering (DICAM), University of Trento (UniTN), Trento, Italy
[2] Institute of Biology, Department of Biology, Chemistry and Pharmacy, Freie Universität Berlin (FUB), Berlin, Germany
[3] Department of Ecohydrology, Leibniz-Institute of Freshwater Ecology and Inland Fisheries (IGB), Berlin, Germany

**Corresponding author, e-mail ga.lopez@unitn.it / ga.lopez@igb-berlin.de*

KEYWORDS
Phytoplankton blooms; nutrient enrichment; ecological modelling; lake physics; lake thermodynamics.

Introduction

Phytoplankton biomass is one of several light-absorbing/scattering components of natural waters. As such, when present in high concentrations, e.g. during the intense blooms that characterise eutrophic lakes, it can significantly alter both the underwater light climate, thus limiting its own further growth in deeper waters; and the thermal dynamics of an aquatic ecosystem (Rinke et al. 2010). In recent years, an increased interest has developed within the hydrodynamic modelling community to better understand in which cases it is necessary to consider the effects of phytoplankton biomass on light penetration if one wants to accurately simulate the physical response of a lake. Coloured dissolved organic matter (CDOM) contributes to light extinction as well (Persson and Jones, 2008) and although its concentrations are steadily increasing in many freshwater lakes, a process known as brownification, the effects of this variability are usually not considered in hydrodynamic models. By means of a process-based vertically-layered one-dimensional model of reduced complexity, where physical, biological and chemical processes are fully coupled, allowing for the simulation of both the spatial and the temporal variation of the light extinction coefficient, we studied the response of lakes subjected to a combination of nutrient enrichment and brownification scenarios.

Materials and methods

For this study, we further developed a model initially proposed by Jäger et al. in 2010. To assess the combined effect of water colour and phytoplankton biomass on the thermal structure of the water column, we conducted simulations for combined gradients of eutrophication scenarios (P-load rates from 0.8 to 5.5 mgP·m^{-2}·day^{-1}) and background light extinction coefficients (k_{bg} from 0.3 to 0.9 m^{-1}). When considering the effect of phytoplankton, the total light extinction coefficient is given by $k_{tot} = k_{bg} + k_{phyto} B_{phyto}$, where k_{phyto} was taken to be 0.0003 m^2·mgC^{-1} and B_{phyto} is the concentration of phytoplankton biomass in mgC·m^{-3}, which naturally increases with P_d, the concentration of dissolved phosphorus, given in mgP·m^{-3}.

Results and discussion

Phytoplankton biomass can significantly alter the thermal structure of the water column, particularly in eutrophic systems with a low background light extinction coefficient (Figure 1). During the warm-up phase, higher surface water temperatures can be expected if one considers the effect of phytoplankton (Figure 2a). Slightly lower surface temperatures are also observed during the cool-down phase (Figure 2b), with a shallower thermocline throughout the whole stratified period. The effect of phytoplankton biomass on the thermal structure of the water column can be important at low background light extinction coefficients (Figure 3a), especially in eutrophic/hypereutrophic lakes. It becomes relatively less important as water becomes browner (Figure 3b).

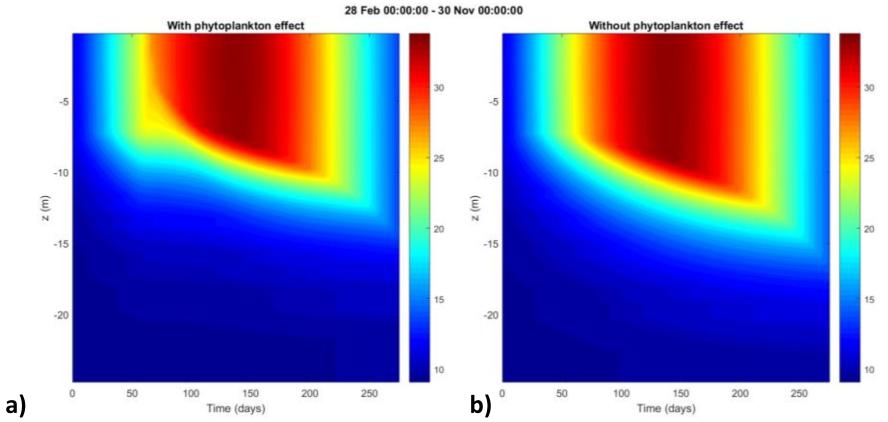

Figure 1. Modelled water temperature throughout the stratified period when: **a)** considering light extinction by phytoplankton biomass; and **b)** not considering this effect (k_{bg} = 0.30 m^{-1}; P-load rate = 5.5 mg P·m^{-2}·day^{-1}).

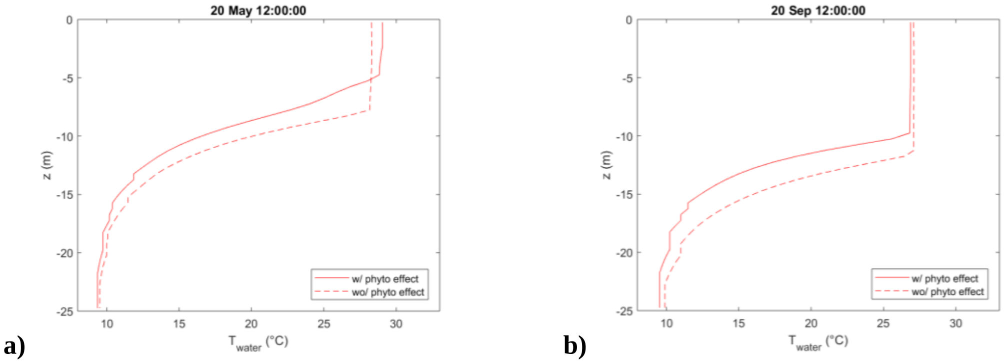

Figure 2. Modelled water temperature (T_{water}) profiles for a representative time of the: **a)** warm-up phase; and the **b)** cool-down phase.

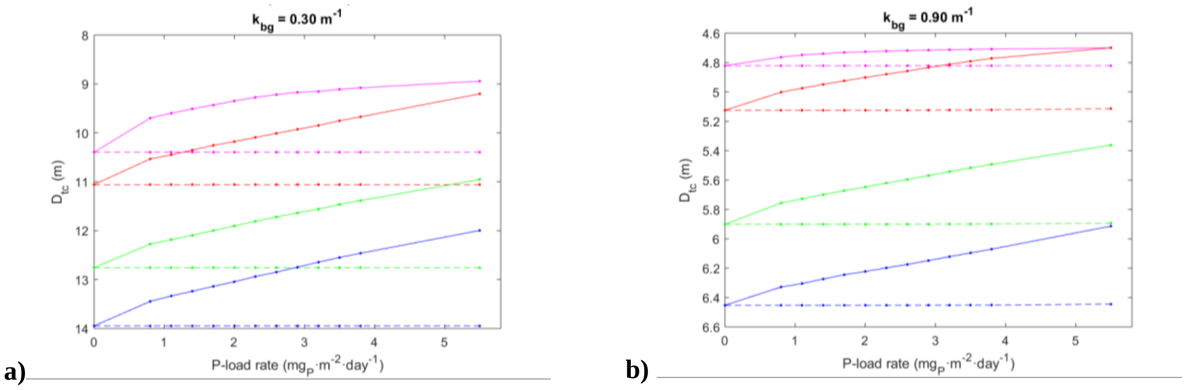

Figure 3. Thermocline depth (D_{tc}), in meters, as a function of phosphorus loading rate (P-load rate), in mg_P·m^{-2}·day^{-1}, for a background extinction coefficient of: **a)** k_{bg} = 0.30 m^{-1}; and **b)** k_{bg} = 0.90 m^{-1}

REFERENCES

Rinke, K., P. Yeates, K.-O. Rothhaupt (2010), A simulation study of the feedback of phytoplankton biomass on thermal structure via light extinction, *Freshwater Biol.*, *55*, 1674-1693, doi:10.1111/j.1365-2427.2010.02401.x

Persson, I., I. D. Jones (2008), The effect of water colour on lake hydrodynamics: a modelling study *Freshwater Biol.*, *53*, 2345-2355, doi:10.1111/j.1365-2427.2008.02049.x

Jäger, C. G., S. Diehl, and M. Emans (2010), Physical Determinants of Phytoplankton Production, Algal Stoichiometry, and Vertical Nutrient Fluxes, *Am. Nat.*, *175*(4), E91-E104, doi: 10.1086/650728

Why is deepwater oxygen depletion not decreasing despite reoligotrophication?

Alfred Wüest[1,2,]*, Thomas Steinsberger[1], Beat Müller[1] and Robert Schwefel[2]

[1] *Eawag, Swiss Federal Institute of Aquatic Science and Technology, Surface Waters - Research and Management, Kastanienbaum, Switzerland*
[2] *EPFL. Physics of Aquatic Systems Laboratory – Margaretha Kamprad Chair, ENAC-IEE-APHYS, Lausanne, Switzerland*

**Corresponding and presenting author, e-mail alfred.wueest@eawag.ch*

KEYWORDS
Primary production; phosphorus; sedimentation; organic carbon; reduced substances.

Introduction

In Switzerland, as in many other western countries, nutrient inputs and the level of algae production in lakes reached their maxima in the late 1970s / early 1980s. Since then, the production-limiting phosphorus has decreased - by partly more than 90% - in response to the rigorous national implementation of waste water treatment. However, the enthusiasm about this unprecedented success of water quality management was damped by the discovery that oxygen depletion in the stratified deepwaters did not decrease correspondingly in the last decades. In certain lakes, oxygen depletion increased even more during reoligotrophication. For the last ten years, we performed several studies to answer this practical management question. In this presentation the lessons learned will be summarized.

Study sites

The Cantonal agencies, responsible for water quality monitoring on their territories, perform usually monthly CTD profiles on lakes, which either exceed a minimal size or are of specific management interest. During the periods of eutrophication / reoligotrophication, many tens of thousands of oxygen concentration values have been acquired in various lakes over decades. These data allowed to reconstruct the nutrient and oxygen depletion histories. Unfortunately, on almost none of those lakes, primary production estimates are available so that the intermediate process of the organic matter build-up is not well documented. For this reason, we tried to acquire as many as possible sediment cores, to reconstruct the carbon accumulation related to the eutrophication history (*Steinsberger et al. 2017*).

Materials and methods

Oxygen concentrations were either directly provided as monitoring data (see comment above) or measured by CTD profiles and Winkler titration. Oxygen depletion rates were estimated by balancing the oxygen below a depth level of 10 m over ~200 days during the stratified period (including oxygen input by artificial aeration). The fluxes of reduced substances (CH_4, NH_4, Mn(II), and Fe(II)) were calculated based on the concentration gradients measured in the topmost layer of the sediment cores (*Steinsberger et al. 2017*). The oxygen fluxes into the sediment were measured using a MP4/ 8 Microprofiler (Unisense A/S) equipped with oxygen microsensors (*Schwefel et al. 2017*).

Results and discussion

By analysing tens of thousands of oxygen measurements from former eutrophic lakes, we were able to disentangle oxygen depletion pathways in the deepwater. In shallow lakes, oxygen depletion is determined by the molecular fluxes of oxygen into the sediment and reduced substances out of the sediment (*Müller et al. 2012*). As an effect, the oxygenation / aeration of eutrophic lakes on the Swiss Plateau basically increased the oxygen uptake by the sediment, increased the oxygen depletion and improved the quality of the sediment. The amount of reduced substances leaving the sediment is strongly correlated to the organic carbon content in the sediment (*Steinsberger et al. 2017*) and therefore the reduced substances fluxes decreased in those treated lakes.

In deep lakes, oxygen is additionally depleted in the open hypolimnetic waterbody and this portion of the total vertically-integrated oxygen depletion is in fact increasing with the maximum lake depth and reaches ~70% in the 309 m deep Lake Geneva (*Schwefel et al. 2018*). Compared to shallow lakes, the amount of carbon settling in the deep layers is decreasing and subsequently also respiration at the sediment surface and storage in the sediment is decreasing with depth. Measurements in the deepwaters of Lake Geneva and Lake Constance showed consistent low sediment oxygen uptake, low reduced substances fluxes and increased thickness of the sediment oxic zone in the deepest regions of the hypolimnion (*Schwefel et al. 2018*). In both these deep lakes, the replenishment during deep convective mixing in winter is crucial for oxygen levels at great depth. The analysis by Schwefel et al. (2016) revealed that climate change will worsen the deepwater oxygen level, however, a complete anoxia is not expected. The low oxygen uptake by the sediments of the deeper reaches are of great support for this rather positive perspective.

The development of the oxygen depletion during eutrophication and reoligotrophication phases set these findings in a historic context and reveal two managerial relevant results: (a) The oxygen depletion reached is maximum as soon as the phosphorus content exceeded ~25 mg P/m^3 and (b) during reoligotrophication the oxygen depletion did not return to the level before due to the organic carbon accumulated in the sediment (*Steinsberger et al. 2017*). This finding shows clearly that the high, and partially still increasing, oxygen depletion stems from decades ago and is the result of the past eutrophication. With this talk we synthesize almost a decade of research which contributes strongly to the understanding of the *functioning of freshwaters in light of global environmental change (eutrophication and climate change).*

REFERENCES

Müller, B., L.D. Bryant, A. Matzinger, and A. Wüest (2012). Hypolimnetic oxygen depletion in eutrophic lakes. *Environ. Sci. Technol*. ***46***(18): 9964–9971, doi: 10.1021/es301422r.

Schwefel, R., A. Gaudard, A. Wüest and D. Bouffard (2016). Effects of climate change on deepwater oxygen and winter mixing in a deep lake (Lake Geneva): Comparing observational findings and modeling. *Water Resources Research* **52**(11): 8811–8826, doi:10.1002/2016WR019194.

Schwefel, R., M. Hondzo, A. Wüest, and D. Bouffard (2017). Scaling oxygen microprofiles at the sediment interface of deep stratified waters. *Geophysical Research Letters* **44**(3), 1340–1349, doi:10.1002/2016GL072079.

Schwefel, R., T. Steinsberger, D. Bouffard, L.D. Bryant, B. Müller, and A. Wüest (2018) Using small-scale measurements to estimate hypolimnetic oxygen depletion in a deep lake. *Limnology and Oceanography* **63**: S54–S67, doi: 10.1002/lno.10723.

Steinsberger, T., M. Schmid, A. Wüest, R. Schwefel, B. Wehrli and B. Müller (2017). Organic carbon mass accumulation rate regulates the flux of reduced substances from the sediments of deep lakes. *Biogeosciences*, **14**(13): 3275–3285. doi:10.5194/bg-14-3275-2017.

Wind forcing and planetary rotation as key drivers of ventilation in deep elongated lakes: evidence from Lake Garda (Italy)

S. Piccolroaz[1]*, M. Amadori[2], H. Dijkstra[1], and M. Toffolon[2]

[1] Institute for Marine and Atmospheric research Utrecht,
Department of Physics, Utrecht University, Utrecht, The Netherlands
[2] Department of Civil, Environmental and Mechanical Engineering,
University of Trento, Trento, Italy

**Corresponding author, e-mail s.piccolroaz@uu.nl*

KEYWORDS
Deep elongated lakes; Coriolis force; deep ventilation; field observations; analytical and numerical modeling

Introduction

Vertical mixing in lakes controls the redistribution of mass and energy along the water column, thus being a key factor affecting water quality and trophic status. The occurrence of deep mixing events (DMEs) is highly relevant especially in lakes that undergo irregular mixing and less frequently than once per year (i.e., oligomixis). This is the case of several deep alpine lakes, where DMEs are typically associated to buoyancy-driven convection due to intrusion of denser surface water, e.g., following harsh winters [*Schwefel et al., 2016; Salmaso et al., 2017*]. However, convective mixing is not the only mechanism of deep ventilation and other factors may play a role. For example, in narrow and elongated lakes (such as alpine, glacial, rift valley, and fjord lakes) strong and persistent winds can generate large-scale, along-lake overturning circulations [*Ambrosetti et al., 2010*]. Theoretical and numerical studies have shown that these along-lake circulations can be affected by planetary rotation, generating closed secondary flows in the cross-sections orthogonal to the wind with up and downwelling at the shores [*e.g., Toffolon, 2013*]. These secondary flows have never been explicitly measured in narrow deep lakes, and are often neglected or confused in relatively small enclosed basins [*Winant, 2004*]. Based on evidence from Lake Garda (Italy), here we provide explicit proof for the development of such secondary flows in a narrow lake and show their relevance as deep ventilation mechanism.

Materials and methods

Lake Garda is one of the largest lakes in the Alpine region, and the largest in Italy (surface area of 368 km^2 and water volume of 49 km^3). The lake is oligomictic and is characterized by a narrow and deep northern trunk (average width of 4 km and maximum depth of 350 m) connected to a wider and shallower southern basin lying in a flat plain (see Figure 1a). In the norther part, the wind regime is strongly controlled by the surrounding topography, which constrains the winds along the major axis of the lake.

Since March 2017, monthly high resolution profiles of temperature and chlorophyll-a are measured in the upper 100 m of the lake using a micro-profiler (MicroCTD, by Rockland Scientific). The measurements are performed at three reference stations along a cross transect in the northern trunk. As a complement to *in-situ* measurements, a one-way coupled three-dimensional atmosphere-lake numerical model is available for the lake (WRF-Delft3D).

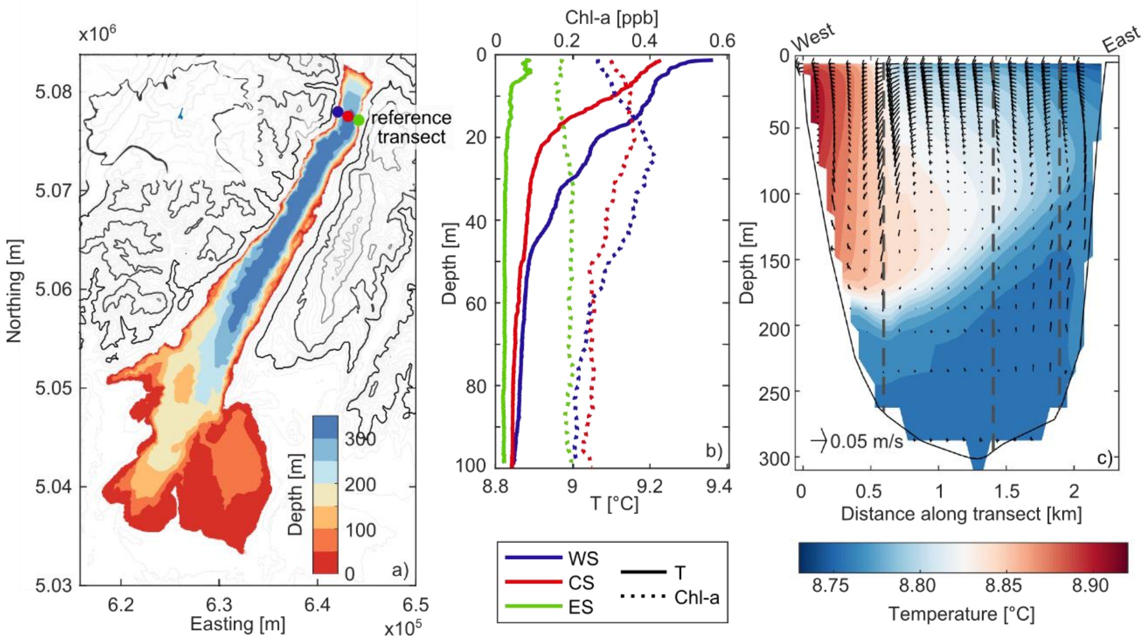

Figure 1: a) Bathymetry of Lake Garda, its location in Northern Italy, and position of the monitoring stations. b) Vertical profiles of temperature (solid lines) and chlorophyll-a (dotted lines) measured at the three stations (West: WS, Central: CS, East: ES) on 21/04/2017. c) Temperature and flow field (arrows) at the reference transect for the same day resulting from Delft3D simulation.

Results and discussion

After strong and uniform synoptic northerly wind events, significant lateral gradients of temperature and chlorophyll-a have been detected along the reference transect. Figure 1b shows the existence of such lateral variation after a persistent wind event occurred between 19 and 21 April 2017 (6.5 ±1.6 m/s). A clear westward transport is recognizable, with accumulation of chlorophyll-a and warm water at the West Station (WS), while profiles at the East Station (ES) were nearly homogeneous. This pattern is the result of the water transport deviated to the right by the Coriolis force, generating a secondary closed circulation bounded by lateral shores.

The observed pattern is reproduced with a three-dimensional numerical model (Figure 1c). The combination of observations and simulated flow fields indicates that such secondary flows are relevant for the ventilation of deep layers, and that these can be detected also in the case of relatively narrow lakes. This result calls into question the reliability of choosing the width of a lake as the discriminating factor for neglecting the effect of Earth's rotation. In this regard, we also propose a theoretical framework for quantifying the Ekman-type lateral transport in closed water bodies. We use this theory to relate the dependence of the secondary circulation on the width of the lake and the shear stresses due to horizontal mixing.

REFERENCES

Ambrosetti, W., L. Barbanti, and E. Carrara (2010), Mechanisms of hypolimnion erosion in a deep lake (Lago Maggiore, N. Italy), *Journal of Limnology*, *69*(1), 3–14, doi:10.4081/jlimnol.2010.3.

Salmaso, N., A. Boscaini, C. Capelli, and L. Cerasino (2017), Ongoing ecological shifts in a large lake are driven by climate change and eutrophication: evidences from a three decade study in Lake Garda, *Hydrobiologia*, doi:10.1007/s10750-017-3402-1.

Schwefel, R., A. Gaudard, A. Wüest, and D. Bouffard (2016), Effects of climate change on deepwater oxygen and winter mixing in a deep lake (Lake Geneva): Comparing observational findings and modeling, *Water Resources Research*, *52*(11), 8811–8826, doi:487 10.1002/2016WR019194.

Toffolon, M. (2013), Ekman circulation and downwelling in narrow lakes, *Advances in Water Resources, 53*, 76–86, doi:10.1016/j.advwatres.2012.10.003.

Winant, C. (2004), Three-dimensional wind-driven flow in an elongated, rotating basin, *Journal of Physical Oceanography, 34*(2), 462–476.

Towards an integrated hydrodynamic, water quality, and ecological modelling approach for Lake IJssel and Lake Marken.

Menno Genseberger[1]*, Arnout Bijlsma[1], Pascal Boderie[1], Mart Borsboom[1], Clara Chrzanowski[1], Miguel Dionisio Pires[1], Carlijn Eijsberg - Bak[1], Marieke Eleveld[1], Asako Fujisaki[1], Valesca Harezlak[1], Thijs van Kessel[1], Nienke Kramer[1], Ruurd Noordhuis[1], Sibren Loos[1], Jamie Morris[2], Arno Nolte[1], Sacha de Rijk[1], Alfons Smale[1], Bas Stengs[1], Christophe Thiange[1], Tineke Troost[1] and Migena Zagonjolli[1]

[1] Deltares, Delft, The Netherlands
[2] Wood Group, Dartmouth, Canada

**Corresponding author, e-mail Menno.Genseberger@deltares.nl*

KEYWORDS
Lakes; hydrodynamics; water quality; ecology; modelling.

Introduction

For Lake IJssel and Lake Marken in the Netherlands, various societal aspects are important (flooding, ship navigation, sand mining, salt intrusion, drinking water quality, water quality, ecology). Natural and human pressures require these aspects to be quantified. For example forecasting of flooding and water quality on a daily basis, ecological impact assessments of measures, and predictions of future climate change scenarios. Despite the diversity of aspects, many are related to common underlying physical, chemical, and biological processes. This allows for an integrated approach to quantify different aspects simultaneously. At Deltares we started working on this for Rijkswaterstaat (Dutch public works). Here we sketch the outline of the approach with two practical examples of its use.

Materials and methods

Lake IJssel and Lake Marken resulted from the construction of two dikes and land reclamation in an inland sea to protect the surrounding land from floodings. The first dike (1932) separated the inland sea from the Wadden Sea, turning the inland sea into a fresh water lake. The second dike (1975) splitted the fresh water lake into two: Lake IJssel and Lake Marken. The lakes are quite shallow: Lake IJssel has a depth of 5-7 m with some deep channels (remainders from the inland sea) and Lake Marken has a depth of 2-4 m with a deeper navigation channel in the south. The bottom of Lake IJssel is covered by sand, while the bottom of Lake Marken is composed of loam and clay. Lake IJssel is fed with fresh water from the River Rhine via the River IJssel, a fixed water level is maintained by flushing surplus water to the Wadden Sea. Lake Marken is more isolated resulting in relatively high residence times of water**.** In the lakes, the dynamic behavior of the surface water consists mainly of waves (driven by wind) and currents (driven by wind for Lake Marken, driven by wind and river discharges for Lake IJssel). This is a driving force for other physical and biological processes such as salt intrusion, resuspension of sediments, transport of nutrients, and algal blooms. See the scheme for important underlying physical, chemical, and biological processes and their interconnections in both lakes. For Lakes IJssel and Lake Marken, many of the societal aspects (as listed in the introduction) are directly related to this: they have important underlying processes in common. Therefore, the key idea is to use computational components [1, 2, 3] for modelling these common underlying processes as building blocks. This allows for an integrated approach to quantify different aspects simultaneously. To connect the building blocks we use a modelling chain of meteorological model, shallow water model, near shore wave model, and advection-diffusion-reaction model (including an extensive set of process definitions for suspended sediments, water quality, and ecology). In the scheme we marked the physical processes that are strongly related to the dynamic behaviour of the surface water with an orange dashed line and the chemical and biological processes with a blue dotted line. The biological processes marked by a green dash dotted line are less responsive to this dynamic behaviour. Final goal is to have all computational components included in an operational system [4], with the existing one for flooding around the lakes [5, 9] as a basis, to simulate the dynamic physical, chemical, and biological processes. Less responsive biological processes can be quantified afterwards.

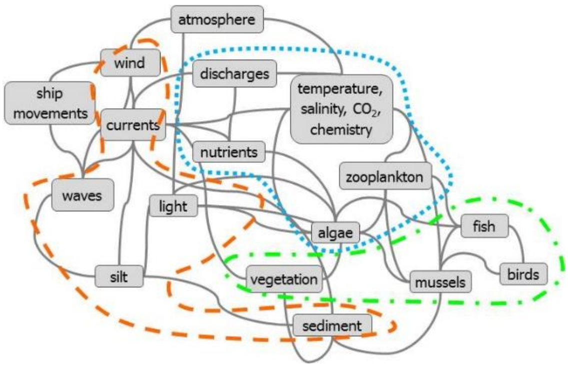

Example 1: The fresh water from Lake IJssel is used for drinking water and agriculture. However, measures for fish migration from the Wadden Sea to the lake may lead to salt intrusion in the lake (in addition to a.o. natural trends and climate change). With the integrated approach these aspects can be quantified simultaneously. This is of practical use to manage these aspects in a balanced way. Currently, a field measurement campaign is being set up, which will provide data for calibration and validation of the model.

Example 2: In Lake Marken, suspended sediments cause light limitation. Combined with decreasing nutrient concentrations, this prevents the achievement of ecological targets. Improved water transparency may provide opportunities for a more diverse and productive ecosystem. For this purpose, measures are being studied and built, such as the natural islands Marker Wadden. Impacts of these measures on water quality and ecology in Lake Marken will be assessed with a combination of the integrated modelling approach, measurements/monitoring, and expert knowledge [7, 5, 11].

Results and discussion

The integrated approach is of major interest for impact assessments of the future masterplan for Lake IJssel and Lake Marken. Although the plan making process started recently, it has to be an integral plan that takes into account all important societal aspects.

REFERENCES

[1] Delft3D https://oss.deltares.nl/web/delft3d/home

[2] SWAN http://swanmodel.sourceforge.net/

[3] HABITAT https://oss.deltares.nl/web/habitat

[4] FEWS https://oss.deltares.nl/web/delft-fews

[5] Donners et al.: Using High Performance Computing to enable interactive design of measures to improve water quality and ecological state of Lake Marken. Proceedings 15th World Lake Conference, 2014.

[6] Genseberger, Smale, Hartholt: Real-time forecasting of flood levels, wind driven waves, wave runup, and overtopping at dikes around Dutch lakes. Proceedings 2nd European Conference on FLOODrisk Manag., 2013.

[7] Genseberger, Noordhuis, Thiange, Boderie: Practical measures for improving the ecological state of lake Marken using in-depth system knowledge. Lakes & Reservoirs: Research & Manag. 21(1), pp. 56-64, 2016.

[9] Genseberger, Spee, Voort: Domain decomposition in shallow lake modelling for operational forecasting of flooding, proceedings of the 22nd International Conference on Domain Decomposition Methods, 2012.

[10] Genseberger et al.: A new D-Flow FM (Flexible Mesh) shallow water model for Lake Marken area. Poster at SIAM Conference on Mathematical and Computational Issues in the Geosciences 2017.

[11]http://content.oss.deltares.nl/delft3d/animations/reference_and_Markerwadden_silt_model_lake_Marken/reference_and_Markerwadden_silt_model_lake_Marken.mp4

Will climate change enhance the effects of pumped-storage on the thermal properties of the connected waterbodies?

U.G. Kobler[1], M. Schmid[1]*, A. Wüest[1,2]

[1] *Eawag, Swiss Federal Institute of Aquatic Science and Technology, Surface Waters - Research and Management, Kastanienbaum, Switzerland*
[2] *EPFL. Physics of Aquatic Systems Laboratory – Margaretha Kamprad Chair, ENAC-IEE-APHYS, Lausanne, Switzerland*

**Corresponding and presenting author, e-mail martin.schmid@eawag.ch*

KEYWORDS
pumped-storage; climate change; water quality; modelling; reservoir management.

Introduction

Pumped-storage (PS) hydropower plants are increasingly important facilities to stabilize the electrical grid by balancing intermittent renewable electricity sources such as wind power and photovoltaics. However, the water exchange between the two water bodies connected by a PS facility affects their thermal properties and water quality. A previous study on a planned PS system between Lago Bianco and Lago di Poschiavo had indicated strongest impacts in warm years, suggesting that climate change would likely aggravate the PS effects on the connected waterbodies (*Bonalumi et al*., 2012). In the present study we aimed at testing this hypothesis by simulating the combined impacts of climate change and PS operations on temperature, stratification, ice cover, and water quality of the two connected waterbodies.

Study site

We investigated the interactions between the effects of PS operations and those of climate change for the case of Etzelwerk, a PS hydropower plant that connects the natural lake Upper Lake Zurich to the artificial reservoir Sihlsee. At present, only about 12% of the power produced by this plant stems from PS, but the power plant is currently in the process of concession renewal, and several options for extending PS operations have been discussed.

Kobler et al. (2018) investigated the impacts of both the current and an extended PS scenario (with the pumping flow increased by a factor of ~20) on temperature, stratification, and water quality in the two water bodies. Impacts on Upper Lake Zurich were comparably small due to its larger size and higher natural inflows. For Sihlsee, however, extended PS operations were shown to increase hypolimnion temperatures, to shorten the duration of inverse stratification and ice cover in winter, and to increase hypolimnetic oxygen concentrations, especially towards the end of summer stratification. However, the effects of PS operations were smaller compared to those caused by the location of the water withdrawal in the hypolimnion of Sihlsee, which caused, among other things, a strong warming of the hypolimnion in autumn and a distinctive shortening of the summer stratification.

Materials and methods

The system of the two water bodies connected by a PS facility was implemented in a modified version of CE-QUAL-W2, a two-dimensional, laterally averaged, hydrodynamic and water quality model. Meteorological forcing for future climate scenarios, based on the climate scenarios CH2011 for the end of the 21st century in Northeastern Switzerland, were developed using the weather generator described by Schlabing et al. (2014). Simulations were performed for the current and an extended PS scenario as well as for two reference scenarios without PS and water withdrawal from either the epilimnion or the hypolimnion of Sihlsee.

Results and discussion

The results of the simulations showed significant synergistic and antagonistic effects of climate change and PS operations. As an example for a synergistic effect, summer hypolimnion temperatures were projected to increase by ~0.5 °C in the near-natural reference scenario, but by ~2.0 °C in the extended PS scenario – on top of the warming that is already induced by PS under current climate conditions. Conversely, oxygen concentrations show antagonistic effects, where the duration of the period with hypolimnetic O_2 concentrations below the legal target of 4 mg L^{-1} is projected to increase by ~1 month in the near-natural reference scenario, but only by ~1 week in the extended PS scenario.

Hydropower concessions are often issued for a duration of 50 years or longer. Significant climate change must be expected within that time frame, and we therefore recommend to include an analysis of potential interactions between climate change and PS effects in the environmental assessment of new or extensions of existing PS hydropower plants.

REFERENCES

Bonalumi, M., F. S. Anselmetti, A. Wüest, M. Schmid (2012), Modeling of temperature and turbidity in a natural lake and a reservoir connected by pumped-storage operations. *Water Resources Research*, *48*, WR01184.

Kobler, U. G., A. Wüest, and M. Schmid (2018), Effects of lake-reservoir pumped-storage operations on temperature and water quality, *Sustainability*, *in revision*.

Schlabing, D., M. A. Frassl, M. M. Eder, K. Rinke, and A. Bárdossy A (2014), Use of a weather generator for simulating climate change effects on ecosystems: A case study on Lake Constance. *Environmental Modelling & Software, 61*, 326-338.

Human-induced changes in lake forcing: the impact of the Kárahnjúkar hydroelectric scheme in the hydrodynamics of Lake Lagarfljót

C.L. Ramón[1,2]*, F.J. Rueda[1], M. Priet-Mahéo[2,3] and H.Ó. Andradóttir [2]

[1] Department of Civil and Environmental Engineering and Water Research Institute, University of Granada, Spain.
[2] Faculty of Civil and Environmental Engineering, University of Iceland, Reykjavík, Iceland.
[3] Icelandic Meteorological Office, Reykjavík, Iceland.

**Corresponding author, e-mail crcasanas@ugr.es*

KEYWORDS
Arctic lakes; dam impact; modelling; stratification; river intrusion depths.

Introduction

Un-dammed rivers and lakes could become affected by the damming of rivers that are located in other drainage basins, when the water diverted from dammed reservoirs — once used for power generation— is transferred to them. In that case, the added water could have physical-chemical characteristics that are different to those of the receptor stream (Bonalumi et al. 2012; Eiriksdottir et al. 2017). These different characteristics could lead, among others, to changes in the natural forcing of downstream lakes and, thus, to changes in their flow conditions and stratification regime (e.g., Bermúdez et al., 2017). The magnitude of the impacts will depend on the magnitude of the outflows from the powerplant with respect to the inflows of the other natural tributaries to the lake (e.g., Bonalumi et al., 2012). The Kárahnjúkar Hydroelectric Project in NE Iceland is an example of massive man-made interbasin transfer in the subarctic: two separate glacial rivers originating in the Vatnajökull glacier —the largest glacier of Europe— were dammed, united and discharged into Lake Lagarljót, one of the largest and deepest lakes in Iceland. This largest singular project in Icelandic construction history has increased the downstream water turbidity, reduced the primary production and influenced the flux of most dissolved elements towards the ocean (Eiriksdottir et al. 2017). The impact of the inter-basin transfer on internal physics within Lake Lagarfljót have to date not been clear. This research, funded by the National Power Company of Iceland (Landsvirkjun), aims to improve the knowledge and methodological framework for assessing the environmental impacts of hydropower projects on downstream lakes hydrodynamics. Changes in inflow characteristics (discharge, temperature and sediments) on hydrodynamical processes such as density stratification and river intrusion depths are assessed.

Materials and methods

Historical hydrological data was analyzed in order to assess the impacts of damming on riverine inputs to the lake, such as river temperature, suspended sediments and flow rates. Secondly, an Eulerian model (Smith 2006) already validated for Lake Lagarfljót post dam (Priet-Mahéo, unpubl.) was used to simulate lake hydrodynamics post dam during an average year from hydrological and meteorological perspectives. The same model was used to simulate lake hydrodynamics as prior to the dam project, by maintaining the meteorological forcing while modifying the hydrological forcing based on the analysis of pre-vs. post dam data. Thirdly, and to calculate river intrusion depths, the three-dimensional hydrodynamic fields generated by the Eulerian model both in the reference and deconstructed scenarios were used to simulate the trajectories of neutrally-buoyant particles originally seeded in the southern-inflows (glacial rivers) to the lake, using the 3-D Lagrangian particle-tracking routines of Rueda et al. (2008).

Results and discussion

Once the powerplant became operational in 2008, the residence time of water in the lake has decreased from 1.4 to 0.5 years and the seasonal cycle of suspended solids entering the lake has been highly impacted, with higher and lower than naturally occurring concentrations in winter and summer, respectively, and an overall increase of suspended solid concentrations within the lake demonstrated by the one-order-of-magnitude increase (from O(10) to O(10^2) mg L^{-1}) in the concentration of the lake outflows. Lake inflow and outflow temperatures are also on average 0.7ºC and 0.3ºC lower than prior to the project as a result of the outflows from the powerhouse which reach a maximum of only 6ºC in summer. The results of numerical simulations show that these human-induced changes in the natural forcing of the lake are responsible for, among others, a decrease in the length of the stratification period, a weaker strength of the lake-stratification (Fig. 1a) due to lower top-bottom density differences in the water column and the presence of a thicker metalimnion, and generally shallower and deeper river intrusions (Fig. 1b) before and during the stratification period (days 180-280), respectively.

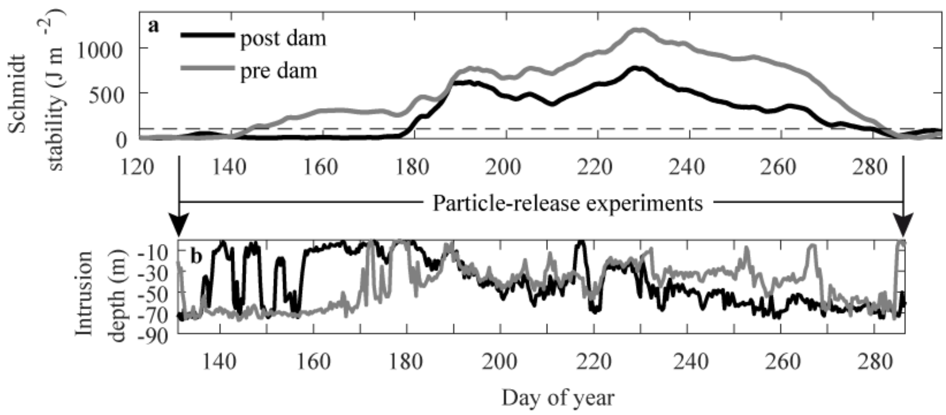

Figure 1. Modeled (a) water column stability and (b) intrusion depths pre and post dam.

REFERENCES

Bermúdez, M., L. Cea, J. Puertas, N. Rodríguez, and J. Baztán (2017), Numerical Modeling of the Impact of a Pumped-Storage Hydroelectric Power Plant on the Reservoirs' Thermal Stratification Structure: a Case Study in NW Spain, *Environmental Modeling & Assessment*, 23(1), 71–85, doi: doi: 10.1007/s10666-017-9557-3.

Bonalumi, M., F. S. Anselmetti, A. Wüest, and M. Schmid (2012), Modeling of temperature and turbidity in a natural lake and a reservoir connected by pumped-storage operations, *Water Resources Research*, 48(8), W08508, doi: 10.1029/2012WR011844.

Eiriksdottir, E. S., E. H. Oelkers, J. Hardardottir, and S. R. Gislason (2017), The impact of damming on riverine fluxes to the ocean: A case study from Eastern Iceland, *Water Research*, 113(Supplement C), 124–138, doi: 10.1016/j.watres.2016.12.029.

Rueda, F. J., S. G. Schladow and J. F. Clark (2008), Mechanisms of Contaminant Transport in a Multi-Basin Lake. *Ecological Applications*, 18(sp8), A72–A87, doi:10.1890/06-1617.1.

Smith, P. (2006), A Semi-Implicit, Three-Dimensional Model of Estuarine Circulation, Open File Report 2006-1004, USGS, Sacramento, USA.

Effects of hydropower operation on turbidity in a glacially-fed reservoir

D.M. Robb[1]*, R. Pieters[1,2], and G.A. Lawrence[1]

[1] *Civil Engineering, University of British Columbia, Vancouver, Canada*
[2] *Earth, Ocean and Atmospheric Sciences, University of British Columbia, Vancouver, Canada*

**Corresponding author, e-mail drobb@eoas.ubc.ca*

KEYWORDS
Hydroelectric reservoir; stratification; turbidity; glacial fines; aquatic productivity.

Introduction

While hydropower offers many benefits, there is an increasing desire to consider ecological values in water use planning. Of particular interest is the effect of changes in reservoir operation on aquatic productivity. Here we focus on one part of this complex problem, by looking at observations and model results of glacial inflow moving through a reservoir, and the effect of this inflow on turbidity and light extinction within the reservoir.

We examine Carpenter Reservoir, located in southwest British Columbia, Canada. The reservoir is long (50 km) and narrow (~1 km), with a surface area of 46 km^2 and a maximum depth of 50 m. The reservoir is a drowned river valley (Fig 1) formed from the Bridge River by the construction of Terzaghi Dam in 1960. Inflows into the reservoir are high in glacial fines, which are slow to settle, and which give the water a cloudy (turbid) appearance. There is concern that glacial meltwater is limiting light penetration within the reservoir, reducing algal growth, and in turn decreasing fisheries productivity.

Materials and methods

Field observations were collected over the biologically active season (May to October) in 2015 and 2016. Data included monthly surveys of the reservoir and tributaries, meteorological measurements, and a temperature mooring. To evaluate various reservoir operation scenarios, we used the two-dimensional laterally-averaged model, CE-QUAL-W2.

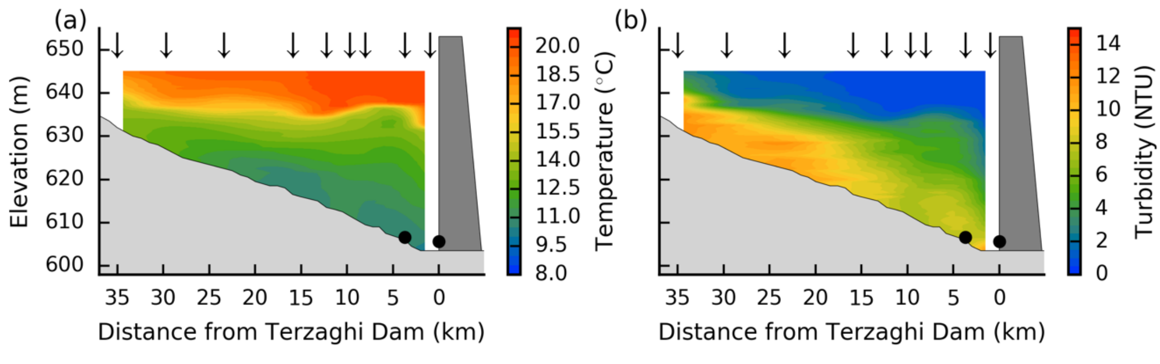

Figure 1. (a) Temperature and (b) turbidity profiles collected at Carpenter Reservoir on 16 July 2015. The downward arrows mark the location of each CTD cast and the black dots mark the location of the withdrawals.

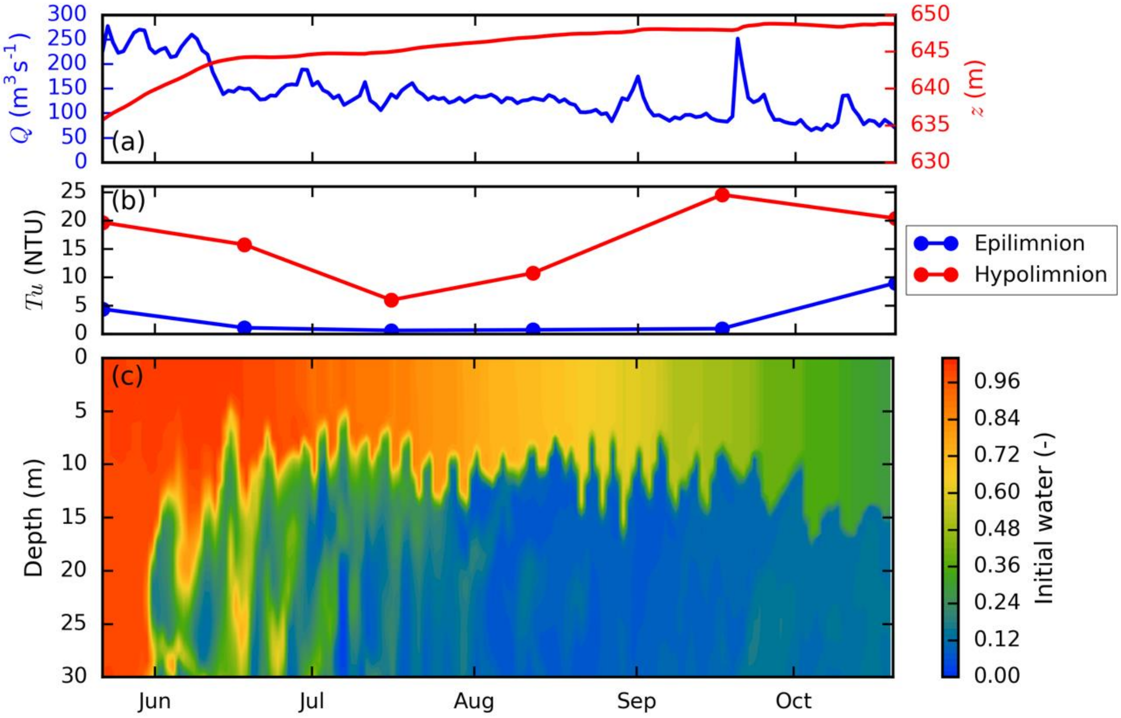

Figure 2. (a) Total inflow (blue) and water level (red) in Carpenter Reservoir; (b) measured turbidity in the epilimnion (blue) and hypolimnion (red); (c) fraction of water in the reservoir at the start of the model run, 22 May to 20 October, 2015.

The model was run from May to October, starting at the first sampling trip and ending at the last. Initial conditions for temperature, conductivity, and turbidity were given by profiles from the first trip. Boundary conditions included inflow, outflow, tributary temperature, tributary water quality and meteorological data. Model temperature agreed well with the measurements (RMSE ~0.9°C). To match observed turbidity required a settling rate of 0.2 m day^{-1}. We added passive tracers to the model to examine the mixing and transport of water originating from different sources, including a tracer to track the fraction of water in the reservoir at the start of the model run.

Results and discussion

The CTD profiles collected on 16 July 2015 are an example of the temperature and turbidity observed during the summer months (Fig 1). Given the high inputs of glacial fines, we expected the epilimnion to be turbid, so we were surprised to observe such a clear (~1 NTU) epilimnion over most of the summer (Fig 2b). The model tracer helps explain this as follows. At the beginning of the model run (May 22), the entire water column was occupied by the initial water in the reservoir (Fig 2c). After 10 days, much of the initial water below 20 m was replaced by water from the inflows, and by July, essentially all the initial water in the hypolimnion had been flushed. In contrast, the initial water in the epilimnion remained for most of the stratified season. It was not until fall that appreciable quantities of turbid water from depth were mixed into the epilimnion (Fig 2b,c). In other words, the epilimnion—with a long residence time—clears as the initial turbidity settles, while the large volume of turbid inflow short circuits through the hypolimnion below.

Future work involves identifying reservoir operations associated with extremes in turbidity. Preliminary results indicate that maintaining a lower water level during the spring leads to higher turbidity in the epilimnion, thereby limiting light availability.

Impact of different dredging scenarios on circulation and environmental parameters in Lake Viljandi.

T. Liblik, F. Buschmann, G. Väli, I. Suhhova, M-J. Lilover, U. Lips and J. Laanemets

Department of Marine Systems at Tallinn University of Technology
Akadeemia tee 15A, 12618 Tallinn, ESTONIA

**Corresponding author, e-mail madis.lilover@ttu.ee*

KEYWORDS
Lakes; dredging; environment; modelling.

Introduction

The lake Viljandi (located in southern Estonia (Fig. 1a)) rowing centre currently allows competition at 2000 m distance in three lines. To add three additional lines to carry out international competitions the lake has to be partly widened. In this study, the impact of different scenarios of planned dredging was evaluated on the lake currents, circulation scheme, vertical mixing and thermal regime using GETM (General Estuarine Transport Model) numerical experiments.

Materials and methods

Lake Viljandi is a long narrow valley lake: 4.6 km long, predominantly 300-400 m wide with thalweg depth about 10 m (Fig. 1b), surface area 1.55 km^2. The Järvekael is the narrowest area (120 m wide) and divides lake to the SW and NE sub-basins. The Uueveski and Valuoja streams flow into the northern part of the lake and Raudna river flows out from the SW end of the lake.

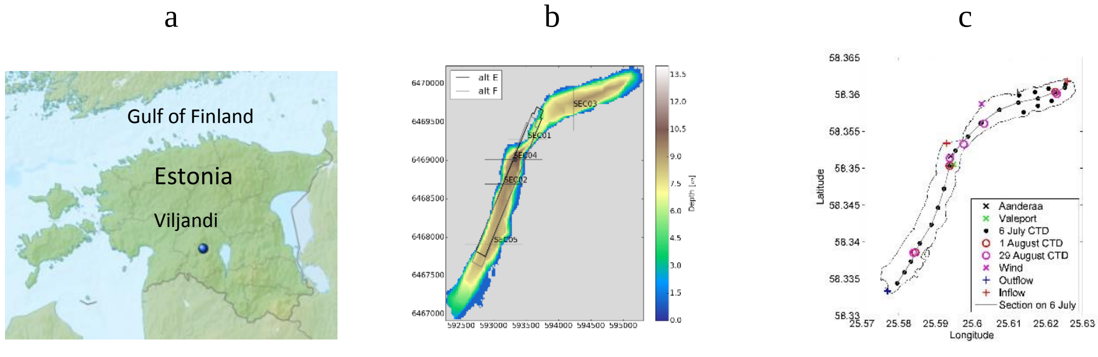

Figure 1 (a) Localisation of Lake Viljandi (Estonia), (b) bathymetry and rowing competition areas for scenarios E and F, (c) scheme of *in situ* measurements in summer 2017.

GETM has been used for simulations of the Lake Viljandi circulation for different dredging scenarios. GETM is a primitive equation 3-dimensional, free surface, hydrostatic model with a vertically adaptive coordinate scheme embedded. The horizontal model grid had a resolution of 20 m; ten layers were applied in vertical. Model is forced with observed wind data, and other atmospheric parameters were taken from HIRLAM (High Resolution Limited Area Model). For model validation wind, current and temperature *in situ* measurements were carried out in summer 2017. Altogether three CTD campaigns (at 6.07, 1.08 and 29.08) and one RDCP and rotor current meter time series were carried out (Fig. 1c). In addition oxygen and chl *a* concentrations were measured parallel to CTD casts.

Results and discussion

For summer period the SW winds with speed of 2-4 m/s prevailed. The analysis of CTD *in situ* data showed that the vertical temperature and oxygen distributions were in accordance with wind forcing. Both, CTD and simulation data showed an upwelling at upwind, and downwelling at downwind ends of the lake (Fig. 2a and 2b). In average, the wind generated current speed varied within 2–5 cm/s, but in extreme cases exceeded 15 cm/s. The narrow-necked region in the middle of the lake caused the division of circulation into two cyclonic gyres. The two widening scenarios of the narrow-necked region foresee different amounts of dredging. The model runs indicated that the reconstruction work will lead to an intensification of vertical mixing in some extent and the merging of two circulation cells to one. Still, the metalimnion remained for both studied scenarios. In the narrow neck, transport increased by 17 or 23% according to the used scenarios (Fig. 2c). Thus, the dredging will lead to increased vertical and horizontal (between two sub-basins of the lake) exchange of water and substance.

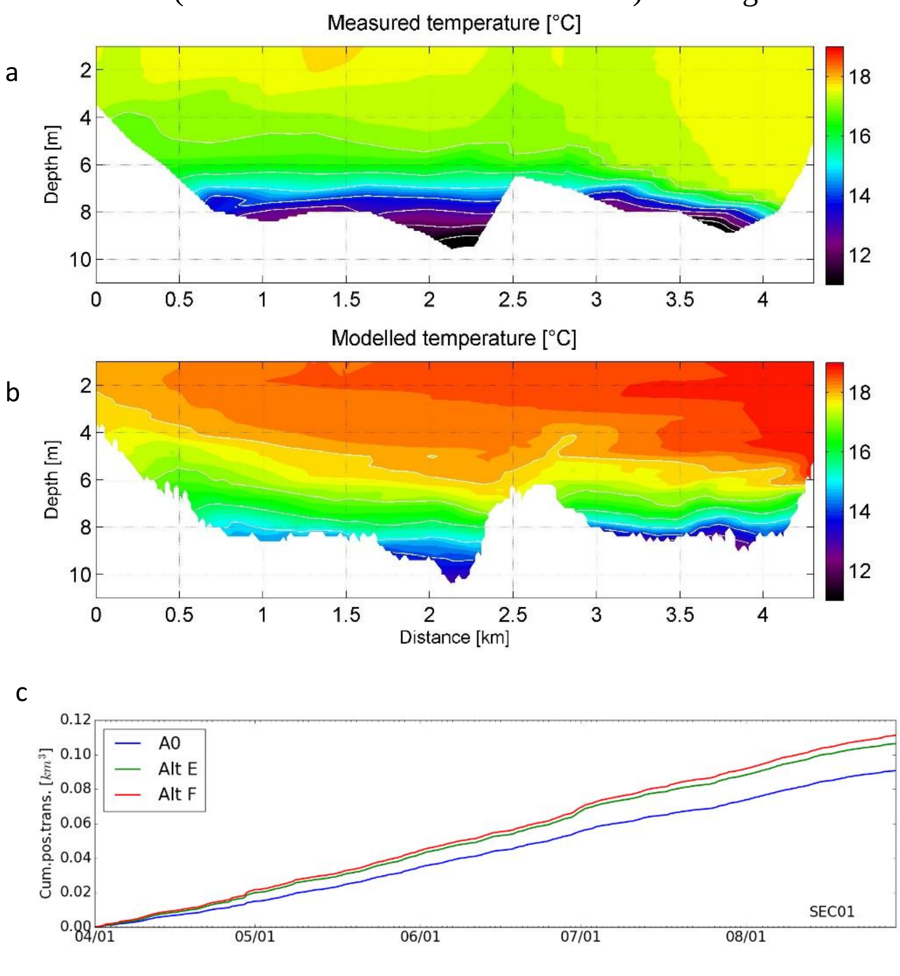

Figure 2 (a) Measured vertical temperature structure along the thalweg on 6 July and (b) concurrent simulated temperature structure. (c) A simulated cumulative northward transports through section SEC01 (A0) for the present lake and (Alt E and Alt F) for dredged lake scenarios E and F respectively (time interval 1.04-31.08.2017).

Keynote Speaker

Dr. Amber J. Ulseth

Scientist, Stream Biofilm and Ecosystem Research

Ecole Polytechniqe Fédérale de Lausanne (EPFL)

Address:	EPFL ENAC IIE SBER
Phone:	+41 (0)21 293 63 65
Email:	amber.ulseth@epfl.ch OR amber.ulseth@gmail.com
Website:	https://sites.google.com/site/amberjulseth/home

Research interests	*Ecosystem Ecology, Biogeochemistry, Stream and River Ecology, Stream Metabolism Carbon and Nutrient Cycling, Anthropogenic Stressors on Freshwater Ecosystems*
University education	*University of Vienna (Post-doc), University of Wyoming (PhD), University of North Carolina Greensboro (MS), University of Minnesota Duluth (BS)*

The main focus of Amber's work is on ecosystem ecology and biogeochemical cycling in streams and rivers. Amber uses a combination of field, laboratory, and modeling approaches to understand how streams and rives transform, store, and export carbon and nutrients. She is particularly interested in the interaction of abiotic forcing, such as changes in hydrology, and biotic drivers (from microorganisms to people) on biogeochemical cycling in fluvial freshwaters. Currently, Amber is a Scientist within the Stream Biofilm and Ecosystem Research (SBER) laboratory at EPFL working on gas-exchange, ecosystem metabolism, and CO_2 dynamics in alpine streams. Prior to working at EPFL, Amber was a post-doctoral researcher at the University of Vienna working on ecosystem metabolism in subalpine streams. Amber received her PhD from the University of Wyoming, USA, where she worked on organic carbon dynamics in the Colorado River Basin. In January 2019, Amber will be starting a new position as a tenure-track Assistant Professor at Sam Houston State University (Texas, USA) where she will continue her pursuits in aquatic ecological research and teaching.

Two-state gas-exchange in streams and the implications of bubbles on scaling CO_2 fluxes

Amber J. Ulseth[1*], Robert O. Hall Jr.[2], Åsa Horgby[1], Marta Boix Canadell[1], Amin Niayifar[1], Daniel McGinnis[3], and Tom J. Battin[1]

[1]*Stream Biofilm and Ecosystem Ecology, Ecole Polytechnique Fédérale de Lausanne, Lausanne, Switzerland*
[2]*Flathead Biological Station, University of Montana, Montana, USA*
[3]*Department F.-A. Forel, Faculty of Science, University of Geneva, Geneva, Switzerland*

**Corresponding author: amber.ulseth@gmail.com*

Keywords
gas-exchange; k_{600}; streams; Alpine; CO_2; energy dissipation

Introduction

Inland waters are significant components of the global carbon cycle. Carbon dioxide (CO_2) fluxes from streams, rivers and lakes to the atmosphere are of the same order of magnitude than CO_2 fluxes from the atmosphere to the oceans. Gas exchange across the air-water interface in these ecosystems is critical for the flux of climate-relevant gases and for ecosystem processes, including ecosystem metabolism and nutrient cycling. While the physical forcing of gas exchange in the ocean and lakes has received substantial attention over the last decades, it remains poorly understood in streams and rivers, thereby making global estimates of gas fluxes from these ecosystems difficult to constrain. Data driven models to scale gas exchange in streams and rivers have been based on gas-tracer experiments conducted mostly in low-energy, low-sloped (<4%) streams. However, the world is not flat. A significant proportion of streams worldwide have steep slopes (>4%), but we know little how gas exchange may scale to these high-energy streams. Furthermore, while scientists working on lake and marine ecosystems have recognized that bubbles affect gas exchange when scaling less soluble gases to more soluble CO_2, recognizing the potential roles of bubble mediated gas exchange in streams and rivers is extremely limited.

Methods

We used a combination of experimental and modeling approaches to address scaling gas exchange in streams. To address scaling gas exchange from low- to high-energy streams, we combined a new set of data on gas transfer velocities (k_{600}) from tracer gas additions in mountain streams with published k_{600} values to cover an unprecedented range of streams differing in energy, geomorphology and hydraulics. Additionally in these mountain streams, we conducted dual tracer gas-releases, using both a less soluble gas (argon) in combination with CO_2 to address the role of bubbles on scaling CO_2 fluxes.

Results and Discussion

We found differing scaling relationships between stream energy dissipation ($eD = gSV$, g is gravitational acceleration, S is stream slope, and V is streamflow velocity) and k_{600} for low- and high-energy streams. This indicates two different physical regimes with differing behavior in how k_{600} responds to turbulence in low versus high-energy streams. In low-energy streams (with $eD < 0.08$), we suggest that Fickian diffusion drives k_{600} with an attenuating increase with eD (maximum k_{600} of 35 m d^{-1}). In comparison, in high-energy streams ($eD > 0.08$), turbulence entrains air bubbles in the water resulting in an explosive increase in k_{600} with increasing eD. k_{CO2} was approximately half that of k_{argon}, based on the dual gas tracer experiments in these high-energy streams. This difference indicates that in high-energy streams, when scaling gas exchange from less-soluble gases to more soluble CO_2, both solubility and Schmidt scaling should be considered. These findings offer a framework to properly include steep sloped streams draining the numerous mountainous regions on Earth in future estimates of gas fluxes from streams and rivers at the global scale.

Listening to air-water gas exchange in running waters

M. Klaus[1]*, E. Geibrink[1], E.R. Hotchkiss[2] and J. Karlsson[1]

[1] Department of Ecology and Environmental Science, Umeå University, Umeå, Sweden
[2] Department of Biological Sciences, Virginia Polytechnic Institute and State University, Blacksburg, VA, USA

**Corresponding author, e-mail marcus.klaus @posteo.net*

KEYWORDS
Stream; gas exchange coefficient; turbulence; air bubbles; acoustics.

Introduction

Air-water gas exchange coefficients (k) are critical components of biogeochemical mass balance models in aquatic systems and particularly relevant for ecosystem metabolism calculations and greenhouse gas budgets (Hall & Hotchkiss, 2017; Wallin et al., 2011). New high resolution sensor technology is now widely applied to account for spatiotemporal variability in gas concentrations (e.g. Bernhardt et al. 2017; Crawford et al. 2017). Yet, this technology can only be exploited to its full potential to estimate air-water gas fluxes, if combined with high resolution k estimates. Because k measurements are labor intense, new affordable methods with minimal logistical efforts are needed to efficiently capture the large spatiotemporal variabilities of k in running waters (Wallin et al., 2011).

Air-water gas exchange rates are controlled by turbulence at the air-water interface and bubble-mediated transfer (Woolf et al., 2007). Turbulence and air bubbles create sound of characteristic frequencies (Minnaert, 1933; Proudman, 1952). Sound spectra of flowing water may therefore contain unique information to estimate k. This is especially relevant in steep systems where k is largely mediated by bubbles and traditional methods based on turbulence measurements, physical models or tracer gases are biased (Hall & Madinger, 2018).

Materials and methods

Here, we develop a new method to quantify k in running waters based on spectral sound analysis. We expand on pioneering work by Morse et al. (2007) that showed high correlations between above-stream band-integrated sound pressure levels and k, but here target sound where it is produced (underwater) and frequency bands associated with turbulence and bubbles. We explored the relationship between k and sound spectra in a laboratory flume experiment and in three Swedish boreal headwater streams, with 36 sites nested in 12 reaches, each sampled 4-8 times during a wide range of flow conditions. We estimated k at the lab- and site scale using gas flux chambers and at the reach scale using propane injection experiments, and recorded sound above and below the water surface by microphones and hydrophones, respectively. Observations were complemented by lab measurements of turbulence and field measurements of morphological and hydrological parameters. We established statistical models of k based on the difference in sound pressure levels (SPL) at octave bands affected and not affected by bubbles (125 Hz - 2 kHz), and explored the variability in exact band selection and model parameterizations relative to turbulence and hydro-morphological stream characteristics.

Results and discussion

In the lab experiment, we found strong sinusoidal relationships between k and differential SPLs (R^2=0.94-0.99). Under field conditions, differential SPLs were excellent linear proxies of k when calibrated for each site or reach (median R^2=0.85-0.95). Predictive power was weaker for general calibration models (R^2=0.22-0.83). Calibration parameters and octave band selection were strongly linked to hydro-morphological stream characteristics. Above-stream and under-water sound predicted k equally well. In both the lab and field experiment, SPLs associated with bubbles (1 kHz) increased relative to SPLs associated with turbulence (31.5 Hz) with expected increases in bubble contributions to air-water gas exchange.

We summarize our mechanistic insights in the acoustic signatures of air-water gas exchange in a conceptual figure (Fig. 1). While SPLs generally rise with faster gas exchange, the increase is strongest at frequencies associated to turbulence and bubbles. Hence, underwater sound spectra can potentially be used to separate turbulence- and bubble mediated contributions to k. This information is difficult to obtain simultaneously with existing methods but critical for developing mechanistic k models that could relieve our current heavy dependence on site-specific statistical models.

Passive acoustic techniques are increasingly used to survey aquatic ecosystems, yet their potential to monitor biogeochemical processes remain largely unexplored (Linke et al., 2018). Here, we demonstrate that acoustics can be used to infer k, but with much less sampling efforts and costs relative to traditional methods. Combined with data loggers, acoustic sensors could be used to estimate k continuously in time. Properly calibrated, they could also allow quick spatial snap-shot surveys. This opens the opportunity of acoustics to better constrain magnitudes and variabilities in biogeochemical fluxes and ecosystem processes.

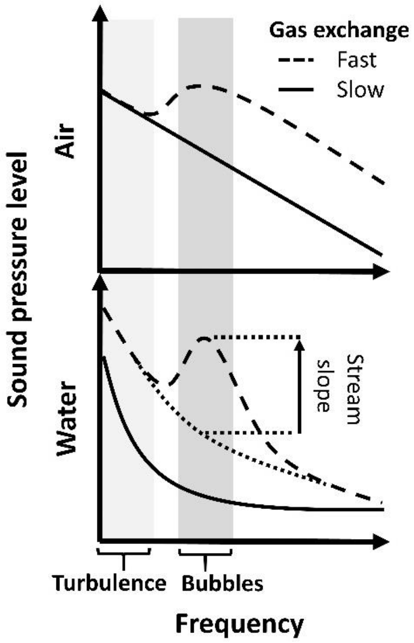

Fig. 1 Conceptual diagram of the acoustic signature of air-water gas exchange in running waters.

REFERENCES

Bernhardt, E.S., J.B. Heffernan, N.B. Grimm, E.H. Stanley, J.W. Harvey, M. Arroita, et al. (2017), The metabolic regimes of flowing waters. *Limnology and Oceanography*, *63*(S1), S99-S118.

Crawford, J.T., E.H. Stanley, M. M. Dornblaser and R. G. Striegl (2017), CO2 time series patterns in contrasting headwater streams of North America. *Aquatic Sciences*, *79*(3), 473-486.

Hall, R.O. and E.R. Hotchkiss (2017), Stream metabolism. In F. R. Hauer & G. A. Lamberti (Eds.), *Methods in Stream Ecology* (Volume 2,). Academic Press.

Hall, R.O. and H.L. Madinger (2018), Use of argon to measure gas exchange in turbulent mountain streams. *Biogeosciences Discussions*, 1-16.

Linke, S., T. Gifford, C. Desjonquères, D. Tonolla, T. Aubin, L. Barclay, et al. (2018), Freshwater ecoacoustics as a tool for continuous ecosystem monitoring. *Frontiers in Ecology and the Environment 16(4), 231-238*.

Minnaert, M. (1933), On musical air-bubbles and the sounds of running water. *The London, Edinburgh and Dublin Philosophical Magazine and Journal of Science*, *16*(104), 235-248.

Morse, N., W.B. Bowden, A. Hackman, C. Pruden, E. Steiner and E. Berger (2007), Using sound pressure to estimate reaeration in streams. *Journal of the North American Benthological Society*, *26*(1), 28–37.

Proudman, I. (1952), The generation of noise by isotropic turbulence. *Proceedings of the Royal Society A. Mathematical, Physical and Engineering Sciences*, *214*(1116), 119-132.

Wallin, M.B., M.G. Öquist, I. Buffam, M.F. Billett, J. Nisell and K. H. Bishop (2011), Spatiotemporal variability of the gas transfer coefficient (KCO2) in boreal streams: Implications for large scale estimates of CO2 evasion. *Global Biogeochemical Cycles*, *25*(3), 1-14.

Woolf, D. K., I.S. Leifer, P.D. Nightingale, T.S. Rhee, P. Bowyer and G. Caulliez (2007), Modelling of bubble-mediated gas transfer : Fundamental principles and a laboratory test. *Journal of Marine Systems*, *66*, 71-91.

Spatial and temporal scales of flow and morphological diversity in gravel bed streams

A. Lorke[1*], C. Anlanger[1*], U. Risse-Buhl[2], M. Weitere[2] and C. Noss[1]

[1] *Institute for Environmental Sciences, University of Koblenz-Landau, Fortstrasse 7, 76829 Landau, Germany.*

[2] *Department River Ecology, Helmholtz Centre for Environmental Research – UFZ, Brückstraße 3a, 39114 Magdeburg, Germany.*

**Corresponding author, e-mail: lorke@uni-landau.de*

ABSTRACT

Biodiversity in fluvial ecosystems is closely linked to habitat heterogeneity. Although the processes by which habitat heterogeneity is shaped by hydro-morphologic processes are well studied, the relationships between abiotic and biotic diversities are largely unknown. While biological diversity and its scale dependence is usually expressed using indices based on species number and relative abundance, corresponding metrics describing the diversity of abiotic patterns are lacking. In a novel approach, we combine existing ecological and physical theories and present a concept based on additive variance partitioning for abiotic variables, like flow velocity and streambed morphology. The overall diversity within a region (gamma diversity) is the sum of alpha and beta diversities, which constitute temporal and spatial averages at smaller scales. The concept is exemplarily applied to a comprehensive data set of near-bed flow velocity and streambed morphology in two gravel bed streams. Flow diversities were consistently increasing with increasing spatial scale, which was mainly caused by increasing variability of temporarily averaged flow velocities (beta diversity). Morphologic diversity explained 33% of the observed flow diversity. Temporal and spatial extrapolation of diversities showed that flow alpha diversity (turbulent velocity fluctuations) on time scales between 0.1 – 100 s, contributed on average 20% to the long-term (16 years) flow diversity, while most of the morphologic diversity was present at spatial scales between 100 m and ~2 km. The proposed concept facilitates estimation of abiotic and biotic diversity at identical spatial and temporal scales and can be integrated into a broadened biodiversity concept in stream ecology.

Keynote Speaker

Prof. Dr. Werner Eugster

Institute of Agricultural Sciences, ETH Zürich

Head of Micrometeorology Subgroup of Grassland Sciences Group

Address: LFW C 55.2, Universitätstrasse 2, 8092 Zürich
Phone: +41 (0)44 632 68 47
Email: werner.eugster@usys.ethz.ch
Website: http://homepage.usys.ethz.ch/eugsterw/

Werner Eugster obtained his Ph.D.in 1994 from the University of Bern where he was the first to carry out eddy covariance flux measurements of NO_2, O_3 and other gases. During his postdoctoral research at the University of California at Berkeley (1995-1996) he measured CO_2 fluxes in a broad range of arctic tundra ecosystems, including the very first eddy covariance flux measurements carried out on Toolik Lake in northern Alaska. This brought him in touch with limnologists in Switzerland, the USA, Finland and elsewhere. Thus, measuring energy exchange fluxes from lakes, as well as CO_2 and CH_4 fluxes, using the eddy covariance technique has become one of his main research interests.

Direct gas flux measurements from surface waters

W. Eugster[1]*, T. DelSontro[2] and G. W. Kling[3]

[1] Department of Environmental Systems Science, ETH Zürich, Zürich, Switzerland
[2] Department F.-A. Forel for environmental and aquatic sciences
Faculty of Science, University of Geneva, Geneva, Switzerland
[3] Department of Ecology & Evolutionary Biology, University of Michigan, Ann Arbor, MI 48109-1085, USA

**Corresponding author, e-mail werner.eugster@usys.ethz.ch*

KEYWORDS

Lakes; gas fluxes; short-term variability; environmental drivers; water–air gas gradients.

Introduction

Measuring CO_2 and CH_4 exchange fluxes between water bodies and the atmosphere remains a challenge. Eddy covariance flux measurements increase the temporal coverage of flux data of a relevant water surface area known as the "flux footprint". Using such data allows analyses of diel and seasonal dynamics of fluxes, and has the potential to cover singular events such as lake turnover or partial mixing during storm events. Nevertheless, CO_2 and CH_4 fluxes are typically close to the detection limit that eddy covariance fluxes can resolve. Moreover, if a lake is small, local non-steady-state micrometeorological conditions may confound the eddy covariance flux measurements that assume steady-state turbulence and horizontally homogenous fetch conditions. Methods that cope with such conditions are still experimental and not well established in the scientific literature.

Materials and methods

CO_2 and CH_4 fluxes were measured via the eddy covariance method on four lakes and one run-of-river reservoir. In the special case of Toolik Lake, we also deployed an automatic gas extraction unit during the summer season of 2015 that simultaneously measured CO_2 and CH_4 gas concentrations in the water.

Eddy covariance flux measurements — Direct flux measurements are still not the standard in limnology, but an increasing number of scientists are employing these methods. Thus, we added a specific chapter on eddy covariance flux measurements over lakes (Vesala et al., 2012) to the text book on eddy covariance that is typically read by terrestrial ecologists using this method. For soil scientists we wrote a short overview (Eugster and Merbold, 2015) that also provides insight for people working in aquatic systems. The measurement technique that we deploy over lakes and rivers was documented for advanced users by Eugster and Plüss (2012), and our first eddy covariance measurements of CO_2 fluxes over Toolik lake were published by Eugster et al. (2003). As a short summary for participants that have not been exposed to eddy covariance flux measurements it suffices to say that this method typically requires two separate instruments—one for measuring wind and the other for the gas in question. Both instruments should provide a fast response time and sufficient temporal resolution to measure the covariance between the vertical wind velocity fluctuations (w') and the associated fluctuations of the gas concentrations (c') for which the flux is to be determined ($w'c'$ or covariance of w and c). Here we take the viewpoint of an atmospheric scientist measuring the gas flux (e.g., CO_2 or CH_4) leaving a water surface in oversaturated conditions or resupplying it in undersaturated conditions. The same principle also holds for eddy covariance flux measurements inside the water body, but technical constraints on both sensors and the time scales that must be resolved to correctly quantify the turbulent flux are much stronger inside the water than in the atmosphere. In both cases, the physical flux is the covariance between the vertical velocity speed and the concentration fluctuations. To calibrate and correct the flux, a suite of procedures and assumptions are normally made, but these should be considered fine-tuning of the precision and accuracy of such flux measurements.

Lake water gas concentration measurements — Turbulent fluxes across the water interface are more complicated to measure and understand than fluxes over terrestrial surfaces, since both the water body and the atmosphere above are typically turbulent media, whereas vegetation or soil are nonturbulent media. This means it is not clear *a priori* whether the limiting factor in water–atmosphere exchange is the turbulent transport in the water body or the turbulent transport in the atmosphere. The key to understanding these effects is the measurement of the gas gradient across the water–air interface. During summer 2015, we performed gas measurements with a newly developed continuous flow gas extraction unit consisting of a Liqui-Cel (Charlotte, NC, USA) membrane with a closed gas loop and an open water circulation with a flow rate of 1 L/min. Gas concentrations were measured with a Los Gatos Research (San Jose, CA, USA) CH_4 analyzer and a Licor (Lincoln, NE, USA) model 840 CO_2/H_2O analyzer.

Results and discussion

This presentation will show successful deployments of eddy covariance systems on various lakes and a run of river reservoir using a variety of experimental approaches and discuss remaining open issues and challenges. In combination with gas concentration measurements in water and the atmosphere above, a direct determination of gas exchange piston velocity is possible. These experimentally determined piston velocities do not perfectly agree with values obtained from large water bodies far from the shore, indicating that both atmospheric turbulence and circulation patterns in a lake interact in governing gas exchange rates. We present a description of how piston velocities for CO_2 and CH_4 were determined over Toolik Lake in the summer of 2015, when direct gas concentration measurements of CO_2 and CH_4 were available from the peak ice-free season, and what was learned from this effort.

In the last part of this contribution, ideas and suggestions for future work with the eddy covariance method over small and medium-size water bodies will be discussed with the participants. The goal will be to encourage such measurements, but raise awareness that the eddy covariance flux measurement technique on water bodies poses additional challenges compared to terrestrial deployment, and while promising it is not yet a “plug-and-play” technique.

REFERENCES

Eugster, W., and L. Merbold (2015), Eddy covariance for quantifying trace gas fluxes from soils, *SOIL, 1*, 187–205, doi:10.5194/soil-1-187-2015.

Eugster, W., G. Kling, T. Jonas, J. P. McFadden, A. Wüest, S. MacIntyre, and F. S. Chapin, III (2003), CO_2 exchange between air and water in an Arctic Alaskan and midlatitude Swiss lake: Importance of convective mixing, *J. Geophys. Res.*, *108*(D12), 4362, doi:10.1029/2002JD002653.

Eugster, W., and P. Plüss (2012), A fault-tolerant eddy covariance system for measuring CH_4 fluxes, *Agric. Forest Meteorol.*, *150*(6): 841–851, doi:http://dx.doi.org/10.1016/j.agrformet.2009.12.008.

Vesala, T., W. Eugster, and A. Ojala (2012), Eddy covariance measurements over lakes, in: Aubinet, M., T. Vesala, and D. Papale (eds.) *Eddy Covariance: A Practical Guide to Measurement and Data Analysis*. Springer Verlag, pp. 365–376, doi:http://dx.doi.org/10.1007/978-94-007-2351-1_15.

Physical process impacting methane emission from Swedish lakes

A. Verlet-Banide*, A. Rutgersson, E. Sahlée

Department of Earth Science. Uppsala University, Uppsala, Sweden

**Corresponding author, e-mail antonin.verlet-banide@geo.uu.se*

KEYWORDS
Lakes; methane; seasonal cycle;eddy covariance

Introduction

The large number of studies on increasing concentrations of greenhouse gas (GHG) in the atmosphere supports the idea that the increasing in concentration has an impact on climate change. Due to its high anthropogenic emission, CO_2 in the atmosphere is highly researched on, however the concentration of CH_4 in the atmosphere has also a forcing impact on climate change due to its high warming potential [Kirschke et al., 2012] . Indeed, it is estimated around 23 times more important then CO_2, per unit over a time period of 100 years. Lakes are contributing in significant amount to CH_4 emissions in the atmosphere. Fresh water body are estimated to emit approximatively 103 $Pg.C.yr^{-1}$, the high impact of lake can outweigh 25% of the terrestrial carbon sink for CH_4 emission [Bastviken et al., 2011]. Numerous studies show the use of eddy covariance (EC) method over coastal zone, ocean and terrestrial area to measure GHG fluxes,more and more study show the specific interest in of EC method for methane flux observations [Eugster et al. 2011, Podgrajsek et al, 2014]. This study is a comparison between three Swedish lakes. The impact of specific physical process om methane flux differs depending of the lake characteristic. The following result focus on the seasonal process impacting the methane flux. The three long term studies are ideal for a lake comparison over similar time periods.

Materials and methods

Lake Erken

The first set of flux measurements are taken at lake Erken in the east center part of Sweden (59 o 51’ 00 ” N, 18 o 34’ 00 ” E). Lake Erken as a mean depth of 9 meter,the maximum depth is 21 meter and a surface area of 24 km^2. The northern and south west part of the lake is surrounded by forest whereas the east and south-east part is surrounded by agricultural land. Five inlet and outlet are studied and measured by Erken laboratory. A 6 meter tower is located on a small island on the southeast part of the island. The north side shore of the island contains the deepest water area, the closest shore is about 500 meter south of the island. The measurement are taken at two levels. The first level at 4.10 m and the second level at 6.17 m height above the tower base, measure wind speed, wind direction,water vapor, gas concentration. CH_4 flux measurement are realized at the first level with a sonic anemometer (WindMaster,Gill instrument, Lymington,UK) for wind measurements, thermocouples for temperature and a LI-7700 (LI-COR Inc.,Lincoln,NE,USA) for the methane measurements. The use of LI-7700 is justified by the well agreement in CH_4 flux measured by close path and LI-7700 [Peltola et al,2013 and Detto et al, 2011]. Air pressure, global radiation and relative humidity are additionally measured on the tower.

Lake Erssjön

See article [Podgrajsek et al, 2015].

Lake Tämnaren

See article [Podgrajsek et al, 2014]

Data Coverage and selection

The data selection for lake Erken, Tämnaren and Erssjön is for open water period. For lake Erken the data overlap a period from September 2014 to August 2017. Lake Tämnaren data is over the period from Sept 201 to August 2012. Lake Erssjön data cover the period from April and December 2013.The receive signal strength indicator criteria is set higher then 20 % for lake Erken,Tämnaren and Erssjön. The skewness and the kurtosis are set in the following range -2 to 2 and 1 to 8 as advided in Vickers and Mahrt (1997).

Results and discussion

Seasonal cycle

In figure 1 the methane flux represented on the entire half-hour mean data sets in respect of the months. The data sets are laid out in a box-plot .X axes represent the months of the years. Y axis represent the methane flux, 0 to 35 nmol.m^{-2}.s^{-1} for lake Erken, 0 to 50 nmol.m^{-2}.s^{-1} for lake Erssjon ,0 to 150 nmol.m^{-2}.s^{-1} for lake Tamnaren.

The lake comparison for between lake Erken Erssjön and Tämnaren show some clear similarities.The common trend between the three lake is the a clear decrease from summer period to fall period, the mean flux emission is significantly higher during summer then fall for all tree lake. Both lake Erken and lake Erssjön show a clear increase of methane flux from spring period to summer period however this trend is less clear for Lake Tämnaren since August data are not available.Lake Erken show lower methane fluxes in April then May, but May fluxes are significantly smaller then the summer period and similar to some of the fall period fluxes (October andNovember). Methane fluxes in Spring for lake Erssjön and lake Tämnaren are both significantly higher then the fluxes in October and November. This is in contradiction high peak of methane out-gassing in Autumn observe lake Lugano by Blees et al (2015).

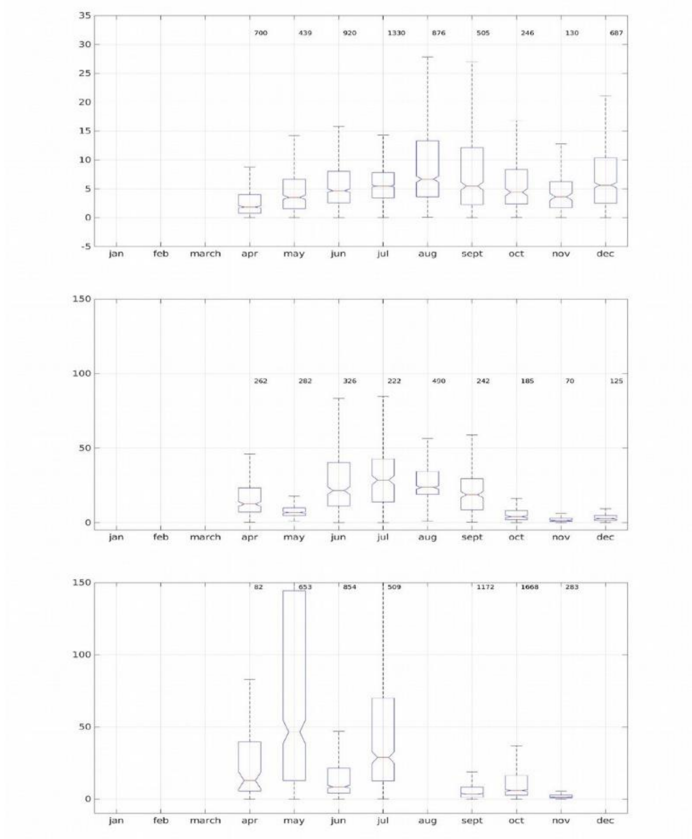

Figure 1: Methane seasonal cycle for Erken (upper graph), Erssjön (middle graph) and Tämnaren (bottom graph). The y-axes represent the methane flux in nmol.m^{-2}.s^{-1}. The center line in the boxes represent the median values, the edges of the boxes are the 25th(Q1) and 75th(Q1) percentiles, and the upper and lower whiskers represent161 Q3+1.5(Q3- Q1) and Q1-1.5(Q3-Q1)

REFERENCES

Bastviken, D.; Tranvik, L. J.; Downing, J. A.; Crill, P. M.; Enrich-Prast, A. Freshwater methane emissions offset the continental carbon sink. Science 2011,331(6013), 50-50

Blees J, Niemann H, Wenk CB, Zopfi J, Schubert CJ, Kirf MK, et al. Micro-aerobic bacterial methane oxidation in the chemocline and anoxic water column of deep south-Alpine Lake Lugano (Switzerland). Limnol Oceanogr. 2014;59: 311–324. tto, M., J. Verfaillie, F. Anderson, L. Xu, and D. Baldocchi (2011), Comparing laser-based open- and closed-path gas analyzers to measure methane fluxes using the eddy covariance method, Agr. For. Meteorol., 151, 1312–1324,

Eugster, W.; DelSontro, T.; Sobek, S. Eddy covariance flux measurements confirm extreme CH4 emissions from a Swiss hydropower reservoir and resolve their short-term variability. Biogeosciences 2011,8 (9), 2815-2831.

Peltola, O., I. Mammarella, S. Haapanala, G. Burba, and T. Vesala (2013), Field intercomparison of four methane gas analysers suitable for eddy covariance flux measurments, Biogeosci. Discuss., 9, 17,651–17,706.

Podgrajsek, E., Sahlée, E. & Rutgersson, A. (2014). Diurnal cycle of lake methane flux. Journal of Geophysical Research, 119(3), 236-248

Podgrajsek, E., E. Sahlée, D. Bastviken, S. Natchimuthu, N. Kljun, H. E. Chmiel, L. Klemedtsson, and A.Rutgersson (2015), Methane fluxes from a small boreal lake measured with the eddy covarianc method, Limnol. Oceanogr.

Vickers, D., and L. Mahrt. 1997. Quality control and flux sampling problems for tower and aircraft data. J. Atmos. Ocean Technol. 14: 512–526.

(Semi-) Continuous measurements of dissolved greenhouse gases with Cavity Ring-Down Spectrometers

M. Hofmann[1]*, R. Winkler[2]

[1] *Picarro Inc., Netherlands*
[2] *Picarro Inc., Switzerland*

**Corresponding author, e-mail mhofmann@picarro.com*

KEYWORDS
dissolved greenhouse gases; Cavity Ring-Down Spectrometers; (semi-) continuous measurements

ABSTRACT

The budget of atmospheric greenhouse gases is significantly affected by air-water exchange fluxes. Analysis of dissolved gases like CO_2, CH_4 and N_2O can therefore provide significant insight on sources and sinks of atmospheric trace gases.

Picarro Inc. provides a range of greenhouse gas analysers that can be coupled with different front-ends to analyse the concentration and isotopic composition of dissolved gases like CO_2, CH_4 and N_2O with highest precision. Depending on the peripheral, our Cavity Ring-Down Spectrometers (CRDS) allow continuous or semi-continuous measurement of dissolved gases. The performance of our CRDS isotope analysers is comparable to isotope ratio mass spectrometry, with the advantage of being portable, easy to operate and service, and less expensive. As such, our analysers have been used in a range of innovative configurations and applications for dissolved gas analysis.

Here, we want to highlight a few applications where we coupled conventional dissolved gas extraction methods to our CRDS analysers:

(1) Greenhouse gas concentrations alone can be analysed e.g. with our Picarro G2508 analyser that allows simultaneous measurement of N_2O, CH_4, CO_2, NH_3 and H_2O concentrations. Alternatively, the Picarro GasScouter G4301 is a new generation, light-weight, battery-powered CRDS for CO_2 and CH_4 measurements in the field. Both instrument can easily be coupled to floating chambers to measure continuously air-water gas exchange fluxes.

(2) The Picarro G2201-i Dual Carbon isotope analyser measures simultaneously the $\delta^{13}C$ signature of CO_2 and CH_4. Coupling the G2201-i to a showerhead equilibrator allows you to identify different CO_2 and CH_4 source contributions.

(3) Dissolved inorganic carbon (DIC) concentration and its isotopic signature are critical to study processes such as photosynthesis, respiration, calcification and the penetration of anthropogenic carbon into the surface ocean and its subsequent ocean acidification effect. We will present how coupling of a DIC extraction front end with the Picarro G2131-i allows to measure in a fast and cost-effective way the stable carbon isotope composition of DIC.

High-frequency productivity estimates for a lake from free-water CO_2 concentration measurements

M. Provenzale[1]*, A. Ojala[1,2,3], J. Heiskanen[4], K-M. Erkkilä[1], I. Mammarella[1], P. Hari[3] and T. Vesala[1,3]

[1] Institute for Atmospheric and Earth System Research/Physics, Faculty of Science, University of Helsinki, Helsinki, Finland
[2] Faculty of Biology and Environmental Sciences, University of Helsinki, Lahti, Finland
[3] Institute for Atmospheric and Earth System Research/Forest Sciences, Faculty of Agriculture and Forestry, University of Helsinki, Helsinki, Finland
[4] ICOS ERIC Head Office, Helsinki, Finland

**Corresponding author, e-mail: maria.provenzale@helsinki.fi*

KEYWORDS
Lakes; productivity; free-water approach; CO_2; PI curves.

Introduction

In freshwater ecology, productivity studies have traditionally relied on the dark and light bottle method and the ^{14}C labelling technique. Both these methods require sampling and incubation, conditions far from the natural ones, and thus may lead to unrealistic results. Moreover, they have a low temporal resolution that does not allow the non-linear relationship between photosynthetically active solar radiation (PAR) and net ecosystem productivity (NEP)
to be properly investigated. As a consequence, the NEP cannot be robustly parameterised as a function of ambient variables.

In the last 15 years, free-water approaches have become more common. They are, however, usually based on the measurement of the O_2 concentration in the water, which is then used as a proxy for CO_2. This introduces uncertainties: the respiratory quotient that has to be applied when transforming rates from O_2 to CO_2 has, in fact, large variations.

In 2008 Hari et al. proposed a free-water method based on the high-frequency measurement of CO_2 in the water. At that time, the method was tested on a short dataset of 3 days, and only validated qualitatively. Here, we used it to collect 40 days of data on a boreal lake in Finland.
We were able to calculate the NEP at a high-frequency, and quantitatively verify its dependence on PAR and T, with a very good agreement between model and data.

Materials and methods

The measuring method proposed in Hari et al. (2008) consists of non-dispersive infrared air CO_2 probes and an air-circulating system in which the air equilibrates with the water at the desired depth. By measuring the CO_2 concentration in the air in the system and using Henry's law, the concentration in the water is obtained. Our set-up was completed by an eddy-covariance system, and water PAR and T sensors for the parameterisation of NEP.

The other key feature of the method is calculating the NEP with an equation similar to those typically adopted in terrestrial ecology, where high-frequency measurements are more widespread. Using shared procedures is beneficial in the framework of integrating research in the different ecosystems that form the continuum through which carbon is cycled.

Thus, from the mass balance of CO_2 in the lake:

$$NEP = -\int_{-h_{mix}}^{0} \frac{\partial C(z,t)}{\partial t} dz - F_a + F_u,$$

where z is depth, t is time, h_{mix} the depth of the mixed layer, C the CO_2 concentration in the mixed layer, F_a the CO_2 flux from the lake to the atmosphere and F_u the CO_2 flux from the deeper to the mixed layer of the lake. Our analysis was limited to stratified conditions and hence $F_u = 0$.

For the dependence of NEP on PAR and T, we used the Michaelis-Menten equation:

$$NEP = \frac{p_{max}\,PAR}{PAR + b} - r_0 Q_{10}^{T/10},$$

where T is the water temperature, Q_{10} a known non-dimensional temperature coefficient; p_{max}, b and r_0 are parameters typical of the algal communities and represent the maximum potential photosynthetic rate, the half-saturation constant and the basal respiration, respectively.

Results and discussion

We were able to calculate the NEP at a temporal resolution of minutes, and we found a very good agreement between the Michaelis-Menten model and the data (see Fig. 1).

Overall, we believe that the method represents an improvement over the traditional approaches, given its time resolution. We also think that it is promising compared to the other more common free-water approach, the O_2 method, since it is direct. However, at the present stage it can be applied under a limited set of conditions (isothermal or stable stratification). Still, given the scarcity or even lack of high-frequency direct CO_2 measurements for productivity studies (we are aware of only one other study where free-water CO_2 measurements were used for metabolism studies; see Hanson et al., 2003), we feel our work is an important step towards testing and developing the method so that it becomes more general, and we are looking for further contributions by the research community.

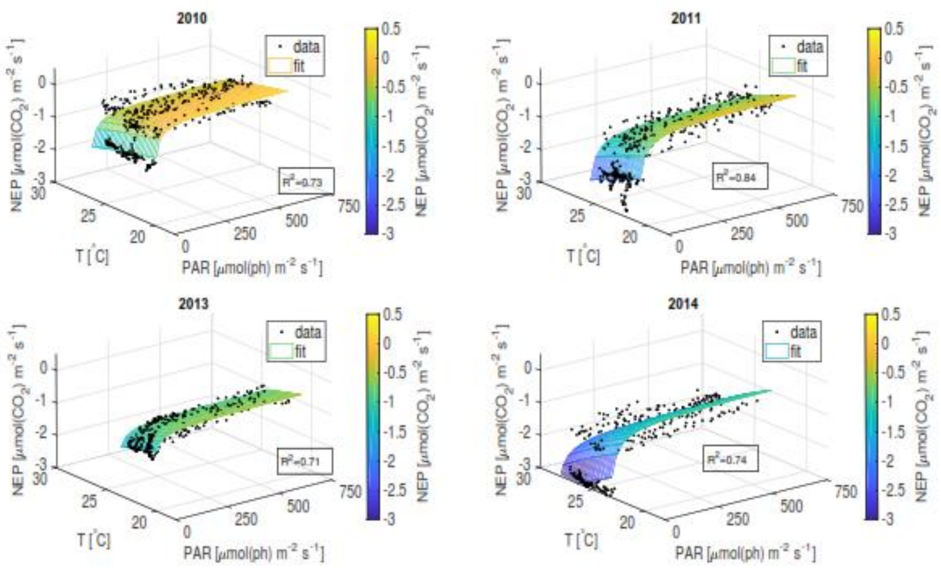

REFERENCES

Hanson, P., D. Bade, S. Carpenter, and T. Kratz (2003), Lake metabolism: Relationships with dissolved organic carbon and phosphorus, *Limnol. Oceanogr.*, *48*, 1112–1119.

Hari, P., J. Pumpanen, J. Huotari, P. Kolari, J. Grace, T. Vesala, T., and A. Ojala (2008), High frequency measurements of productivity of planktonic algae using rugged nondispersive infrared carbon dioxide probes, *Limnol. Oceanogr.-Meth.*, *6*, 347–354.

Methane bubbles under ice in Base Mine Lake

Edmund Tedford[1]*, Sarah Chang[1]*, Kai Zhao[1]*, Jason Olsthoorn[1]*, Roger Pieters[1,2]*, and Gregory Lawrence[1]

[1] *Civil Engineering,* University of British Columbia, Vancouver, Canada
[2] *Earth, Ocean and Atmospheric Sciences,* University of British Columbia, Vancouver, Canada

**Corresponding author, e-mail ttedford@eos.ubc.ca*

KEYWORDS
Reverse stratification; methane ebullition; ice; echosoundings; mine tailings.

Introduction

Base Mine Lake (7.9 km^2, depth ~10 m, 57^{o}1' N, 112 ^{o}31'W) is a pit lake in the oil sands region of northern Alberta, Canada. Within the underlying fluid fine tailings methane bubbles are generated that rise through the water cap throughout the year. Under winter ice cover, these bubbles get trapped within the forming ice. We look at how these bubbles from the bottom, affect the ice at the surface.

Results

1. Relatively minor depressions (< 0.5m) of the underlying fine tailings are correlated with conspicuous features in the ice in the weeks before ice off (Figure 1). The ice melt patterns repeated themselves over three years of available satellite imagery. The depressions are also correlated with higher ebullition of methane bubbles (Tedford et al 2015) which suggests that the ice is strongly affected by the bubbles.
2. Similar to the ice melt patterns in Figure 1, recovered ice is generally thicker in regions with less ebullition. We found that the concentration of bubbles in the ice is related to the rate of ice growth such that ice that formed early in the winter (rapid ice growth) has a lower concentration of bubbles than ice that formed late in the winter (slow ice growth). Ice formation predicted following Lepparanta, 2015 was compared with layers in the ice that have a high bubble concentration.
3. During the winter of 2017 low pressure events were associated with jumps in turbidity. A downward pointing echo sounder (Echologger EA400) was deployed under the ice during the winter of 2018 and recorded increased ebullition during similar low pressure events.
4. Bubbles in the lake ice are, in some cases, frozen at a fixed horizontal location indicating a persistent source in the underlying mud and that horizontal advection of bubbles rising through the water cap is limited (Figure 2).

REFERENCES

Leppäranta, Matti. (2015), Thermodynamics of Seasonal Lake Ice. Freezing of Lakes and the Evolution of their Ice Cover. Springer, Berlin Heidelberg.

Tedford, T., R. Pieters and G. Lawrence. 2015. Echo soundings in an end pit lake. Proceedings of the 22nd Canadian Hydrotechnical Conference Montreal, Quebec, April 29 – May 2, 2015. 2pp.

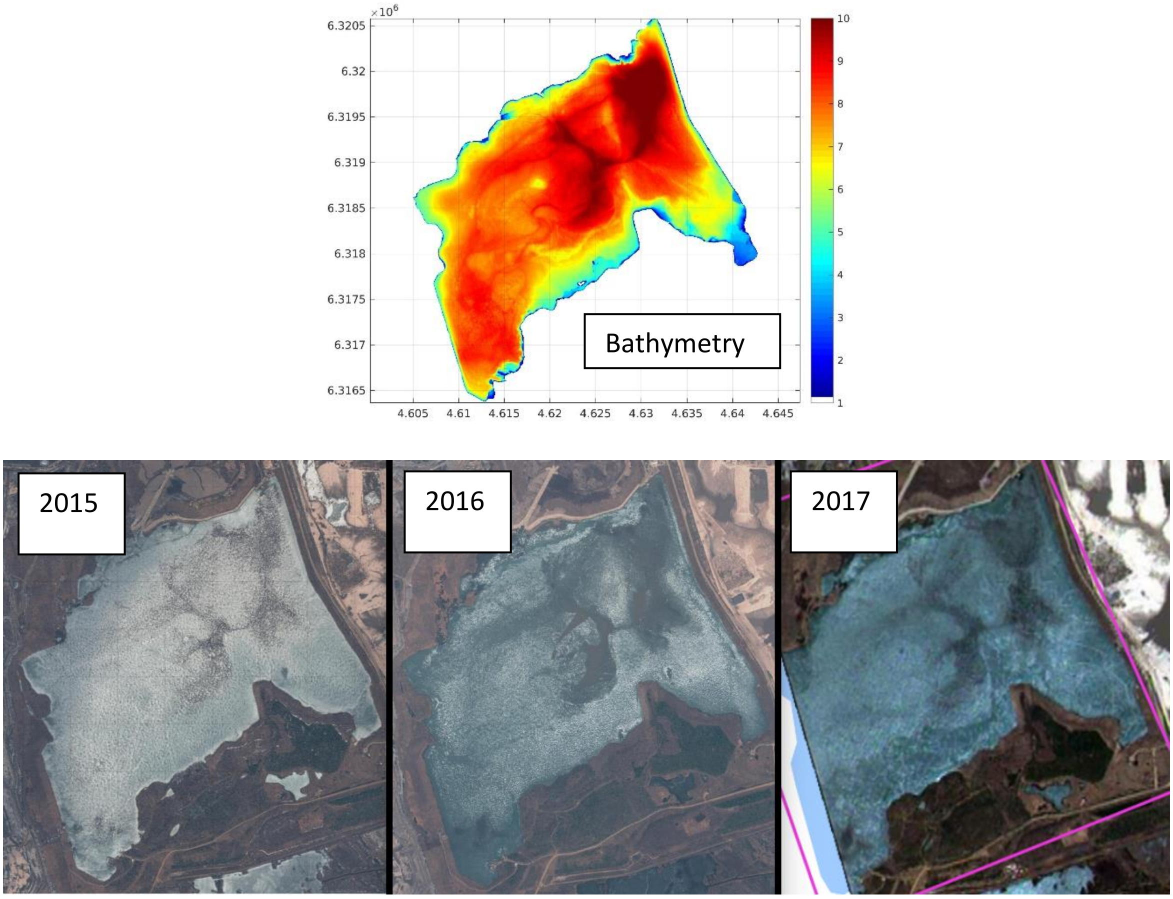

Figure 1. Bathymetry (top panel) and satellite imagery of Base Mine Lake during early April 2015, 2016 and 2017.

Figure 2. Photograph of a column of bubbles in Base Mine Lake ice. Note the scale is on the left is millimetres and that the ice grows downward at a rate of approximately 5mm a day.

The control of surface sediment gas accumulation on spatial distribution of ebullition in Lake Kinneret

L. Liu[1]*, Klajdi Sotiri[2], Yannik Dück[3], Stephan Hilgert[2], Ilia Ostrovsky[4], Ernst Uzhansky[5], Regina Katsman[5], Boris Katsnelson[5], Revital Bookman[5], Jeremy Wilkinson[1] and A. Lorke[1]

[1] *Institute for Environmental Sciences, University of Koblenz-Landau, Landau, Germany*
[2] *Institute for Water and River Basin Management, Karlsruhe Institute of Technology, Karlsruhe, Germany*
[3] *Cologne University of Applied Science, Institute of Hydraulic Engineering & Water Resources Management, Cologne, Germany*
[4] *Yigal Allon Kinneret Limnological Laboratory, Israel Oceanographic & Limnological Research, Migdal, Israel*
[5] *The Dr. Moses Strauss Department of Marine Geosciences, University of Haifa, Mount Carmel, Haifa, Israel*
**Corresponding author, e-mail: liu@uni-landau.de*

KEYWORDS
Anaerobic methane production, anaerobic methane oxidation, sulfate reduction, methane bubble, hydro-acoustic measurement, ebullition

Introduction

Ebullition in Lake Kinneret has been well characterized by hydro-acoustic measurements [Ostrovsky et al. 2008]. The seasonal/inter-annual variability of ebullition has been found well correlated to lake water level [Ostrovsky et al. 2013], suggesting the potential role of sediment gas storage. Recent process-based modelling demonstrated the significant contribution of ebullition to total methane (CH_4) emissions from the lake regardless of the great depth of Lake Kinneret [Schmid et al. 2017], which makes this lake ideal for testing our hypothesis. With two field campaigns, we mapped the spatial distribution of free gas accumulation in lake sediment; we quantified anaerobic sediment CH_4 production rate (MP); finally, we examined the link of ebullition to spatial distribution of sediment free gas.

Materials and methods

Hydro-acoustic measurements with varied frequencies were performed in early December 2016 (Fig. 1). Freeze cores were sampled from 3 sites for characterizing in situ sediment gas content. Four long sediment cores (> 1 m) (Fig. 1) were taken in late November 2017 for porewater dissolved CH_4 concentration and MP measurement (under 20 ^oC).

Results and discussion

Anaerobic methane oxidation (AMO) coupled to sulfate reduction was observed at the 30 cm depth of Lake Kinneret sediment (Fig. 2). A minimum of MP can be seen at the uppermost layer of sediment, which is significantly lower than predicted from power-law depth dependence of MP at lower depths that are unaffected by AMO. The sulfate concentrations are low (< 0.3 mM) but > 0.03 mM at certain depths, which allow sulfate reduction to outcompete MP when concentrations are above this threshold concentration. The role of AMO in CH_4 budget is significant: ~25-59% methane was oxidized in the upper layer of sediment in the surface 1 m sediment. The spatial distribution of ebullition is controlled by sediment gas content. Active ebullition was not observed at sites where sediment free gas accumulation did not occur (Fig. 3).

We quantified the role of AMO in methane budget, which has been previously under investigated in freshwaters. The net methane production (8.2-14.9 mol m^{-2} yr^{-1}) calculated by integrating the surface 1 m agrees well with previous estimates (10-15.4 mol m^{-2} yr^{-1}), which proves the effectiveness of estimating methane budget by measuring sediment MP.

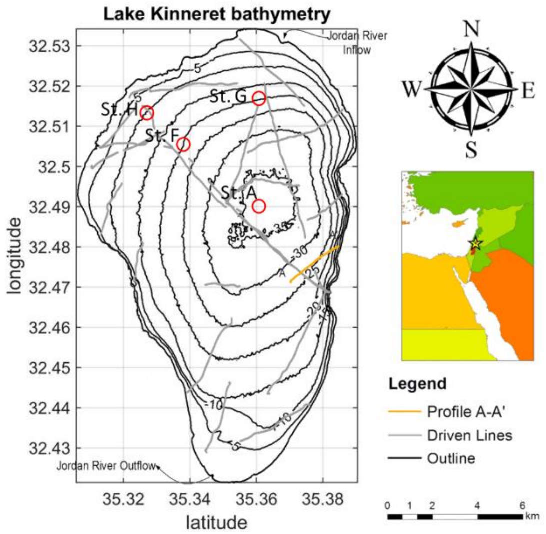

Fig. 1. Lake Kinneret bathymetry. The 4 sites where sediment cores were taken are marked by red circles. Freeze cores were taken from St. H, F and A, and gravity cores from the 4 sites. Gray and yellow lines show the trajectories of hydro-acoustic survey.

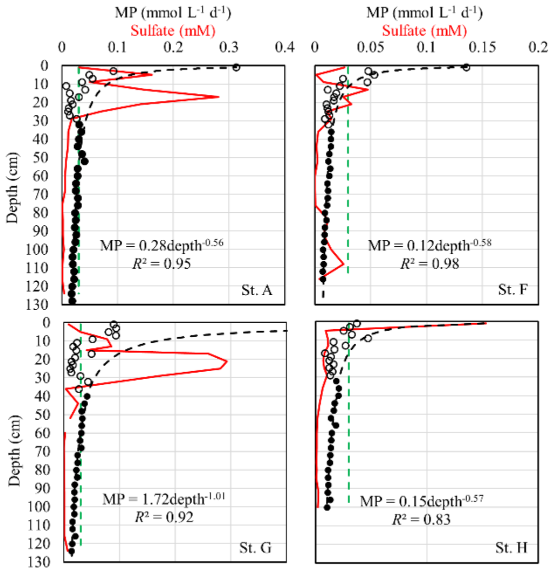

Fig. 2. Depth profiles of methane production (MP) and sulfate concentration in sediment porewater (red line). The equations of power-law depth distribution of MP are shown. The open circles represent MP affected by sulfate reduction and solid dots are unaffected.

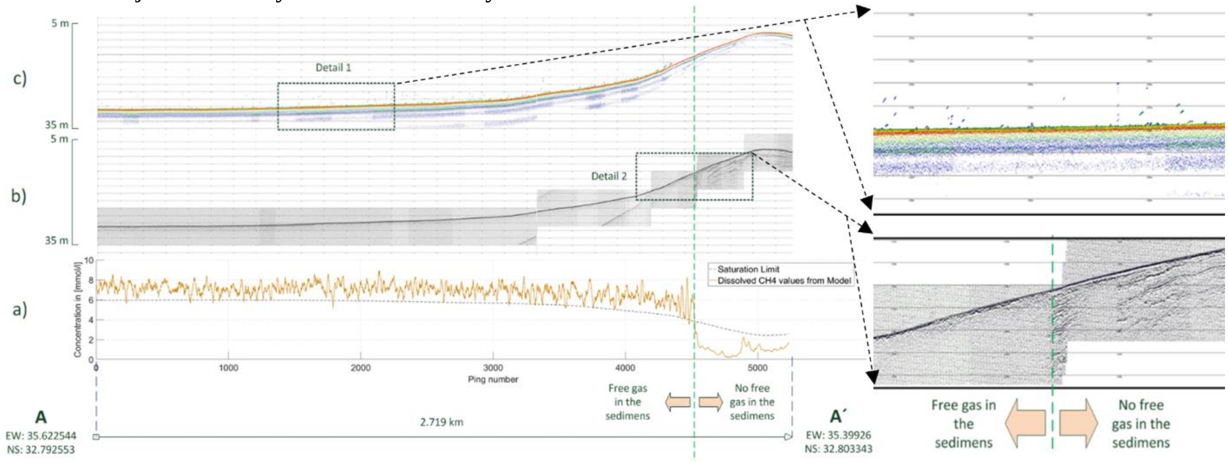

Fig. 3. Example of a selected transect "A-A´" of acoustic survey showing the transition of free gas accumulation to gas free zone. a) By applying inversion model for porewater dissolved CH_4 concentration, a Savitzky-Golay filter (first order polynomial function and window length 15) was applied to the results to smooth the data. b) The 10 kHz echogram shows a clear deep penetration in the gas-free zone, while the echo is blocked in the first meter of sediment in the gas-accumulated zone. c) Echogram of 100 kHz shows intense ebullition in the gas-accumulated zone, while the activity is minimal in the gas-free zone.

ACKNOWLEDGEMENTS

We would also like to thank Daniel McGinnis for providing access to Piccaro for $^{13}\delta C_{CH4}$ measurement and Wang Si for helping measure sediment CH_4 production. This study was financially supported by the German Research Foundation (grant LO 1150/5).

REFERENCES

Ostrovsky, I., D. F. McGinnis, L. Lapidus, and W. Eckert (2008), Quantifying gas ebullition with echosounder: the role of methane transport by bubbles in a medium-sized lake. *Limnol. Oceanogr.: Meth.* 6: 105-118.

Ostrovsky, I. et al. 2013, Long-term changes in the Lake Kinneret ecosystem: the effects of climate change and anthropogenic factors. Climatic change and global warming of inland waters: Impacts and mitigation for ecosystems and societies: 271-293.

Schmid, M., I. Ostrovsky, and D. F. McGinnis (2017), Role of gas ebullition in the methane budget of a deep subtropical lake: what can we learn from process-based modeling? *Limnol. Oceanogr.* 62: 2674-2698.

What the CH_4 bubble knows: CH_4 fluxes revealed by sediment bubble gas composition

T. Langenegger[*1], D. Vachon[1,2], D. Donis[1], D. F. McGinnis[*1]

[1] *Aquatic Physics Group, Department F.-A. Forel for Environmental and Aquatic Sciences (DEFSE), Faculty of Science, University of Geneva, Uni Carl Vogt, 66 boulevard Carl-Vogt, 1211 Geneva, Switzerland*
[2] *now at Department of Ecology and Environmental Sciences, Umeå Universitet, 901 87 Umeå, Sweden*

**Corresponding authors: timon.langenegger@unige.ch, daniel.mcginnis@unige.ch*

Keywords: greenhouse gases, methane ebullition, methane diffusion, methane production, sediment modelling

Atmospheric methane (CH_4) concentrations have more than doubled in the past ~200 years, though the sources of this potent greenhouse gas remain poorly constrained. Inland freshwaters contribute ~20% of natural CH_4 emissions, about half attributed to ebullition. As ebullition is a direct pathway for sediment CH_4 to the atmosphere, accurate measurements are crucial. Estimates remain uncertain since ebullition is stochastic, making measurements difficult, time-consuming and costly with current methods (e.g. floating chambers, funnel gas traps and hydro-acoustics). Fortunately, sediment CH_4 production, diffusion, and ebullition are interrelated not only by the sediment CH_4 balance (Production = Diffusive Transport + Ebullition) but also by the stripping of atmospheric gasses (e.g. N_2) out of the sediment via bubbles. Here, we present a novel approach to quantify basin-wide hypolimnetic CH_4 fluxes at the sediment level based on measurements of bubble gas composition and modelling of dissolved porewater gases. We show that the ebullition flux relative to production is resolved by knowledge of the bubble gas composition only. Further, the entire sediment CH_4 balance can be quantified if additional observations are available. Such additional information could be any of the depth of bubble formation in the sediments, sediment diffusive fluxes, ebullition, sediment production or the hypolimnetic CH_4 mass balance. The measurement of bubble gas content is particularly useful for identifying local ebullitive hotspots and integrating spatial heterogeneity of CH_4 fluxes. Our modeling results also revealed the crucial effect of water column depth, production rate profiles and overlying water dissolved CH_4 concentrations on sediment CH_4 dynamics. Applying our approach to lakes will certainly provide a deeper understanding of in-lake CH_4 budgets, and thus further help improving CH_4 emission estimates from inland freshwaters at the regional and global scales.

Oxygen ebullition from lakes

Bertram Boehrer, Isabell Hentschel, Matthias Koschorreck

Helmholtz Centre for Environmental Research - UFZ, Department Lake Research, Brückstrasse 3a, D-39114 Magdeburg, Germany

**Corresponding author, e-mail Bertram.Boehrer@ufz.de*

KEYWORDS
Lakes; environment; water quality; modelling; internal waves.

Introduction

Lakes can emit significant amounts of oxygen by emerging gas bubbles - a process called ebullition. This part is mostly neglected in numerical models and in consideration about the net flux of oxygen between lakes and atmosphere. We know of no previous quantification of the oxygen flux from a lake by ebullition. We found oxygen (maximum 34 %) in emerging gas bubbles in two shallow eutrophic reservoirs. In the studied reservoirs, O_2 emission by ebullition was of similar magnitude as diffusive oxygen fluxes. By re-analyzing previous studies we show that the process is ubiquitous and probably quantitatively relevant in many places. We present evidence that O_2 in bubbles originates both from photosynthetic oxygen production and hence bubble formation in the oxic water as well as from stripping by emerging methane bubbles. Ebullition can turn lakes under saturated in respect to the atmosphere into a net O_2 source. Neglecting O_2 ebullition has lead to an over estimation of lake internal respiration.

Materials and methods

Gas samplers were deployed in two small and shallow lakes called Wolfersgrün and Filzteich over period from early spring to autumn, and retrieved at intervals between 2 and 4 weeks. The samples were quantified to calculate gas flux and the content of oxygen, nitrogen (plus Argon) and carbon dioxide were quantified. We found oxygen concentrations between 2 and 34 %.

Results and discussion

We expect two different origins for the gas bubbles: firstly, gas bubbles that originate from methane production in the sediment during decomposition of organic material: these bubbles start with a mix of methane and nitrogen (and possibly traces of carbon dioxide) from the sediment and acquire oxygen by stripping while they pearl through an oxic water column; secondly bubbles can form at the surface of photosynthetically active plants. They start with a composition of nitrogen and oxygen, and are exposed to exchange with the surrounding water while they ascend through the water column. The bubbles should tremendously differ in their oxygen content (see Fig.1)

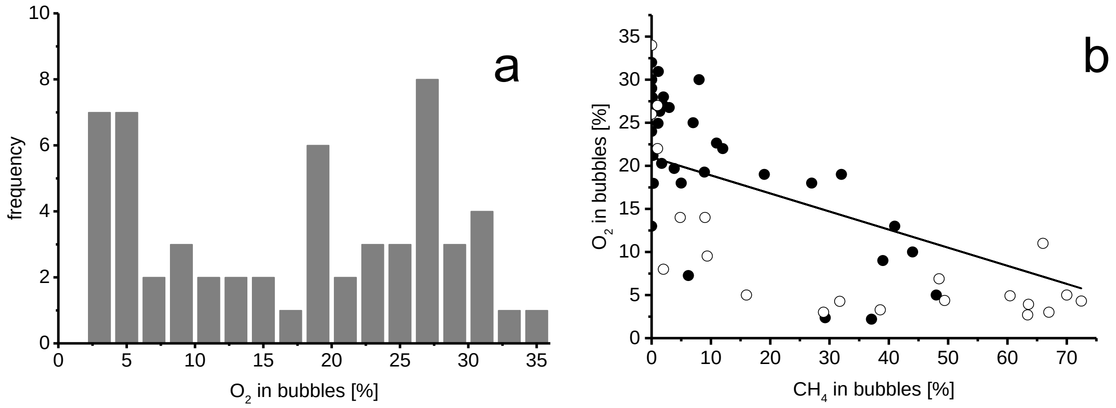

Figure 1. *Histogram of bubble O2 concentration (a), and O_2/CH_4 ratio in the bubbles in Wolfersgrün reservoir (closed circles) and Filzteich (open circles) (b). The line in (b) indicates the O_2 content under the assumption that the bubbles are composed of CH_4 and atmospheric air (from Koschorreck et al., 2017).*

We measured O2 ebullition fluxes between 0 and 5.4 mmol m-2 d-1. O_2 ebullition followed a seasonal trend with higher fluxes during summer. These numbers compared with O_2 ebullition fluxes, which we calculated from existing literature data, which ranged from 0 to 20 mmol m-2 d-1 (Table 1). To quantify the importance of the process, we compared ebullition fluxes with typical O_2 diffusion rates. O_2 diffusion was calculated for different O2 surface concentration and gas transfer velocities (Figure 4). Possible realistic diffusive fluxes ranged from -90 to 90 mmol m-2 d-1.

In conclusion, the oxygen flux by ebullition reaches the same order of magnitude of the net flux by diffusion. Hence, neglecting the ebullition flux biases the trophy of a lake considerably towards heterotrophy; the carbon dioxide flux from a lake ma yhave overestimated or the carbon fixation underestimated, respectively. Including oxygen flux by ebullition may change a lake previously considered heterotroph even to autotroph with the potential of even changing the global balance significantly.

REFERENCES

Koschorreck, M., Hentschel, I., & Boehrer, B. (2017). Oxygen ebullition from lakes. Geophysical Research Letters, 44. https://doi.org/10.1002/2017GL074591

Keynote Speaker

Dr. Ali Mashayek

Department of Civil and Environmental Engineering

Imperial College London

Email: mashayek@imperial.ac.uk
Website: https://www.mashayek.com/

Ali is a faculty member in Civil and Environmental Engineering at Imperial College London. His research is focused on studying (I) ocean turbulence processes, (II) their role within the larger context of ocean circulation and (III) the role of general circulation in regulating the global heat and tracer budgets, thereby the climate system. His work brings observations and theory together with the help of numerical models of varying complexity. Prior to Imperial College, Ali spent time at the University of Oxford, Scripps Institution of Oceanography and MIT. He received his PhD in Ocean physics from the University of Toronto.

Turbulence induced by overturning breaking waves: from small scale mixing to large scale overturning circulation

Ali Mashayek

Department of Civil and Environmental Engineering, Imperial College, London, UK

**Corresponding author, e-mail ali.mashayek@gmail.com*

ABSTRACT

Turbulent mixing in the deep ocean, where stratification is relatively weak and shear is strong in vicinity of rough topographic features, is facilitated by continuous formation and breaking of large overturns which can arise in different forms such as shear instabilities or convectively breaking internal waves, among others. I will connect the fluid dynamical basis of such breaking events to their corresponding mixing rates as diagnosed from models or inferred from observations. I will highlight the significant contribution to mixing of the phase of turbulence in which large scale overturns and small scale isotropic turbulence coexist. Such phase is often systematically ignored in parameterization schemes used to infer mixing from observations and is frequently left out of analysis of direct numerical simulations in favor of better agreement with assumptions made in the aforementioned parameterization schemes: this poses a circular problem. I will review inaccuracies that such assumptions and systematic biases introduce in estimates of mixing. I will finish by putting most recent findings into a big-picture perspective by showing that such errors are leading order insofar as the diagnosis of the rate of overturning of the mixing-induced deep branch of global meridional overturning circulation is concerned.

Turbulence and restratification from glider measurements

Arthur V. S. Rodrigues[1]*, Jeff Carpenter[1], Lucas Merckelbach[1]
[1] *HZG, Helmholtz-Zentrum Geesthacht, Geesthacht, Germany.*

**Corresponding author, e-mail arthursecato@posteo.de*

KEYWORDS
ocean turbulence; mixed layer; Baltic Sea; ocean gliders; mixing.

INTRODUCTION

The oceanic surface mixed layer (SML) is a layer of essentially turbulent nature in which different mixing processes occur. The SML plays a decisive role in the energy exchange between atmosphere and deep ocean. Understanding how energy is absorbed, transported and dissipated in the SML is an important task towards improved vertical budgets modelling (Ivey et al, 2008). However the mixing energetics in a stratified environment is very different from its homogeneous counterpart. Other parameters which account for the intensity of the stratification are needed. Likewise, horizontal gradients in the SML are also believed to have an important influence in its energetics. These gradients act as reservoirs of both kinetic and potential energy which might be released when submesoscales instabilities occur.

This work aims to investigate the stratified ocean dynamic response to atmospheric forcing during a storm with the data collected by an autonomous underwater glider, focusing particularly on the interplay between turbulent dissipation, stratification and shear in the SML and at its base.

MATERIALS AND METHODS

The Baltic Sea is considered to be a good „natural laboratory“ for studying the energetic processes in the SML, since it is a large and semi-closed estuary with permanent deep-water stratification and virtually no tidal currents. For this purpose an autonomous underwater ocean glider (Teledyne Webb Research Slocum Electric) was deployed in the Gotland Basin mid-autumn 2017 during the cruise EMB169. Equipped with a CTD, an acoustic doppler current profiler (ADCP) and turbulent microstructure sensors, the glider successfully collected data over ten days, during which a storm happened.

Turbulent dissipation rate ϵ[W/kg] is calculated using the microstructure measurements. The ADCP velocities are subjected to different quality control routines before horizontal shear squared (S^2[1/s^2]) is computed.

RESULTS AND DISCUSSION

Combining classical CTD based thermophysical seawater properties with turbulent dissipation and current measurements from the same scientific platform, this campaign provided a unique dataset to observe the behaviour of the upper ocean during storm conditions.

Figure 1 shows an overview of the results. In a top to bottom order, the first plot gives the wind magnitude and direction (black arrows) and its induced surface stress (red dashed line). The data was taken from a ICON (Icosahedral Nonhydrostatic Model) reanalysis of the German Forecast Service (Deutscher Wetterdienst). Wind surface stress was calculated with the parametrization presented by Yelland and Taylor, (1996). The onset of an autumn storm can be seen with winds up to 20 m/s at its peak. Potential density is subtracted by 10^3 kg/m^3 and is shown in the second plot. A cut of maximum potential density at 6 kg/m^3 was done in order to get more visual resolution of the features in the SML. Third plot gives the horizontal shear squared $S^2[1/s^2]$ scaled by a factor 10^3, while the fourth the turbulence dissipation ϵ[W/kg].

First thing to notice is the strong heaving of the pycnocline as consequence of the storm event. It is pushed down more than 20 meters during the strong winds and it is pressed against the deeper halocline and topography before relaxing back as the storms weakens. It can be noticed an increase of the turbulent intensity within the pycnocline during the storm,

It is important to notice how the horizontal density gradients in the SML determine the distribution of turbulent dissipation. Even small gradients have a considerably damping effect on turbulent transport. Particularly at the end of the storm, where we believe that a restratification is occurring due to a submesoscale instability, releasing some of the potential energy seen in the potential density plot. Density gradients seem to dominate the dynamics. Small horizontal gradients in the SML can act as absorbers of the turbulent energy that entrains from the surface. Even at the peak of the storm, with high energy transfer rates between ocean and atmosphere, the strong vertical stratification in the pycnocline was able to hinder turbulence entrainment (mixing) into the deep ocean.

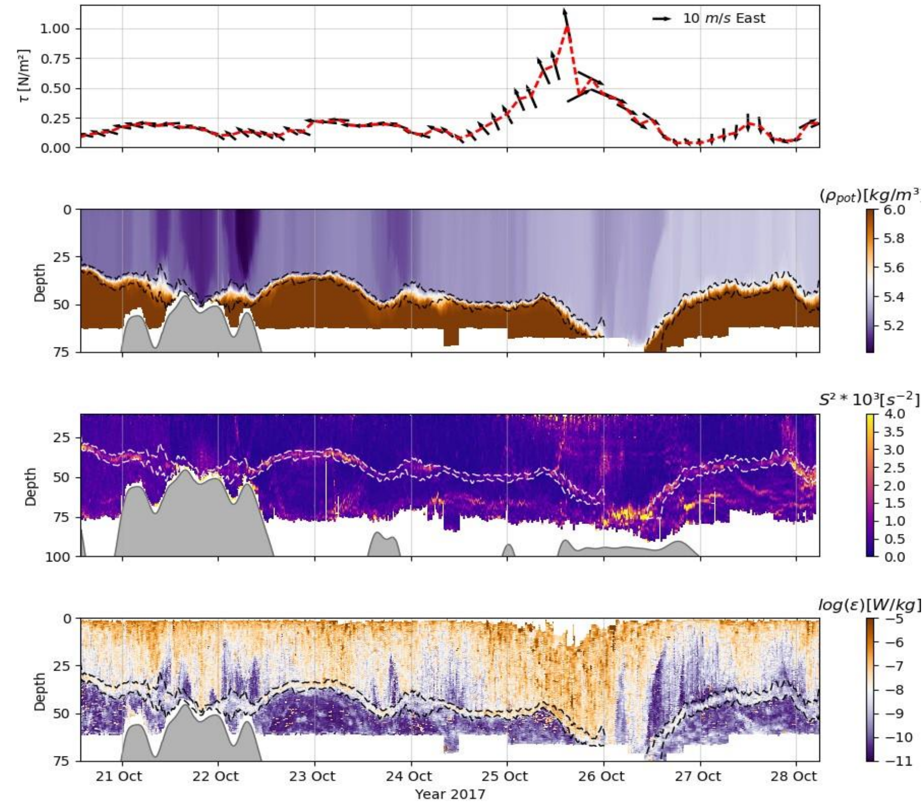

Figure 1: top to bottom: a) Surface stress (red) , magnitude and direction (black arrows) of wind taken from DWD ICON reanalysis. b) Potential density beyond 1000 kg/m³ with maximum cut on 6 kg/m³. c) Horizontal shear squared computed with the ADCP measurements. d) Turbulent dissipation. Bathymetry of the seabed is indicated in gray and the position of the pycnocline in dashed lines.

REFERENCES

Ivey, G., K. Winters, and J. Koseff (2008): *Density Stratification, Turbulence, but How Much Mixing?* Annual Review of Fluid Mechanics, 40, 169–184.

Yelland, Margaret & K. Taylor, Peter. (1996). *Wind Stress Measurements from the Open Ocean*. Journal of Physical Oceanography - Journal of Physical Oceanography 26. 541-558

Seasonality of internal wave action in a large alpine lake

J.B.T. McInerney[1,2]*, A.L. Forrest[1,2], S.G. Schladow[1,2]

[1] *Civil & Environmental Engineering, University of California – Davis, Davis, CA, USA*
[2] *Tahoe Environmental Research Center (UCDavis), Incline Village, NV, USA*

**Corresponding author, e-mail jmcinerney@ucdavis.edu*

KEYWORDS
Large Lakes; internal waves; seasonality; autonomous underwater glider.

INTRODUCTION

Internal waves in large lakes (e.g. Lake Tahoe, USA) have the potential to drive significant vertical mixing as they propagate along the metalimnion after surface wind forcing. Water- sediment interactions from turbulence generated by internal waves at boundaries at the depths of the thermocline can be responsible for driving gas and nutrient flux into the water column (Lemckert & Imberger, 1998). Study of how internal wave fields in large lakes vary throughout the year can inform our understanding of seasonal variation in other lake processes. Internal waves shoaling around the perimeter of the lake (including Kelvin waves) and waves decaying via Kelvin-Helmholtz billowing in the pelagic region contribute to turbulent mixing equally . As a result, both the nearshore and pelagic regions of a deep lake must be included to fully characterize internal wave fields.

MATERIALS AND METHODS

Lake Tahoe (USA) is a large sub-alpine lake with a summer thermocline depth of around 20 m. Lake Tahoe's thermocline deepens in Fall to a maximum depth of 50 m and may result in complete mixing over the full depth (500 m) by the end of winter (end of March), before the onset of stratification in Spring. While mixing to depth still potentially happens, it is becoming increasingly common for partial mixing in the range of 100 – 300 m to occur. As a result of these constraints, in each season from Summer 2017 until Winter 2017/18 a thermistor chain (measuring at 0.001 ºC accuracy, at ~10 m depth intervals) and a 600 kHz downwards facing Acoustic Doppler Current Profiler (ADCP) were moored at the 80 m isobath. The selected location was approximately midway along the west side of the lake, 350 m offshore.

Observations collected with the mooring were then linked to the pelagic region using a G2 Slocum Glider (buoyancy driven autonomous underwater vehicle), equipped with a Sea-Bird CTD. It was programmed to run repeated east-west 15 km transects across the lake, cutting a sawtooth pattern through the water column by diving to 150 m at an angle of ~26°, travelling at ~0.3 m/s. The chosen path allowed the glider to intersect Kelvin waves traveling around the lake in a cyclonic direction and Poincaré waves rotating in the reverse sense.

RESULTS AND DISCUSSION

Temperature collected by the glider and thermistor chain were used to determine integrated potential energy (IPE) of the water column to 75 m (the extent of the thermistor chain) as a time series which were analyzed spectrally. For this analysis, glider data was binned in depth (2 m bins) and time (30 min ~ one dive and surface). The spectrum from each season from the mooring (Fig. 1a-c) and from the glider (Fig. 1d-e) were compared to determine whether the glider was sampling the full range of internal wave activity in the lake.

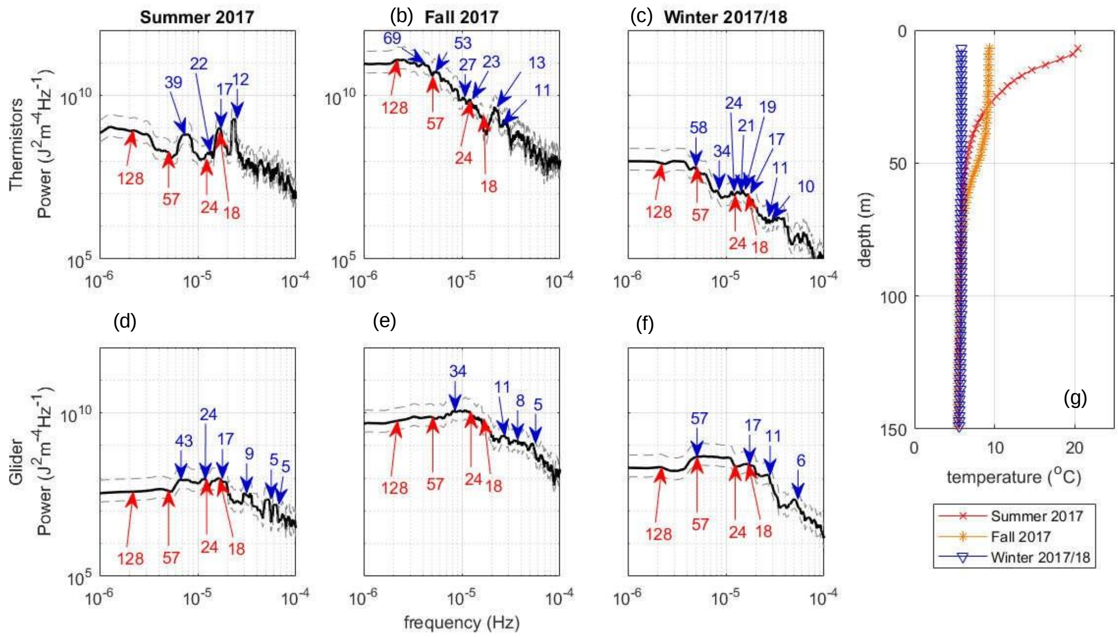

Fig. 1: IPE Power density spectrum. (a) – (c): from data collected by glider; (d) – (f): from data collected from mooring. Periods are indicated with arrows – blue arrows indicate spectral peaks from this data, while red arrows indicate internal wave periods identified by from Lake Tahoe thermistor chain observations in Winter 1999-2000 (thermocline ~75 m). (g) mean temperature profiles from glider data.

Larger amplitude internal waves, driving higher velocities (> 25 cm/s), occurred during Fall when the thermocline was deep with stronger stratification. No Kelvin waves were identified during winter, when the lake was unstratified over the water column sampled by the glider. Completing each transect in ~15 hrs, the glider was better able to resolve the faster moving Kelvin wave (H3V1, ~40 hr period) and Poincaré wave (H1V1, ~17 hr period). There is inherent aliasing of using a mobile platform to sample an internal wave field, but it is possible that alternate mission parameters (e.g. longer missions and/or spending more time closer to the shore) may be able eliminate this aliasing and/or better resolve longer period Kelvin waves not captured in this study.

CONCLUSIONS

Comparing seasonal spectra allows us to identify seasonal variation in the wave field, and mixing in large, deep lakes. Mode 1 Kelvin waves propagated around the lake during periods of strongest stratification. Conversely, a larger metalimnion can accommodate larger amplitude internal waves of other modes, which have higher associated velocities. This is reflected by higher energy peaks in the IPE spectra occurring during summer.

REFERENCES

Lemckert, C., & Imberger, J. (1998). Turbulent Benthic Boundary Layer Mixing Events in Freshwater Lakes. In J. Imberger (Ed.), *Coastal and Estuarine Studies: Physical Processes in Lakes and Oceans*. Washington, D.C.: American Geophysical Union

Preusse, M., Peeters, F., & Lorke, A. (2010). Internal waves and the generation of turbulence in the thermocline of a large lake. *Limnology and oceanography*, *55*(6), 2353-2365.

Rueda, F. J., Schladow, S. G., & Pálmarsson, S. Ó. (2003). Basin-scale internal wave dynamics during a winter cooling period in a large lake. *Journal of Geophysical Research: Oceans*, *108*(C3).

Experiments on shoaling Mode-2 internal solitary-like waves

Peter A Davies[1]*, Magda Carr[2,5], Marek Stastna[3] and Koen van de Wal[4]

[1] *Department of Civil Engineering, The University, Dundee DD1 4HN, UK*
[2] *School of Mathematics & Statistics, University of St Andrews, St Andrews KY16 9SS, UK*
[3] *Department of Applied Mathematics, University of Waterloo, 200 University Avenue West, Waterloo, Ontario, N2L 3G1, Canada*
[4]*Department of Applied Physics, Technical University of Eindhoven, 5600 MB Eindhoven, NL*
[5]*School of Mathematics, University of Newcastle upon Tyne, Newcastle upon Tyne NE1 7RU, UK (from 1 June 2018)*

**Corresponding author, e-mail p.a.davies@dundee.ac.uk*

KEYWORDS
Modelling; internal waves; solitary waves, shoaling

Introduction

Shoaling internal solitary waves (ISWs) constitute an important agency for boundary mixing in stably-stratified lakes, reservoirs and shallow seas (*e.g* Horn *et al*, 2001; Boegman *et al* 2005). Most of the ISW energy for density profiles typical of these conditions is carried by Mode-1 waves but Mode-2 waves have also been observed widely (*e.g* Shroyer *et al*., 2010; Yang *et al*, 2010) in recent years. Significant progress has been made (*e.g* Salloum *et al*., 2012; Brandt & Shipley, 2014; Carr *et al*., 2015) in modelling the detailed evolution of such waves as they propagate on density interfaces. The present study is concerned with the shoaling of packets of Mode-2 ISWs on sloping boundaries. Results are presented from a combined parametric laboratory and numerical modelling investigation.

Materials and methods

Experiments were conducted in a long rectangular tank (Fig 1) containing a stably-stratified system consisting of two homogeneous layers of miscible fluids of thickness h_1, h_3 ($h_1 = h_3$) and densities ρ_1 and ρ_3 ($\rho_1 < \rho_3$) respectively, separated by a thin diffusive layer of thickness h_2 ($< h_{1,3}$) and density $\rho(z)$. Packets of Mode-2 ISWs of prescribed leading amplitude a and phase speed c were generated by the lock release of a fixed volume of fluid of density ρ_2 ($= (\rho_3 + \rho_1)/2$). The flow was seeded with neutrally buoyant tracer particles, illuminated from below and recorded by 3 fixed digital video cameras set up outside the tank. Numerical simulations of the experimental flows for $a/H \sim 0.1$, $\theta \in [1.9°, 21.8°]$, $s = H_s/1.5 \in [0.03, 0.40]$ were performed using a pseudo-spectral incompressible Navier–Stokes solver (see, for example, Olsthoorn *et al*., 2013).

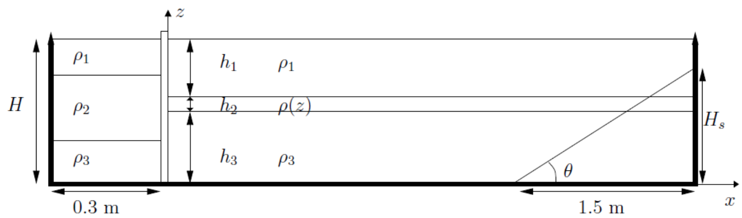

Fig 1: Schematic view (side) of experimental arrangement

Results and discussion

The degree of shoaling modification to the wave properties depends primarily upon slope angle (θ, s) and the ratio a/h. For small values of s and a/h, shoaling results in localised overturning and mixing while for higher values of these parameters the structure of the wave is modified significantly, resulting in extensive run-up of the upper part of the wave and the generation of vortex pairs in the arrested lower part (Fig 2). Excellent qualitative agreement between the laboratory experiments and numerical simulations is found.

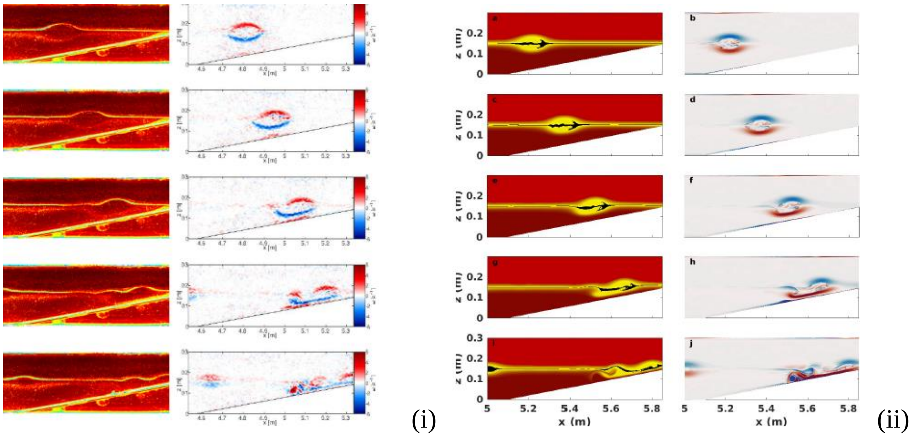

Fig 2. Density interfaces (left column) and vorticity fields (right) for shoaling Mode-2 ISWs (s = 0.20, a/H = 0.11) for (i) lab experiments, (ii) numerical simulation.

For cases of run up, scaling arguments predict the run up length $L \sim ac^2/(g'h_2 \sin\theta)$ where $g' = g(\rho_3 - \rho_1)/\rho_3$. Measurements are seen (Fig 3) to support this scaling.

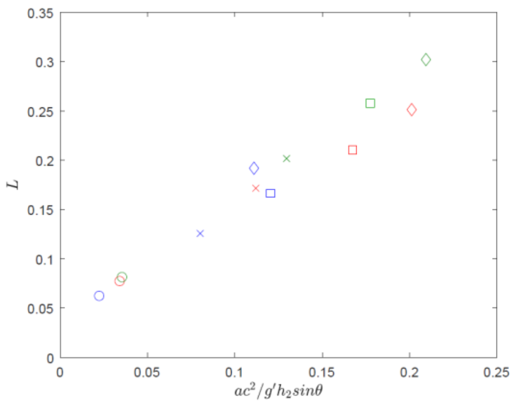

Fig 3: Composite plot of L versus scaling parameter $ac^2/(g'h_2 \sin\theta)$ for $s = \infty$ (○), 0.40 (x), 0.27 (□), 0.20 (◊)

REFERENCES

Boegman, L., J. Imberger, G.N. Ivey & J.P.Antenucci (2003), High-frequency internal waves in large stratified lakes, *Limnol. Oceanogr.*, *48*(2), 895-919.

Brandt, A., & K.R. Shipley (2014), Laboratory experiments on mass transport by large amplitude mode-2 internal solitary waves, *Phys. Fluids*, *26*, 046601

Carr, M., P.A. Davies & R.P. Hoebers (2015), Experiments on the structure and stability of mode-2 internal solitary-like waves propagating on an offset pycnocline, *Phys. Fluids*, *27*, 046602

Horn, D.A., J. Imberger & G.N. Ivey (2001), The degeneration of large-scale interfacial gravity waves in lakes, *J. Fluid Mech*., *434*, 181-207.

Salloum. M., O.M.Knio & A. Brandt (2012), Numerical simulation of mass transport in internal solitary waves, *Phys. Fluids*, *24*, 016602.

Shroyer, E.L., J.N. Moum & J.D. Nash (2010), Mode 2 waves on the continental shelf: Ephemeral components of the nonlinear internal wavefield, *J. Geophys. Res* (*Oceans*), *115*, C07001.

Yang, Y.J., Y.C. Fang, T.Y. Tang & S.R. Ramp (2010), Convex and concave types of second baroclinic mode internal solitary waves, *Nonlin. Processes Geophys*., *17*, 605–614.

Mechanical energy budget and mixing efficiency in an ice-covered and radiatively-forced freshwater basin

Hugo N. Ulloa[1]*, Alfred Wüest[1,2] and Damien Bouffard[2]

[1] *Physics of Aquatic Systems Laboratory (APHYS) – Margaretha Kamprad Chair*
École Polytechnique Fédéral de Lausanne, Switzerland.
[2]*Eawag, Swiss Federal Institute of Aquatic Science and Technology*
Surface Waters – Research and Management, Kastanienbaum, Switzerland

**Corresponding author, e-mail hugo.ulloa@epfl.ch*

KEYWORDS
Ice-covered lakes; radiatively-driven convection; mechanical energy; mixing efficiency

Introduction

In ice-covered enclosed waterbodies, the primary source of energy is supplied by the fraction of solar radiation able to penetrate across the ice and reaches waters usually found below the temperature of maximum density (Kirilling et al. 2012). In this scenario, the radiative buoyancy flux, Φ_r, works directly through the fluid, forcing increments of temperature/density in the upper fluid volume, which can become gravitationally unstable and so drive convection.

In this work, we formulate a mechanical energy budget and the mixing efficiency in a hypothetical ice-covered freshwater basin periodically forced by solar radiation, assuming an adiabatic bottom boundary condition. In particular, we examine the conversion of radiative to potential energy and its role in the available potential energy, E_a (Winters et al. 1995), the primary engine of under-ice water circulation.

Results and discussion

We found that the rate of change of E_a, in our hypothetical system, results from the competition between irreversible mixing, $\Phi_d - \Phi_i$, and Φ_r, and its remaining flux is converted to kinetic energy, E_k, via the buoyancy flux, Φ_z, which in turns is transformed into internal energy at a rate ϵ (Ulloa, Wüest & Bouffard 2018). Based on the mechanical energy budget and the general definition of mixing efficiency, η_m, `the ratio between the change in background potential energy due to mixing and the energy expended', we introduce $\eta = (\Phi_d - \Phi_i)/\Phi_r$ as the metric to quantify the mixing. The above ratio is equivalent to its classical definition $\eta = (\Phi_d - \Phi_i)/(\Phi_d - \Phi_i + \epsilon)$ (Peltier & Caulfield 2003, Gregg et al. 2018) when the available mechanical energy, $\dot{E}_{AM} = \dot{E}_k + \dot{E}_a$ (Tailleux 2009), is found in a statistically steady regime during the active radiative phase (daytime), $\dot{E}_{AM} = 0$. However, the unsteadiness of Φ_r might prevent reaching the above equlibrium, meaning a more robust definition for mixing efficiency is required (Ulloa, Wüest & Bouffard 2018). We sort out this problem by adopting the `cumulative mixing efficiency' in our framework (Peltier & Caulfield 2003). We introduce the integral mixing efficiency over the relevant timescale, T, $\eta^c \equiv \Delta E_{b,T}/E_{R,T}$, where $\Delta E_{b,T}$ and $E_{R,T}$ are the change of background potential energy and the time-integrated radiative energy flux, respectively, over a period T (Ulloa, Wüest & Bouffard 2018). This framework is applied to estimate for the first time the mixing efficiency in an ice-covered lake, finding an integral value of $\eta^c \approx 0.65$ (Ulloa, Wüest & Bouffard 2018).

Despite the similarities among the radiatively-driven convection (RDC) in ice-covered lakes and the classical Rayleigh-Benárd (RBC, $\eta^c = 1/2$) and Rayleigh-Taylor (RTC, $\eta^c = 3/4$) convective frameworks (Hughes, Gayen & Griffiths 2013, Davies-Wykes & Dalziel

2014), the magnitude of η^c, the forcing mechanism, and the signature of temperature/density profiles shown in different in-situ observations (e.g., Kirillin & Terhevik 2011, Bouffard et al. 2016, Bouffard et al. 2018), suggest that RDC might be controlled by Rayleigh-Taylor like convection.

REFERENCES

Bouffard, Damien, Zdorovennov, Roman E., Zdorovennova, Galina E., Pasche, Natacha, Wüest, Alfred & Terzhevik, Arkady Y. (2016) Ice-covered lake Onega: effects of radiation on convection and internal waves. *Hydrobiologia 780 (1), 21-36.*

Bouffard, Damien, Zdorovennova, Galina, Bogdanov, Sergey, Efremova, Tatyana, Lavanchy, Sébastien, Palshin, Nikolay, Terzhevik, Arkady, Vinnå, Love Råman, Volkov, Sergey, Wüest, Alfred, Zdorovennov, Roman & Ulloa, Hugo N. (2018) How to quantify under-ice convection dynamics in lakes. Implication for life under the ice. Inland Waters (Under revision).

Davies-Wykes, Megan & Dalziel, Stuart B. (2014) Efficient mixing in stratified flows: experimental study of a Rayleigh-Taylor unstable interface within an otherwise stable stratification. *J. Fluid Mech. 756, 1027-1057.*

Gregg, M. C., D'Asaro, E. A., Riley, J. J. & Kunze E. (2018) Mixing efficiency in the ocean. *Annu. Rev. Mar. Sci. 10 (1), 443-473*.

Hughes, Graham O., Gayen, Bishakhdatta & Griffiths, Ross W. (2013) Available potential energy in Rayleigh-Bénard convection. *J. Fluid Mech. 729*.

Kirillin, Georgiy, Leppranta, Matti, Terzhevik, Arkady, Granin, Nikolai, Sergey, Palshin, Nikolai, Sherstyankin, Pavel, Zdorovennova, Galina & Zdorovennov, Roman (2012) Physics of seasonally ice-covered lakes: a review. Aquat. Sci. 74(4), 659-682.

Peltier, W. R. & Caulfield, C. P. (2003) Mixing Efficiency in Stratified Shear Flows. *Annu. Rev. Fluid Mech. 35(1), 135-167.*

Tailleux, Rémi (2009) On the energetics of stratified turbulent mixing, irreversible thermodynamics, Boussinesq models and the ocean heat engine controversy. *J. Fluid Mech. 638, 339-383*.

Ulloa, Hugo N., Wüest, Alfred & Bouffard, Damien (2018) Mechanical energy budget and mixing efficiency for a radiatively heated ice-covered waterbody. (*Under submission to J. Fluid Mech.*).

Winters, Kraig B., Lombard, Peter N., Riley, James J. & D'Asaro, Eric A. (1995) Available potential energy and mixing in density-stratified fluids. *J. Fluid Mech. 289, 115-128.*

Extraordinary mixing conditions in ice-covered lakes of Tibetan Plateau

G. Kirillin[1]*, L. Wen[2], T. Shatwell[1]

[1] *Leibniz-Institute of Freshwater Ecology and Inland Fisheries (IGB), Berlin, Germany*
[2] *Key Laboratory of Land Surface Process and Climate Change in Cold and Arid Regions, NIEER, Chinese Academy of Sciences, Lanzhou 73000, China*

**Corresponding author, e-mail kirillin@igb-berlin.de*

KEYWORDS
Winter limnology, lake ice; convection; alpine lakes; Tibet; heat flux.

Introduction

The Tibetan Plateau is covered by thousands of lakes, which play a crucial role in the hydrological regime and climate interactions within the Asian monsoon system. However, the thermal regime of the Tibetan lakes remains largely unknown to date making difficult estimation of their contribution into the regional-scale energy and mass exchange between land and the atmosphere. The lakes are covered by ice during 4-5 months of the year. We present first information on the heat storage by the Tibetan lakes during the ice season.

Materials and methods

Ngoring (Big Blue Lake) is the large freshwater lake of the eastern Tibetan Plateau located at 34.5-35.5°N and 97-98°E, at an altitude of ~4300 m a. s. l., which counts it among the world's highest freshwater lakes. Ngoring Lake has a surface area of 610 km^2.,the mean and maximum depths of 17 and 32 m, respectively. The lake is ice-covered from early December to mid-April. A chain with 18 RBR T-Solo temperature loggers (declared accuracy 0.002°C) was moored in Ngoring Lake on 25 September 2015 at a site with depth of 26 m. The uppermost logger resided at 0.7 m beneath the water surface. Water temperatures were sampled at 0.1Hz throughout the entire ice-covered period.

Results and discussion

Surface cooling and ice formation: The date of ice cover formation was identified from water temperature data as 12 Dec 2015 ± 1 day. The lake became ice-free at 18 Apr 2016. The total ice-cover duration amounted at 126 days. At the moment of ice formation the entire water column cooled down to < 1 °C that can be attributed to strong winds over Tibet, which destroyed the near-surface stratification and prevented ice formation, so that the cooling of the lake surface from TMD to the freezing point took about 3 weeks.

Convection by solar radiation at temperatures below the TMD ("Normal winter"): The high amount of solar radiation at the surface and the low snow amount ensured strong radiative heating of the water column under ice immediately after ice cover formation. Because of the weak stratification at the moment of ice formation, a thermally-homogeneous convective layer driven by under-ice solar radiation quickly developed in the upper 15 meters of the water column. As a result, free convection had mixed the entire 25 m deep water column already in mid-February, 2 months after ice-on.

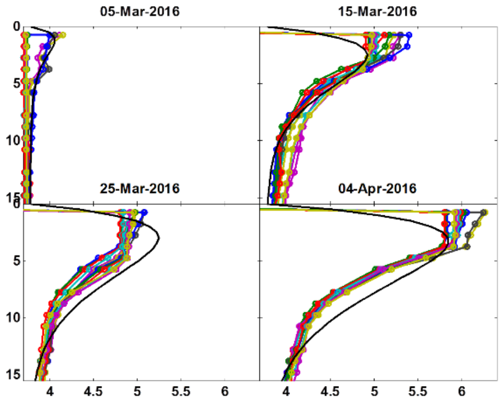

Figure 1 Modeled (black solid lines) and observed (lines with symbols) temperature profiles during the period of inverse stratification. The observed profiles are 2-hour averages for each calendar day

Strong heating and inverse stratification under ice ("Anomalous winter"): In early March, the water temperature beneath the ice achieved the maximum density value. As a result, free convection was cancelled, and stable vertical stratification developed in the bulk of the water column with an inversion layer adjoining the ice-water interface. The stable conditions lasted until the ice breakup in mid-April, with temperatures right beneath the ice cover grown up to 6°C. Mixing conditions during the "anomalous winter" were analyzed using the model of Kirillin and Terzhevik (2011). Several prominent features distinguish the inverse stratification (Fig. 1): (i) 25% of surface radiation penetrates the ice (~60 W m^{-2} daily mean for April). Such a strong warming suggests that any lake of Tibetan Plateau gets warmer than 4°C during the ice-covered period. (ii) A secondary convective layer in the ice vicinity of the ice cover, where temperature drops upward from its maximum to the freezing point. The layer thickness varies strongly following the diurnal cycle of solar radiation and reaches up to several meters. (iii) While the observations from a single thermistor chain did not allow exact quantifying the upward heat flux at the ice base, rough estimations based on the temperature gradients suggest the water-ice heat fluxes to exceed 10 W m^{-2}, and can be much higher in the reality taking into account the strong mixing under ice by secondary convection.

The new findings demonstrate that all freshwater (and apparently the majority of brackish) lakes on Tibet encounter full mixing under ice, so that the convenient concept of winter stagnation, as known from traditional lake science, is inapplicable for these lakes. The direct consequences of the deep convective mixing are aeration of the deep lake waters and upward supply of nutrients to the upper photic layer, both suggesting versatile biogeochemical and ecological interactions specific for high-altitude lakes. The 1-2 month long period of stable stratification at water temperatures above the maximum density value is an exceptional feature of high-altitude freshwaters. The resulting strong temperature gradient at the ice-water interface and a thin unstable layer right beneath intensify the heat flow from water to ice and make by this a crucial contribution to ice cover melting.

REFERENCES

Kirillin, G., and Terzhevik, A. (2011). Thermal instability in freshwater lakes under ice: Effect of salt gradients or solar radiation?. *Cold Regions Science and Technology*, 65(2), 184-190.

Numerical simulation of stratification and ice regime of saline lakes

Victor Stepanenko[1*], Irina Repina[2,1], Arseniy Artamonov[2], Gantuya Ganbat[3], Ganbat Davaa[3]

[1]Lomonosov Moscow State University, Moscow, Russia
[2]A.M.Obukhov Institute of Atmospheric Physics RAS, Moscow, Russia
[3]Information and Research Institute of Meteorology, Hydrology and Environment, Ulaanbaatar, Mongolia

**Corresponding author, e-mail vstepanenkomeister@gmail.com*

ABSTRACT

The presence of dissolved salts in water brings new physical effects into the thermal and ice regime of a lake. However, only a limited number of studies has been conducted to simulate saline lakes. This presentation addresses two distinct effects caused be salinity which have not been well understood on a quantitative level before, and where a numerical model provides new insight into natural phenomena.

The mid-depth temperature maximum (TeM) was measured in an estuarine Bol' shoi Vilyui Lake (Kamchatka peninsula, Russia) in summer 2015. We applied 1D k–ε model LAKE to the case, and found it successfully simulating the phenomenon. We argue that the main prerequisite for mid-depth TeM development is a salinity increase below the freshwater mixed layer, sharp enough in order to increase the temperature with depth not to cause convective mixing and double diffusion there. Given that this condition is satisfied, the TeM magnitude is controlled by physical factors which we identified as: radiation absorption below the mixed layer, mixed-layer temperature dynamics, vertical heat conduction and water-sediments heat exchange. In addition to these, we formulate the mechanism of temperature maximum 'pumping', resulting from the phase shift between diurnal cycles of mixed-layer depth and temperature maximum magnitude. Based on the LAKE model results we quantify the contribution of the above listed mechanisms and find their individual significance highly sensitive to water turbidity. Relying on physical mechanisms identified we define environmental conditions favoring the summertime TeM development in salinity-stratified lakes as: small-mixed layer depth (roughly, $\sim < 2$ m), transparent water, daytime maximum of wind and cloudless weather. We exemplify the effect of mixed-layer depth on TeM by a set of selected lakes.

The saline Lake Uvs (Mongolia) is not stratified by salinity, but salinity plays an important role in ice cover formation here. In order to simulate this lake, the LAKE model was supplemented by a compartment calculating vertical distribution of salinity in the ice cover. The model was compared to data of in situ and satellite measurements of temperature and ice on Lake Uvs for the period from 2000 to 2015. It is demonstrated that neglecting water salinity in the model leads to ice build-up 16-17 days earlier compared to real dates. This error diminishes if the model takes into account the dependence of water density and freezing point on salinity; however, in this case, the model underestimates the maximum ice thickness, on average, by $\approx$0.2 m. The later error, in turn, is reduced by an order of magnitude, if the model accounts for vertical distribution and dynamics of salinity in ice.

The work is supported by Russian Foundation for Basic Research (grant 16-55-44057, Lake Uvs study) and Russian Science Foundation (grant 17-17-01210, Bol'shoi Vilyui Lake study).

Radiatively driven under-ice convection: the impact of lake depth.

S. Volkov[1*], G.Zdorovennova[1], R.Zdorovennov[1], T.Efremova[1], N.Palshin[1], A.Terzhevik[1], D.Bouffard[3], S.Bogdanov[1,2]

[1] Northern Water Problems Institute, Karelian Research Centre of RAS, Petrozavodsk, Russia
[2] Petrozavodsk State University, Petrozavodsk, Russia
[3]Eawag, Swiss Federal Institute of Aquatic Science and Technology, Surface Waters – Research and Management, Kastanienbaum, Switzerland

**Corresponding author, e-mail taranarmo@gmail.com*

KEYWORDS
Ice-covered lakes; under-ice convection; current velocity; energy dissipation; solar radiation.

Introduction

The comparative study of the dynamics and fine-scale structure of under-ice convectively mixed layer was carried out for two significantly different lakes: Petrozavodsk Bay of Lake Onego and small and shallow Vendyurskoe Lake. Both lakes are located in Russian Karelia. Current and solar radiation were recorded by ADCPs and PAR sensors in March-April in 2016-2018 on each site. We focused on the vertical structure of the convectively-mixed layer and investigated the specifics of fine-scale and energy-containing ranges of motion.

Materials and methods

Both beams (Wiles et al, 2006) and ENU coordinates were used in order to derive longitudinal structure function as well as mean current parameters. Different averaging procedure including ping number, burst intervals were tested. The ADCP cell size varied in the range 22-50 mm. The scale of spatial resolution on depth was chosen as the slave one with respect to the Kolmogorov dissipative scale. PAR chains operated with 1 min sampling period and vertical spacing of 0.35-1 m, with parameters tuned for buoyancy flux estimations.

Results and discussion

For both lakes the typical "2/3 power law shapes" of calculated longitudinal structure functions were obtained (Fig. 1). The ranges of energy dissipation rate ε and the extent of Kolmogorov inertial interval were derived after proper analysis. Correlation between the dissipation rate and solar radiation was observed in both lakes, with more extended time delay for Petrozavodsk Bay. To evaluate dependence of ε on depth, we applied the method based on studying the generalized (four-points) structure functions. These functions describe correlations between velocity increments for two pairs of points on the same beam. We also made a comparison of structure parameters during up- and down-welling background flow events. The preliminary conclusion is that alternation of these events is accompanied by periodic enhancement of inhomogeneity. The turbulence activity at night was also observed with reduced but still meaningful values of dissipation rate. In studying the energy-containing range of scales and low-frequency motions we concentrated on applying two complementary tools: velocity hodographs and progressive-vector diagrams (PVD). The velocity components dynamics is very irregular in this range, but PVD trajectories (Fig. 2) reveal some specific features typical for self-organized structures. In particular, the presence of convective cells is manifested by jumps of the velocity direction and loops on hodograph curves, as was previously observed in (Malm et al, 1998). In this context the observed time irregularity of the mixing layer parameters one can treat as the example of chaotic behavior in quasi-deterministic system (Lorenz, 1963).

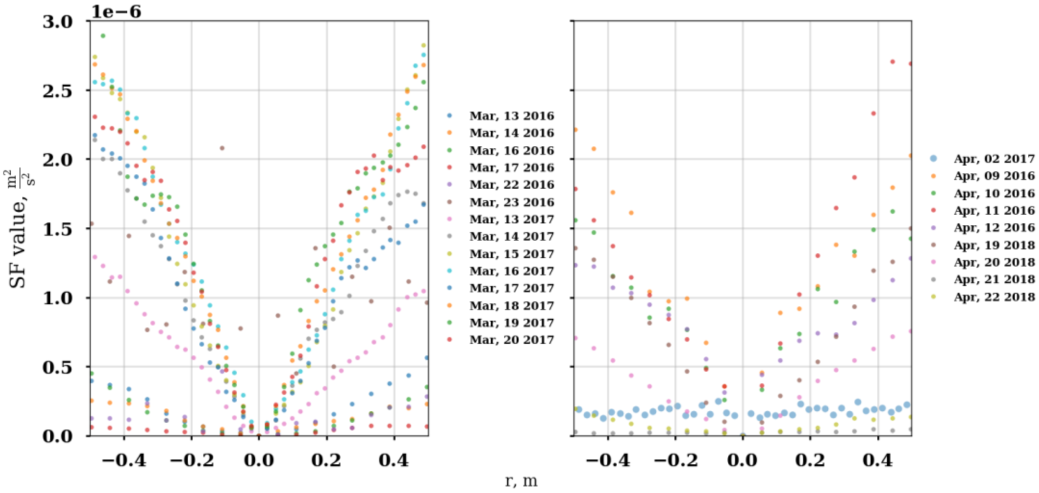

Fig. 1. The sequences of longitudinal structure functions calculated for time intervals close to noons. Left: Petrozavodsk Bay of Onego Lake, depth – 0.9 m; right – Vendyurskoe Lake, depth – 0.9 m.

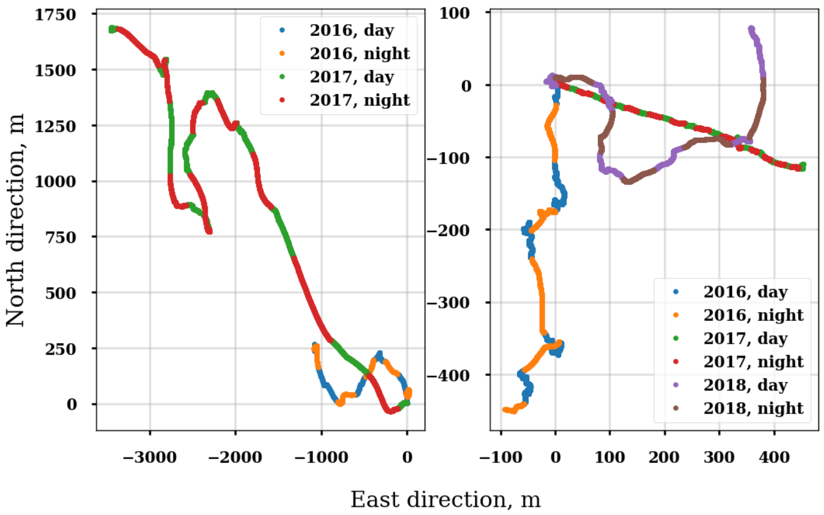

Fig. 2. The progressive-vector diagrams: left – Petrozavodsk Bay, depth – 0.7 m; right – Vendyurskoe Lake, depth – 1m. The almost straight line on the right panel corresponds to the 2017 campaign, when the convection was underdeveloped.

The presence of mean current revealed during all field campaigns, was the key factor, playing the role of scanning mechanism. To put forward the cells images recognition procedure, we carried out the fitting of experimental PVD with trajectories corresponding to the classical convective cells (Lord Rayleigh, 1916; Bisshopp, 1960). By calculating the periods between velocity components extremums and nulls we also derived the estimations of cells horizontal scales. The study was supported by the Russian Foundation for Basic Research (16-05-00436_a) and FEEL Foundation, “Fondation pour l’Etude des Eaux du Léman”.

REFERENCES

Bisshopp, F.E. (1960). On two-dimensional cell patterns. Journal of Mathematical Analysis and Applications - J Math Anal Appl. 1. 373-385.

Lord Rayleigh O.M. F.R.S. (1916): LIX. On convection currents in a horizontal layer of fluid, when the higher temperature is on the under side. Philosophical Magazine Series 6, 32:192, 529-546.

Malm J., Bengtsson L., Terzhevik A., Boyarinov P. , Glinsky A., Palshin N., Petrov M., (1998), Field study on currents in a shallow, ice-covered lake, *Limnology and Oceanography*, 43(7): 1669-1679.

Lorenz E.N. (1963). Deterministic Nonperiodic Flow. J. of Atmospheric Sciences, vol. 20, Issue 2, pp.130-148.

Wiles, P. J., T. P. Rippeth, J. H. Simpson, and P. J. Hendricks (2006), A novel technique for measuring the rate of turbulent dissipation in the marine environment, Geophys. Res. Lett., 33, L21608. doi:10.1029/2006GL027050.

Modeling seasonal and interannual variability of Great Lakes ice cover using FVCOM+ice model

Jia Wang[1*], James Kessler[2], Ayumi Fujisaki-Manome[2], and Philip Chu[1]

[1] *NOAA Great Lakes Environmental Research Laboratory, Ann Arbor, MI, USA.*
[2] *Cooperative Institute for Great Lakes Research, University of Michigan, Ann Arbor, MI, USA*

**Corresponding author, e-mail* Jia.wang@noaa.gov

ABSTRACT

A 3-d, unstructured Finite Volume Coastal Ocean Model with ice model was applied to all five Great Lakes simultaneously to simulate circulation and thermal structure from 1993 to 2016. Model results are compared to available observations of currents and temperature and ice cover. Seasonal cycle and interannual variability for all the five Great lakes were presented. Lake circulation was reasonably reproduced in comparison to the existing observation. The temperature structure was also reproduced reasonably well. The lake dynamics and thermodyanmics exhibit significant annual and interannual variations. Simulated lake ice cover was validated with satellite-measured ice cover for both seasonal cycle and interannual variability. Sensitivity study was conducted on 1) surface wind-wave mixing parameterization, 2) different forcing fields, and 3) different numerical time integration schemes.

Keynote Speaker

Prof. Dr. Roman Stocker

Institute of Environmental Engineering, ETH Zürich

Head of Environmental Microfluidics Group

Address: HIL G 37.2, Stefano-Franscini-Platz, 8093 Zürich
Phone: +41 (0)44 633 30 75
Email: romanstocker@ethz.ch
Website: https://stockerlab.ethz.ch/

Roman Stocker is a Professor in the Institute of Environmental Engineering at ETH Zurich. Roman's research focuses on environmental processes, particularly in the oceans: from harmful algal blooms, to coral bleaching, to oil spills, to the carbon cycle. Roman has pioneered the use of new technology - microfluidics - to zoom in on the smallest players behind these processes: the microbes. Roman’s work has contributed to reveal their importance, frequently appearing in high-profile scientific journals including Science, Nature and PNAS, and being featured in popular media including the BBC, CNN, and the New York Times. When he is not busy creating new technology to understand our environment, Roman is a keen traveler, enthusiastic scuba-diver, and proud father. More about him at http://stockerlab.ethz.ch/.

Plankton in Flow

Roman Stocker

[1]Institute for Environmental Engineering, ETH Zurich, Switzerland

*Corresponding author, romanstocker@ethz.ch

ABSTRACT

Although we now know that microorganisms often rule natural waters - controlling productivity and biogeochemical cycles - we largely ignore how they are affected by typical fluid flow conditions. For example, microbes are routinely exposed to turbulence, yet physicists have ignored microbes and biologists have ignored turbulence. Here I present microfluidic and millifluidic experiments, combined with mathematical models, to show that fluid flow can have profound effects on the biomechanics and the ecology of microorganisms in natural waters. I illustrate this through a series of examples, and will focus in particular on 'gravitaxis', the tendency of many phytoplankton species to swim along the direction of gravity. I will show that, in the presence of flow, gravitaxis results in intense clustering of cells in layers and patches, akin to those often observed in the field, which can have profound effects on plankton population dynamics. Intriguingly, plankton seem to 'know fluid mechanics' and I will present recent evidence that they are able to actively evade turbulence by sensing the simplest among the cues inherent in small-scale turbulent eddies. In addition to representing a new class of active particle problems that promises to keep the fluid mechanician busy for some time to come, these processes are environmentally important because they affect the ecological dynamics and biogeochemical consequences of some of the most important players in aquatic ecosystems.

Day and night bio-convection in Lake Cadagno

Oscar Sepúlveda Steiner[1*], Damien Bouffard[2], and Alfred Wüest[1,2]

[1]Physics of Aquatic Systems Laboratory, Margaretha Kamprad Chair, EPFL-ENAC-IEE-APHYS,Switzerland.
[2]Department of Surface Waters – Research and Management, Eawag, Kastanienbaum, Switzerland.

*Corresponding author, e-mail oscar.sepulvedasteiner@epfl.ch

KEYWORDS
Bio-convection; mixed layers; Lake Cadagno; diffusive time-scale.

Introduction

Bio-convection (Hill and Pedley 2005) is the process in which microorganisms induce local instabilities by displacing parcels of fluid, driving local convection and enhancing mixing. This process develops only if (i) microorganism cells are denser than water, (ii) the concentration of cells is high and within a layer, (iii) the cells are motile and swim upwards, and (iv) above the layer there is a boundary condition that confines the cells. The occurrence of this process is studied in the alpine and meromictic Lake Cadagno – Ticino, Switzerland (1920 m asl, max. depth 21 m and 0.26 km^2 surface area). This lake is divided into an upper layer (top 10 m) rich in oxygen and a deep layer (bottom 10 m) rich in sulfide but depleted in oxygen. In the chemocline of such an extreme environment, anaerobic phototrophic and motile bacteria – *Chromatium okenii* - (~1200 kg m^{-3}) find ideal conditions for their metabolic processes.

Heretofore, mixed layers (MLs) generated by bio-convection in Lake Cadagno were examined by means of vertical microstructure profiles (VMP; Sommer et al. 2017) and were attributed to the upward swimming of *C. okennii* seeking for light on the top of the sulfide-rich layer to perform anoxygenic photosynthesis (i.e. oxygen drives condition iv). During the summer of 2017, two day-night and one night VMP experiments were performed using a VMP-500 (Rockland Scientific, Canada). These experiments revealed a persistent presence of MLs during night time. Occurrence of night bio-convection in Lake Cadagno has not a clear explanation but it can be physically characterized and compared with the diurnal situation. In this work, we study the measured temperature MLs using a model developed from an analytical solution of the 1D-vertical diffusion equation. This approach allows to estimate a diffusive length-scale (and time-scale) which relates the shape of the ML with its convective activity.

Materials and methods

Mixed layer model – The model considers an initial ML h with a step function shape and initial temperature T_o (Figure 1a, green line), subject to Dirichlet boundary conditions on the top (T_{top}) and bottom (T_{bottom}) of the domain. Neglecting lateral gradients, an analytical solution can be encountered by applying the superposition method to recover the boundary condtions. Considering a symmetric temperature step (i.e., $\Delta T = T_o - T_{bottom} + -T_o + T_{top}$) and small times-scales, the solution can be expressed as:

$$\Phi_T(z,t) = \Delta T\left[\operatorname{erf}\left(\frac{\frac{h}{2}-(z-z_o)}{\delta}\right)-\operatorname{erf}\left(\frac{\frac{h}{2}+(z-z_o)}{\delta}\right)\right]+T_o$$

where $\delta = \sqrt{4Dt}$ is the diffusive length-scale of the problem, with D a diffusion coefficient and t time. The center of the ML position is z_o. Furthermore, taking the expression for the diffusive length-scale and solving for t yields to the following expression of the diffusive time-scale:

$$\tau_D = \frac{\delta^2}{4D}$$

Consequently, τ_D can be considered as the time passed since full activity in the ML (step-like function) until the measured situation in each profile with a MLthickness h_{mix} given by:

$$h_{mix} = h - 4\delta$$

Fitting the measured profiles to Φ_T provides insightful information on the activity within the ML during the measurement and on the diffusive time-scale (τ_D) required to form a curved transition to the background temperature of vertical length δ (Figure 1a). Small δ relates to small τ_D and thus high convective activity whereas large suggests large δ suggests large τ_D and negligible convective activity.

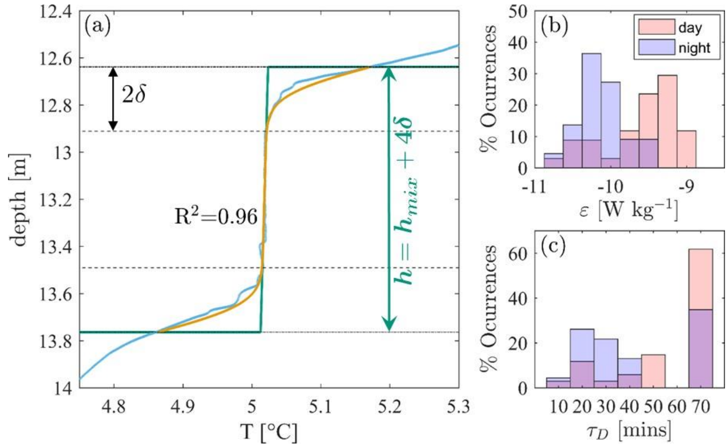

Figure 1:ML example and statistics for a 24 hrs VMP experiment performed during July 2017. (a) Measured ML (blue line), mixed layer model (Φ_T; orange line) and initial step-like function (green line). h_{mix} is represented by the parallel black dashed lines. (b,c) Histograms of turbulent kinetic energy dissipation (ε) in the ML and diffusive time-scale (τ_D) related to the ML.

Results and discussion

Mixed layer model (Φ_T) fitting – An example of the Φ_T fitting against an observed ML is presented in Figure 1a. To estimate τ_D a measured diffusivity $D' = 2{\cdot}10^{-6}$ m^2 s^{-1} (Wuest 1994) was considered. The performance of the model is satisfactory when the layer is well-defined and/or the background temperature gradient persist above and below the ML.

Day and night mixed layer comparison – We present a condensed analysis for a 24 hrs VMP experiment performed during July 2017. After the fitting procedure, only Φ_T with a coefficient of determination $R^2 > 0.75$ were selected for the analysis. The values of τ_D were ~70 minutes for 60 % and 40 % of the observations during day and night respectively. Wihtin the obtained h_{mix}, the rate of turbulent kinetic energy dissipation ε was estimated by means of Batchelor spectral fitting (Ruddick et al. 2000). The mean dissipation rate during day was $\varepsilon = (2.8 \pm 2.3) \times 10^{-10}$ W kg^{-1}, which is in agreement with the values reported by Sommer et al. (2017). During night, the mean dissipation rate was $\varepsilon = (6.8 \pm 6.3) \times 10^{-10}$ W kg^{-1}, which is almost one order of magnitude smaller than day MLs. However, a dissipation $\varepsilon{\sim}1{\cdot}10^{-10}$ W kg^{-1} is not negligible and sheds light on a possible swimming activity during night by *C. okenii*.

REFERENCES

Hill, N. A., and T. J. Pedley (2005), Bioconvection, *Fluid Dyn. Res.*, 37(1–2), 1–20.

Ruddick, B., A. Anis, and K. Thompson (2000), Maximum likelihood spectral fitting: The Batchelor spectrum, *J. Atmos. Ocean. Technol.*, 17(11), 1541–1555.

Sommer, T., et al. (2017), Bacteria-induced mixing in natural waters, *Geophys. Res. Lett.*, 44, 9424–9432.

Wüest, A. (1994), Interactions in lakes: Biology as source of dominant physical forces, *Limnologica*, 24(2), 93–104.

Diurnal variation in the convection-driven vertical distribution of phytoplankton under ice and after ice-off in the large Lake Onego (Russia)

E.L. Suarez[1]*, M.C Tiffay[1], N. Kalinkina[2], T. Chekryzheva[2], A. Sharov[3], E. Tekanova[2], M. Syarki[2], R.E. Zdorovennov[2], E. Makarova[2], E. Mantzouki[1], P. Venail[1] and B. W. Ibelings[1]

[1] *Department F.-A. Forel for environmental and aquatic sciences*
Faculty of Science, University of Geneva, Geneva, Switzerland
[2] *Karelian Research Center, Northern Water Problems Institute, Russian Academy of Sciences, Petrozavodsk, Russia*
[3] *Science Research Centre, Ecological Security of Russian Academy of Sciences, Saint-Petersburg, Russia*

**Corresponding author, ena.suarez@unige.ch*

KEYWORDS:
High DOC; convection; light limitation; thermal bar; primary production.

Introduction

In many of the world`s unproductive lakes, which vary naturally in the input of nutrients and organic matter, it is light and not nutrients that control primary production (Karlsson et al. 2009). The main difference between light and nutrients is the heterogeneous distribution of light underwater that complicates access to this resource. Phytoplankton that lives in a lake with low incoming irradiance, high attenuation or deep mixing, and in particular any combination of these factors, are most likely to be light limited in their development. All these three factors seem to converge in the lake we report here, Lake Onego (Russia). Most of the phytoplankton species are non-motile, so they are dependent on mixing process to stay in suspension and to have access to light. Still, for motile phytoplankton active positioning is only possible when migration rates are fast enough to distrain from turbulent mixing (Ibelings et al. 1991; Granin et al. 2000).

Many of the factors that control and drive winter phytoplankton growth are not fully understood (Kelley 1997; Hampton et al. 2015; Bouffard et al. 2016). In Lake Baikal under ice convection maintains phytoplankton in suspension and within the euphotic zone, so that convection spurs the development of algal blooms (Kelley 1997). When convection is sufficiently strong, even large and dense taxa may thrive (Jewson et al. 2010; Jewson and Granin 2015). However in high DOC lakes convection takes phytoplankton below the euphotic zone, so that the same sunlight that drives photosynthesis reduces access to it.

During spring, differential heating may cause the inshore lake areas to warm up quicker than the deeper central part of a lake, creating a thermal bar (Forel 1880; Holland and Kay 2003). In a lake with steep light attenuation, deep mixing would prohibit phytoplankton growth in open water, while the inshore side of the thermal bar would support the build-up of a spring bloom.

In this paper, we study the impact of convection on phytoplankton growth during ice-on and ice-off, in the large and relatively high-DOM Lake Onego. We aim to test that:

(1) Light is the limiting factor for phytoplankton growth as a consequence of high DOC both during ice-on and ice-off.
(2) Deep convective mixing leads to low phytoplankton biomass due to light limitation.

(3) Diurnal variation in convection restricts the period of the day where phytoplankton has a beneficial top-down distribution which diametrically varies between ice-on and ice-off seasons.

Materials and methods

Two field campaigns were performed in Lake Onego, first in March (winter expedition - under the ice) and later in June 2017 (spring expedition – after ice-off). The surface area of the lake is 9.700 km2, making it the second largest lake in Europe, it has an average depth of 26.8 m and maximum depth of 119 m. The lake is considered as oligo-mesotrophic. Water samples were taken twice per day at different depths, based on the thermal structure of the water column and the depth of the chlorophyll-a maximum. Phytoplankton counts, chlorophyll-a fluorescence, and nutrients (total and dissolved nitrogen, phosphorus and silica) were analyzed for each depth. A mooring system was deployed to capture the physical parameters during both campaigns. Additionally, we ran a full factorial bioassay under ice where different nutrient and light regimes were tested to determine the effect on phytoplankton growth after 5 days of incubation.

Results and discussion

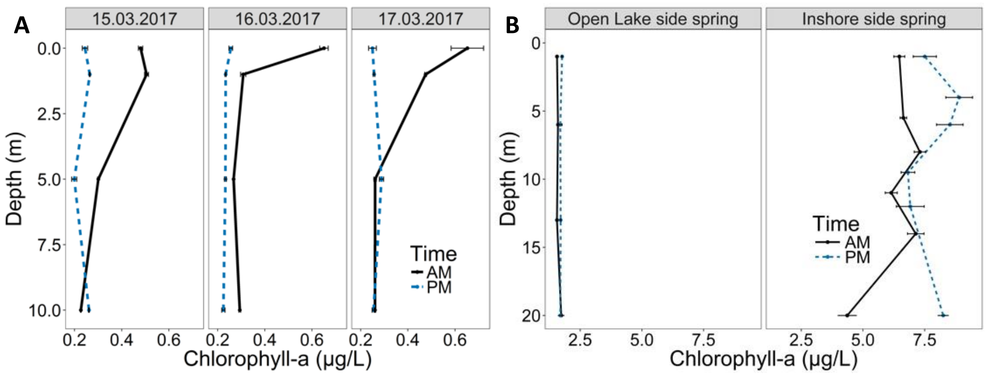

Figure 1. Water column profiles of chlorophyll-a in Lake Onego (Russia) during 2017 campaigns.

We showed that diurnal variation in convection under ice restricts access to light during the morning, while cells are mixed through a deep aphotic layer in the afternoon (Figure 1.A). The bioassay results support the role of light as a key limiting resource. The extension of the convective layer plus the light availability affected phytoplankton development even after ice-off. Very low chlorophyll-a concentrations were found on the open water side of the thermal bar, where convection distributed cells throughout the water column. In contrast on the inshore side of the thermal bar, much higher chlorophyll-a concentrations were found, as over the course of the day microstratification reduced the mixing depth, giving phytoplankton greater access to light (Figure 1.B).

Our results on the diurnal variation in phytoplankton distribution, shows that within the day there are windows of opportunity for a more beneficial top down distribution, where a majority of the cells remain close to the ice and in the euphotic zone. While convection in clear water lakes can be a decisive factor in promoting diatom blooms by maintaining cells in suspension and bringing up nutrients from the deep (Vehmaa and Salonen 2009); in high DOC lakes there is a clear trade-off to these benefits.

REFERENCES

Bouffard D, Zdorovennov RE, Zdorovennova GE, Pasche N, Wüest A, Terzhevik AY. 2016. Ice-covered Lake Onega: effects of radiation on convection and internal waves. Hydrobiologia. 780(1):21-36.

Forel FA. 1880. La congélation des lacs Suisses et savoyards pendant l'hiver 1879-1880. 11 - Lac Léman, Geneva. Vol. 3. L'Echo des Alpes.

Granin NG, Jewson DH, Gnatovsky RY, Levin LA, Zhdanov AA, Gorbunova LA, Tsekhanovsky VV, Doroschenko LM, Mogilev NY. 2000. Turbulent mixing under ice and the growth of diatoms in Lake Baikal. Verh Internat Verein Limnol. 27(5):2812-2814.

Hampton SE, Moore MV, Ozersky T, Stanley EH, Polashenski CM, Galloway AWE. 2015. Heating up a cold subject: prospects for under-ice plankton research in lakes. Journal of Plankton Research. 37(2):277-284.

Holland PR, Kay A. 2003. A review of the physics and ecological implications of the thermal bar circulation. Limnologica - Ecology and Management of Inland Waters. 33(3):153-162.

Ibelings BW, Mur LR, Walsby AE. 1991. Diurnal changes in buoyancy and vertical distribution in populations of Microcystis in two shallow lakes. Journal of Plankton Research. 13(2):419-436.

Jewson DH, Granin NG. 2015. Cyclical size change and population dynamics of a planktonic diatom,Aulacoseira baicalensis, in Lake Baikal. European Journal of Phycology. 50(1):1-19.

Jewson DH, Granin NG, Zhdarnov AA, Gorbunova LA, Gnatovsky RY. 2010. Vertical mixing, size change and resting stage formation of the planktonic diatom Aulacoseira baicalensis. European Journal of Phycology. 45(4):354-364.

Karlsson J, Bystrom P, Ask J, Ask P, Persson L, Jansson M. 2009. Light limitation of nutrient-poor lake ecosystems. Nature. 460(7254):506-509.

Kelley D. 1997. Kelley DE.. Convection in ice-covered lakes: effects on algal suspension. J Plankton Res 19: 1859-1880. Vol. 19.

Vehmaa A, Salonen K. 2009. Development of phytoplankton in Lake Pääjärvi (Finland) during under-ice convective mixing period. Aquatic Ecology. 43(3):693-705.

Phytoplankton response to hydrodynamically determined light and nutrient availability in a stratified reservoir

Brad Sherman

CSIRO, Canberra, Australia

**Corresponding author, email: brad.sherman@csiro.au*

ABSTRACT

The fate of a late summer inflow rich in filterable reactive phosphorus (FRP) to meso-eutrophic Chaffey Dam (New South Wales, Australia) is followed using detailed physical, chemical and biological observations. The inflow was observed to intrude into the reservoir below both the surface layer and the euphotic zone where it remained until surface mixed layer deepening – driven mainly by penetrative convection – resulted in direct entrainment of nutrient into the surface layer. The phytoplankton population, located predominantly within the surface layer and dominated by the cyanobacterium *Anabaena*, remained static for several weeks after the inflow despite high concentrations of immediately bioavailable phosphorus being located just 2 to 3 m below the bottom of the surface layer. As the surface layer deepened, FRP was entrained into it and the phytoplankton population immediately began to grow. Population growth ceased when light availability became limiting due to deepening of the surface layer. Hydrodynamic factors are shown to control both the distribution of nutrients within the water column and the dynamics of the phytoplankton community through concurrent nutrient addition and light reduction.

Effect of vegetated canopies in turbidity current deposits

Marianna Soler[1]*, Jordi Colomer[1], Andrew Folkard[2] and Teresa Serra[1]

[1] *Department of Physics, University of Girona, Girona, Spain*
[2] *Lancaster Environment Centre, Lancaster University, Lancaster, United Kingdom*

**Corresponding author, marianna.soler@udg.edu*

KEYWORDS
Turbidity current, drag-dominated regime, inertial regime, natural vegetation, sediment deposition

Introduction

The structure and function of many disturbed coastal and freshwater ecosystem landscapes result from feedbacks between plant dynamics and the water- and wind-induced transport of sediment (Corenblit et al. 2015). Plants 'engineer' geomorphic processes in a scale-dependent way (Bouma et al. 2013) by developing specific response traits and therefore modifying ecosystem functioning (Corenblit et al. 2015). Thus, bio-geomorphic feedbacks are a major determinant of coastal and freshwater landscape evolution (Bouma et al. 2013). The bio-mechanical properties and structure of plants (density, height, cover and flexibility) mediate interactions between vegetation, hydrodynamics and sedimentary processes. For example, increased plant density, frontal area and stiffness reduce mean flow speed (Västilä and Järvelä 2014), decrease near-bed turbulence intensity (Pujol et al. 2013) and promote sediment deposition (Soler et al. 2017).

Gravity currents are an important type of transport process associated with the fate and distribution of sediments in coastal and fluvial environments. They occur when there are horizontal gradients of density in a fluid under the action of a gravitational field. Gravity currents flowing through vegetated canopies pass through three phases while advancing along the flume (e.g. Huppert and Simpson 1980; Maxworthy et al. 2002). In the initial, 'inertial' phase, the current proceeds as if released from an infinite reservoir, at constant velocity i.e. its frontal position x_C varies in direct proportion to time (Tanino et al., 2005). When the motion is determined by a balance between buoyancy and drag forces caused by obstacles, as vegetation, the flow slows over time such that the position of the front varies as $t^{1/2}$ (Hatcher et al. 2000), this second phase is called 'drag-dominated' phase. The third and last phase occurs when the current has spread so far that it has become thin enough for viscous forces between the two fluids to become important. In this phase, the dominant force balance is between viscous and buoyancy forces, and the position of the front varies as $t^{1/5}$.

Materials and methods

The experiments were carried out in a methacrylate flume with a removable vertical lock gate that separated it into two sections. The shorter section was filled with a mixture of sediment and water that would form the turbidity current, while the longer section was filled with water only. In the latter, a vegetation canopy was distributed along the flume bed. Three species of natural plant vegetation (*Arthrocnemum fruticosum*, *Juncus maritimus* and *Ruppia cirrhosa*) and a single vegetation simulation (PVC) were used in turn. The density of the canopies was quantified using their solid plant fraction, SPF (Pujol, 2013).

In order to mimic natural conditions, the sediment was taken from the Pletera ponds at the Empordà Marshes Natural Park). It was found to have an essentially bimodal size distribution , the coarse fraction having diameters of 6.2 to 104 μm and forming the major volume of sediments (77.7%), and the fine fraction having diameters 2.2 to 6.2 μm and accounting 18.2%. In order to determine the speed of the current front, two CCD cameras were mounted on stationary tripods over the tank. Fourteen sediment traps were located all along the flume bed. These traps collected sediment deposited from the turbidity current as it travelled along the flume. The sediment collected in each trap was analysed with the LISST-100 to obtain the particle volume distribution and the particle volume concentration (Serra et al. 2002).

Results and discussion

The advance of the turbidity current was analysed. Initially, in all cases, $x_C \propto t$ as predicted by theory. Subsequently, the flow slowed. In the non-vegetated runs, $x_C \propto t^{2/3}$ as found by Bonnecaze et al. (1993) for the same configuration. This loss of speed is attributed to particles settling out of the turbidity current. In the vegetated runs, the turbidity current was further slowed by the vegetative drag following $x_C \propto t^{1/2}$.

The effect of the vegetation on sediment transport was found to depend on the hydrodynamic regime of the turbidity current. Regardless of the initial current concentration, vegetation type and particle size, it was found that, while the current is in the inertial regime, depositional flux values remain approximately equal to their initial values at the beginning of the vegetation canopy. This means that currents deposit sediment at a constant rate throughout the inertial regime. In the drag dominated regime, for both the fine and the coarse particles, it was found a linear decrease of sediment deposit depending of the canopy density. This implies that a turbidity current developing in a denser canopy, would provoke a "muddification" of the substrate, i.e. an increase in the fine sediment fraction within the canopy. Coarser particles would have been deposited near the canopy edge.

REFERENCES

Bonnecaze R.T., H.E. Huppert and J.R. Lister (1993), Particle-driven gravity currents, *J. Fluid Mech*., *250,* 339-369.

Bouma T.J., S. Temmerman, L.A. Van Dure, E. Martini, W. Vandenbruwaene, D.P. Callaghan, T. Balke, G.Biermans and others (2013), Organism traits determine the strength of scale-dependent bio-geomorphic feedbacks: A flume study on three intertidal plant species, *Geomorphology, 180-181,* 57-65.

Corenblit D., Baas A, T. Bouma, F. Fromard, V. Garófano-Gómez, E. González, A.M. Gurnel, J.F. Hortobágyi , D. Kim, L. Lambs, J.A. Stallins, J. Steiger, E. Tabacchi and R. Walcker (2015), Engineer pioneer plants respond to an affect geomorphic constraints similarly along water-terrestrial interfaces world-wide, *Global Ecology and Biogeography, 24*, 1363-1376.

Hatcher L., Hogg AJ, Woods, AW. (2000). The effect of drag on turbulent gravity currents, J. Fluid Mech., 416, 297-314.

Huppert, H. E. and J.E. Simpson (1980), The slumping of gravity currents, *J. Fluid Mech.*, 99, 785-799.
Maxworthy T., J. Leilich, J.E. Simpson and E.H. Meiburg (2002), The propagation of a gravity current in a linearly stratified fluid, *J. Fluid Mech*., 453, 371-394.

Pujol D., J. Colomer, T. Serra and X. Casamitjana (2013), Flow structure in canopy models dominated by progressive waves, *Journal of Hydrology*, *486*, 281-292.

Serra T., X. Casamitjana, J. Colomer and T.C. Granata (2002), Observations of the particle size distribution and concentration in a coastal system using an in situ laser analyzer, *Marine Technology Society Journal*, *36*, 59-69.

Soler M., J. Colomer, T. Serra, X. Casamitjana and A.M. Folkard (2017), Sediment deposition from turbidity currents in simulated aquatic vegetation canopies, *Sedimentology, 64,* 1132–1146.

Tanino Y., H.M. Nepf and P.S. Kulis (2005), Gravity currents in aquatic canopies. *Water Resources Research*, 41, W12402, doi: 10.1029/2005WR004216.

Västilä K. and J. Järvelä (2014), Modelling the flow resistance of woody vegetation using physically based properties of the foliage and stem, *Water resources research, 50,* 229-245.

An applied physical oceanography study of Scottish coastal and fjordic waters with regard to sea lice dispersal between aquaculture farms

B. Rabe[1]*, A. Gallego[1], J. Hindson[1] and J. Wolf[2]

[1] *Marine Laboratory, Marine Scotland Science, Aberdeen, UK*
[2] *Marine Systems Modelling, National Oceanography Centre, Liverpool, UK*

*Corresponding author, e-mail b.rabe@marlab.ac.uk

Keywords
Physical oceanography; aquaculture; Scotland; connectivity; bio-physical modelling.

Introduction

Coastal and inshore regions around Scotland are complicated with regard to circulation patterns. The west coast and islands are characterized by complex coastlines with bays, fjords, and surrounding hills. Fjordic estuaries exhibit varying bathymetry, geography, and forcing mechanisms (Asplin et al., 2014, Rabe and Hindson, 2017). Their circulation can be wind-, tide-, and buoyancy-driven, and be influenced by Earth's rotation, depending on their dynamic width.

The aquaculture industry in Scotland and other countries with fjordic systems use these estuarine systems for farming Atlantic salmon. Salmon can be affected by the parasitic sea louse (*Lepeophtheirus salmonis Krøyer*), which has detrimental effects and therefore efforts are made by governments and industry to manage lice burdens.

We here expand previous work from one fjord, Loch Linnhe, which has been investigated with regard to physical forcing mechanisms and connectivity, to a coastal scale, along the whole of the Scottish coast. We investigate the physical processes, circulation, and connectivities to aid the proposed sustainable growth of the aquaculture industry.

Materials and methods

We use a one year climatological output from a FVCOM hydrodynamic model of the Scottish shelf, the Scottish Shelf Model (Wolf et al., 2016). Climatological flow fields (not taking storms into account) force particle-tracking simulations of organisms that represent sea lice (passive particles, no biology, temperature dependent). Particles were released within all Farm Management Areas (FMA) on a regular 2km x 2km grid (100 particles per release point, between 1-100 release points per FMA), were constrained to the surface layer, and the infective stage was captured at all areas that were reached. Four seasons were modelled and results summed up over those four seasons. The connectivity is defined as the degree of dynamic interaction between geographically separated populations via the movement of individuals and we can evaluate connectivity matrices based on different types of analysis. Three different types of analysis were used from worst case (binary presence/absence) to a more realistic approach (evaluating weighted probability above a threshold of 10^{-5}% (Adams et al., 2016, Salama et al., 2017) by active site biomass).

With the use of this coupled bio-physical model we can investigate dispersal and degrees of connectivity between these FMAs (which coordinate the control of sea lice, Code of Good Practice) around Scotland's coast.

Results and discussion

This applied physical oceanography study uses a coupled bio-physical model to investigate sea lice dispersal and connectivity along the Scottish coast. The transmission of the parasite occurs by planktonic larvae; we find that these are transported (in the surface layers by currents) for up to tens of kilometres, leading to interactions between farms.

The analysis focusses on sufficiently discrete geographical areas along the coast. Some areas export particles for considerable distances with the prevailing currents (estuarine circulation out of the fjord and Scottish Coastal Current to the north along the coast) and some particles travel across wide geographical boundaries.

The analysis shows that most management areas self-infect. Probability is highest for self-infecting, neighbouring, and towards downstream locations (generally South to North). Regions to the east of Skye act as both the largest sinks and sources when evaluating probabilities and taking into account biomass at the farms.

We also find that, for example, Shetland is self-contained, not receiving any particles from other islands or the mainland, but is well-connected itself in a clockwise direction. The Western Isles on the other hand can export particles to the mainland and some particles from mainland sites can reach the Western Isles.

Future work could include salmon migration modelling, quantifying interaction pressures from aquaculture to migrating salmonids in coastal and inshore waters, more sophisticated biological behaviour, or taking into account actual sea lice counts. Management areas around the Scottish coast can be evaluated and adjusted with the help of on-going connectivity analysis work.

Overall, our understanding of the physical oceanography of Scottish coastal and fjordic waters, combined with bio-physical modelling, can aid the sustainable growth of aquaculture in Scotland. Knowledge of these interactions to inform management and control of sea lice on farms requires a multidisciplinary approach.

REFERENCES

Adams, T.P., D. Aleynik and K.D. Black (2016): Temporal variability in sea lice population connectivity and implications for regional management protocols. Aquacult Environ Interact 8: 585-596.

Asplin, L., I. Johnsen, A. Sandvik, J. Albretsen, V. Sundfjord, J. Aure, and K. Boxaspen, (2014), Dispersion of salmon lice in the Hardangerfjord. *Mar. Biol. Res.* 10 (3), 216-225.

Code of Good Practice for Scottish Finfish Aquaculture (http://thecodeofgoodpractice.co.uk/).

Rabe, B., and J. Hindson (2017), Forcing mechanisms and hydrodynamics in Loch Linnhe, a dynamically wide Scottish estuary, *Estuarine, Coastal and Shelf Science*, 196, 159–172.

Salama, N.K.G., A. Dale, V.V. Ivanov, P.F. Cook, C.C. Pert, C.M. Collins, and B. Rabe (2017): Informing sea lice management in Loch Linnhe, a Scottish sea loch, using biological-physical modelling. Journal of Fish Diseases, DOI: 10.1111/jfd.12693.

Wolf, J., C. Struiver, D. Price, H. Johnson, A. Gallego and R. O'Hara Murray (2016): The Scottish Shelf Model. Part 6: Wider domain and sub-domains integration. Scottish Marine and Freshwater Science Vol 7 No 8.

Poster Presentation Abstracts

(Poster abstracts are ordered alphabetically by family name)

Simulation of the Effects of Climate Change on Lake Erken Thermal Structure

A. I. Ayala, D. C. Pierson

Department of Ecology and Genetics, Uppsala University, Sweden.

**Corresponding author, isabel.ayala.zamora@ebc.uu.se*

KEYWORDS
Lakes; modelling; climate change; thermal structure; stratification.

Introduction

Lakes hold a large majority of Earth's liquid freshwater, support enormous biodiversity, and provide key provisioning and cultural ecosystem services to people around the world (O'Reilly et al., 2015). A substantial body of research demonstrates the sensitivity of lakes to climate and shows that physical, chemical, and biological lake properties respond rapidly to climate-related changes (ACIA, 2004; Rosenzweig et al., 2007; Adrian et al., 2009).The goal of this study, as part of the Inter-Sectoral Impact Model Intercomparison Project (https://www.ISIMIP.org), is to assess the impacts of different levels of global warming on the thermal structure of Lake Erken (Sweden). These are the first site specific simulations made for the ISIMIP lake sector, and allow us test of the methodologies that will be used for a larger set of simulations that will be run using a global lake data set (~50 lakes). For this purpose, a one dimensional-hydrodynamic model (GOTM Burchard 2002) is used to simulate water temperature when driven with input meteorological scenarios supplied by ISIMIP.

Materials and methods

The Global Climate Models (GCMs) scenarios have a daily time step, while lake model simulations are often forced with meteorological data at hourly or shorter time steps. Therefore, it was necessary to systematically test the ability of the GOTM model to simulate Lake Erken water temperature using daily vs hourly meteorological forcing data, and to evaluate the need to disaggregate the daily GCM scenarios to a shorter time step. We compared water temperatures from simulations forced using measured mean hourly and mean daily data and synthetic hourly data created from mean daily data using Generalized Regression Artificial Neural Network methods (GRNN). In all the cases the GOTM model was calibrated based on the comparison of over 56000 simulated and measured mean daily water temperature measurements during the period from 2006 to 2016.

Long-term water temperature simulations were carried out using synthetic hourly series of meteorological data made from ISIMIP scenarios. This allowed us to quantify the impact of historical warming and climate change effects based on two future projections: one for moderate-mitigation (rcp6.0) and another for strong-mitigation (rcp2.6), and evaluate these relative to preindustrial conditions (piControl).

A range of thermal metrics: surface temperature, whole-lake temperature (volumetric mean), epilimnetic temperature, hypolimnetic temperature and bottom temperature were calculated from the simulated lake temperature profiles. From these profiles, we also calculated Schmidt stability and thermocline depth using Lake Analyzer (Read et al., 2011). The onset and length of the stratification defined as the time when the temperature difference between the surface and the bottom of the lake exceeded 1 ^{0} C (Woolway et al., 2014) and lasting more than 5 days (Kraemer et al., 2015) was also calculated. The non-parametric Mann-Kendall test was used to assess the significance of trends and the Theil-Sen method (Theil, 1950; Sen, 1968) was used to estimate the slope of the significant trends in temperature (surface temperature and whole-lake temperature) and stratification indices (epilimnetic temperature, hypolimnetic temperature, Schmidt stability and thermocline depth) during the stratified period.

Results and discussion

The GOTM model, when using an hourly computational time step, can accurately simulate Lake Erken water temperature even when daily forcing data are used. Simulations forced with the synthetic hourly data also provided accurate simulations of Lake Erken water temperature, and since the results the non-parametric Kolmogorov-Smirnov test suggest that there were significant differences between water temperature simulations forced with daily and synthetic hourly inputs, we choose to evaluate ISMIP scenarios using the hourly synthetic data.

Simulated water temperatures for the four emission scenarios and the IPSL-CM5A-LR GCM are presented as temperature isopleths (see Figure 1). These were created by averaging the daily temperature profiles associated with the emission scenarios (N_{piC} = 639 years, from 1661 to 2299; N_{hist} = 145 years, from 1861 to 2005; $N_{rcp2.6}$ = 294 years, from 2006 to 2299 and $N_{rcp6.0}$ = 94 years, from 2006 to 2099). These mean scenario temperature isopleths provide a clear visualization of how for future scenarios the length of the stratification will be longer, surface water temperatures will be greater and vertical gradients in water temperature will increase. Further evaluation of trends showed a significant decrease in the onset of the stratification (Mann-Kendall $p<0.001$) and significant increase in the length of the stratification (Mann-Kendall $p<0.001$) for the future scenario with moderate-mitigation (rcp6.0) by 1.3898 and 2.4242 day decade^{-1} respectively. Epilimnetic temperatures are predicted to increase at a rate of 0.1941 ^{0} C decade^{-1} (Mann-Kendall $p<0.001$) for the rcp6.0 scenario. Extreme epilimnetic temperatures also show a pronounced increase during the future scenarios. The 97.5 percentile from the distribution of epilimnetic temperatures increased by 2.17 ^{0} C for the rcp2.6 scenario and 2.64 ^{0} C for the rcp6.0 scenario relative to preindustrial reference levels. Lake stratification became more stable during the future scenarios. The Schmidt stability increased by 27 % for the rcp2.6 and 35 % for the rcp6.0 scenarios. For rcp6.0 the rate of increase (Mann-Kendall $p<0.001$) was 5.5312 J m^{-2} decade^{-1}. More stable stratification also resulted in a shallower thermocline depth. For the rcp6.0 scenario we estimated a significant decrease (Mann-Kendall $p<0.001$) of 0.8041 m over the period from 2006 to 2099.

REFERENCES

ACIA. 2004, Impacts of a warming Arctic: Arctic climate impact assessment. Cambridge Univ. Press.

Adrian, R., C. M. O'Reilly, H. Zagarese, S. B. Baines, D. O. Hessen, W. Keller, D. M. Livingstone, R. Sommaruga, D. Straile, E. Van Donk, G. A. Weyhenmeyer, (2009), Lakes as sentinels of climate change. Limnology and Oceanography, 54(6part2), 2283–2297, doi:10.4319/lo.2009.54.6_part_2.2283.

Burchard, H. (2002), Applied turbulence modeling in marine waters, Springer, Germany.

Kraemer, B. M., O. Anneville, S. Chandra, M. Dix, E. Kuusisto, D. M. Livingstone, A. Rimmer, S. G. Schladow, E. Silow, L. M. Sitoki, R. Tamatamah, Y. Vadeboncoeur, and P. B. McIntyre (2015), Morphometry and average temperature affect lake stratification responses to climate change, Geophys. Res. Lett., 42, 4981–4988, doi:10.1002/2015GL064097.

O'Reilly, C. M., et al. (2015), Rapid and highly variable warming of lake surface waters around the globe, Geophys. Res. Lett., 42, 10,773–10,781, doi:10.1002/2015GL066235.

Read, J. S., D. P. Hamilton, I. D. Jones, K. Muraoka, L. A. Winslow, R. Kroiss, C. H. Wu, and E. Gaiser, 2011, Derivation of lake mixing and stratification indices from high resolution lake buoy data, Environ. Model. Softw., 26(11), 1325-1336, doi:10.1016/j.envsoft.2011.05.006.

Rosenzweig, C., et al., 2007, Assessment of observed changes and responses in natural and managed systems, p. 79–131. In M. L. Parry, O. F. Canziani, J. P. Palutikof, P. J. van der Linden, and C. E. Hanson [eds.], Climate change 2007—impacts, adaptation and vulnerability. Contribution of Working Group II to the Fourth Assessment Report of the Intergovernmental Panel on Climate Change. Cambridge Univ. Press.

Sen, P. K., 1968, Estimates of the regression coefficient based on Kendall's Tau, J. Am. Stat. Assoc., 63(324), 1379–1389.

Theil, H., 1950, A rank invariant method of linear and polynomial regression analysis, I, II, III, Proc. K. Ned. Akad. Wet., Ser. A Math. Sci., 53, 386–392.

Woolway, R. I., S. C. Maberly, I. D. Jones, and H. Feuchtmayr (2014), A novel method for estimating the onset of thermal stratification in lakes from surface water measurements, Water Resour. Res., 50, 5131–5140, doi:10.1002/2013WR014975.

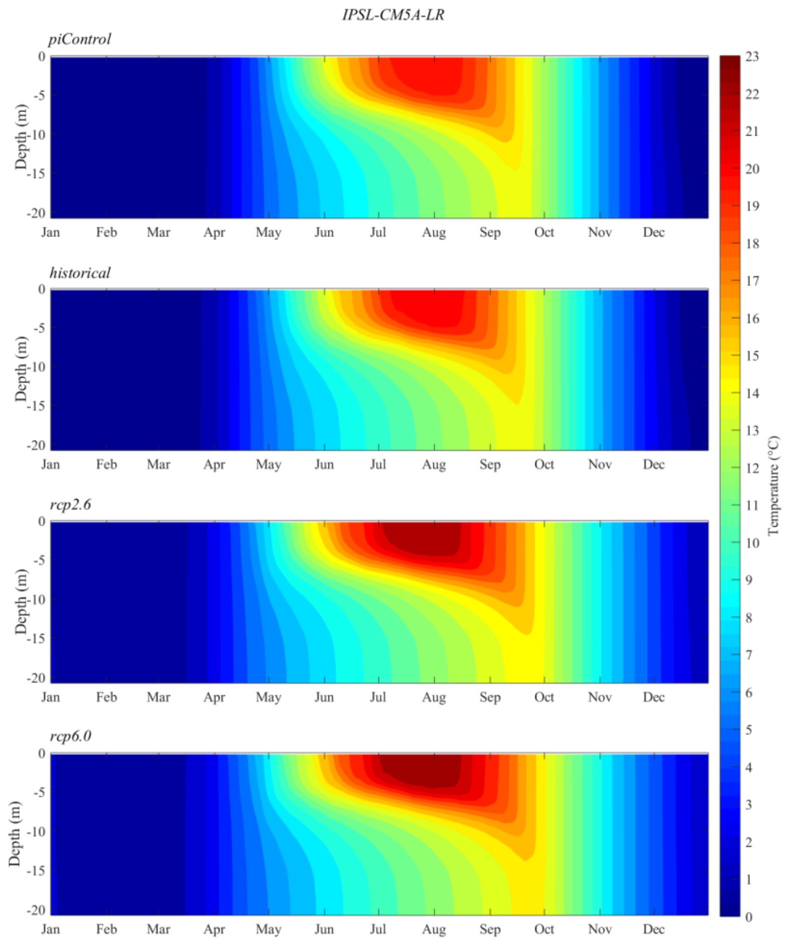

Figure 1. Temperature isopleth diagrams for the GCMs: IPSL-CM5A-LR and scenarios: preindustrial reference levels (piControl), historical, future with strong-mitigation (rcp2.6) and future with moderate-mitigation (rcp6.0). The temperature matrix used to make these plots was created by averaging the simulated daily temperature profiles for every year in each scenario.

On-site analysis of gas concentrations in Lake Kivu, Central Africa

F. Bärenbold[1]*, M. Brennwald[2], R. Britt[2], R. Kipfer[2,3], M. Plüss[1] and M. Schmid[1]

[1] *Eawag, Swiss Federal Institute of Aquatic Science and Technology, Surface Waters - Research and Management, Kastanienbaum, Switzerland*
[2] *Eawag, Swiss Federal Institute of Aquatic Science and Technology, Water Resource and Drinking Water, Dübendorf, Switzerland*
[3] *ETH Zurich, Inst. of Biogeochemistry and Pollution Dynamics & Inst. of Geochemistry and Petrology, Zurich, Switzerland*

**Corresponding author, e-mail fabian.baerenbold@eawag.ch*

Introduction

Lake Kivu is one of the African Great Lakes with a surface area of around 2370 km^2 and a depth of 485 m. Located on the border between Rwanda and the Democratic Republic of the Congo (DRC), meromictic Lake Kivu is particularly known for its uniquely huge reservoir of dissolved CO_2 and CH_4 in the stably stratified deep water (between 250 and 485 m). In fact, the deep water's unusually stable stratification effectively prevents annual mixing and thus keeps the gases trapped in the deep water. While the CO_2 is provided by subaquatic groundwater inflow, CH_4 is believed to be mainly of biologic origin (degradation of organic matter and CO_2 reduction). The CH_4 reservoir is considered a valuable resource for electricity production. Most recently, a 25 MW power plant has been connected to the Rwandan grid and the mid-term goal is to increase production to well beyond 100 MW which would be a substantial share of total electricity production in the region.The last reliable assessment of the lake's CH_4 resources dates from 2003 (Schmid et al, 2005) and the total CH_4 content is estimated to around 65 km^3 at 0°C and 1 atm. (Wüest et al., 2012). This means that the authors measured an increase of CH_4 on the order of 15% since 1974 (Tietze, 1978) which would indicate an increased risk of a spontaneous gas eruption from the deep water. It is therefore of great importance to reassess the reservoir and production rate of CH_4 in the lake periodically. However, accurate gas measurements are challenging in the highly outgassing deep water. Here, we present the results of a field campaign which took place in March 2018 near Gisenyi at the northern shore of the lake. Our campaign was part of a larger project to reassess CH_4 and CO_2 concentrations in Lake Kivu, but we also measured N_2, O_2, Argon and Helium concentrations.

Furthermore, numerical modeling can highlight possible consequences of the ongoing methane harvesting and climate variation on gas concentrations and stability of the density stratification. Measurements of anthropogenic tracers ^3H and SF_6 can be used to constrain mixing processes in the intermediate layer between the mixolimnion and the deep layers and therefore close an important gap of knowledge. We will only present results of tracer concentrations as the work on modeling is still ongoing.

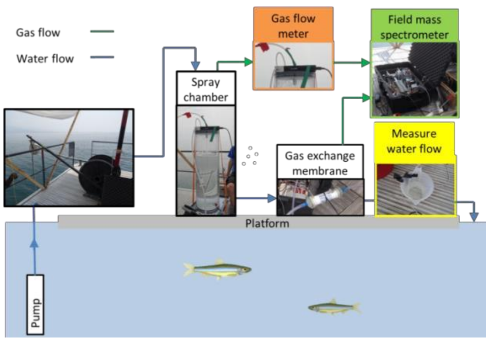

Materials and methods

We used a portable membrane-inlet mass spectrometer operating at gas equilibrium (GE-MIMS, see Brennwald et al., 2016) to derive an on-site vertical profile of gas concentrations. A submersible pump provided the continuous sample water flow required to maintain gas equilibrium at the MS inlet. Below 250 m depth however, gas concentrations quickly increase and thus the buoyancy of the outgassing water alone is capable of lifting the water to the surface. The water-gas mixture is subsequently dispersed through the nozzle of a home-made spray chamber and thus separated into water and gas phase. Both phases are analyzed using the GE-MIMS (gas directly and water via a membrane module). Finally, gas and water flow rates are measured to compute in-situ gas concentrations in the water column.

Results and discussion

CO_2 and CH_4 measurements from 2003 and 2018 in general agree within uncertainty (see Figure). Hence, our measurements do not suggest an increased risk of a gas eruption as hypothesized in Schmid et al., 2005. Oxygen is only found in the top 30 m (mixolimnion), while the N_2 and Argon concentrations stay approximately constant down to the bottom of the lake. However, the uncertainty of these two gases is high due to mass interference with CO and high dilution through CO_2 and CH_4 respectively. Thus, we can't exclude a slight decrease with depth which could imply moderate degassing in the deep water. Finally,

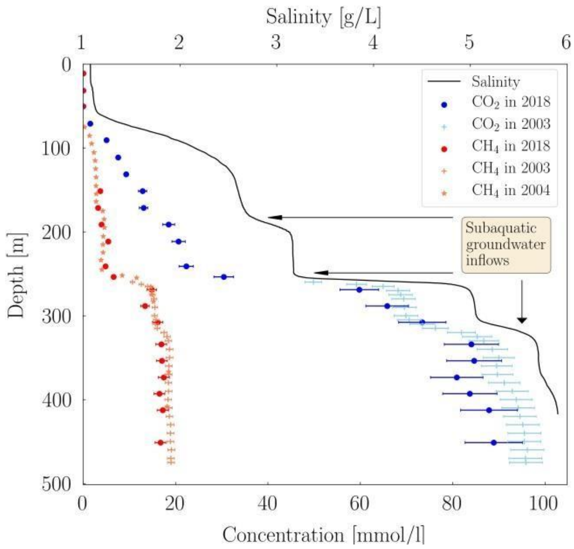

Helium increases by a factor of ~1000 in the deep water compared to surface waters, meaning that the deep groundwater inflows are indeed connected to a magmatic system.

The analysis of SF_6 samples from our campaign in 2017 year suggested that only the mixed surface layer is younger than ~50 years (SF_6 could not be detected below the mixolimnion). Therefore, the result confirms that there is no downward mixing in Lake Kivu from the mixolimnion into the deeper layers because of the unusually weak turbulence and the upwelling due to subaquatic inflows (Schmid et al., 2005). The analysis of our ^3H samples is still ongoing, but the better resolution of this sampling (compared to SF_6) will help to either confirm or reject the current hypothesis about mixing.

REFERENCES

Brennwald M. S., M. Schmidt, J. Oser and R. Kipfer (2016), A portable and autonomous mass spectrometricsystem for on-site environmental gas analysis, *Environ. Sci. Technol.*, 50 (24), 13455–13463

Schmid M., M. Halbwachs, B. Wehrli, and A. Wüest (2005), Weak mixing in Lake Kivu: New insights indicate increasing risk of uncontrolled gas eruption, *Geochem. Geophys. Geosyst. 6(7)*, Q07009.

Tietze K. (1978), Geophysikalische Untersuchung des Kivusees und seiner ungewöhnlichen Methangaslagerstätte – Schichtung, Dynamik und Gasgehalt des Seewassers, Ph.D. thesis, Christian- Albrechts-Univ., Kiel, Germany.

Wüest A., L. Jarc, H. Bürgmann, N. Pasche and M. Schmid (2012), Methane formation and future extraction in Lake Kivu, *Lake Kivu*. Springer Netherlands, pp. 165-180.

Turbulence parameters estimations via inter-beams ADCP correlations.

S.Bogdanov[1,2]*, S. Volkov[1], A.Terzhevik[1], G.Zdorovennova[1], R.Zdorovennov[1], N.Palshin[1], T.Efremova[1], and G.Kirillin[3]

[1] *Northern Water Problems Institute, Karelian Research Centre of RAS, Petrozavodsk, Russia*
[2] *Petrozavodsk State University, Petrozavodsk, Russia*
[3]*Leibniz-Institute of Freshwater Ecology and Inland Fisheries (IGB), Berlin, Germany*
**Corresponding author, e-mail Sergey.R.Bogdanovt@mail.ru*

KEYWORDS
Acoustic current profilers, turbulence fine-scale structure, Reynolds stresses, structure functions.

Introduction

Acoustic Doppler current profilers (ADCPs) are widely used in oceanological and limnological studies. In the case of horizontally homogeneous currents these tools have proven to be rather powerful for mean flow vertical profiling, after proper averaging. In recent years, progress was achieved also in processing raw along-beam velocities *b*. In particular, the longitudinal structural functions $D_{LL}(AA') = \langle (b_{A'} - b_A)^2 \rangle$ and spectral methods (by applying Taylor's hypothesis) were successfully used in studies of fine-scale turbulence, including indirect estimations of energy dissipation rate (Lorke and Wüest, 2005; Lucas et al., 2014). However further development of the methods, including inertial-dissipative one, is restricted by the lack of information on velocity direction.

Concerning the large-scale turbulence parameters, the variance method was developed (Howarth and Souza, 2005) and validated by estimating some components of the Reynolds stress tensor. Thus, estimates of both production and dissipation rates become available, inspiring the further subtle studies of the turbulent kinetic energy balance.

Some problems remain open, including noise exclusion and the averaging algorithms (Kirincich and Rosman, 2011). Even more challenging is the problem of extending ADCP possibilities on deriving the full set of turbulence parameters. First, in fine-scale structure studies, apart from revealing of "2/3 law", information is necessary on isotropy of pulsations and the transverse structural function for an unambiguous conclusion on the direction of spectral energy transfer. On the other hand, all six components of Reynolds stress tensor are necessary for studying the energy-containing range, but their direct calculation is not possible even with five-beams ADCP (Guerra and Thomson, 2017).

Materials and methods

One of the ways to overcome these problems is based on studying the generalized (four-point) structural functions $\tilde{D}$, which describe the correlations between velocity increments for two pairs of points on different beams. For example, two pairs (A, A´) and (B, B´) generate (Fig.1): $\tilde{D}_{12} = \langle (b_{A'1} - b_{A1})(b_{B'2} - b_{B2}) \rangle$. The values of $\tilde{D}_{12}$ for different spacing's AB and AA´ are directly derived from experimental data.

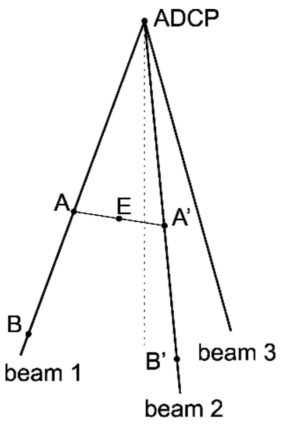

Figure 1. Four-point configuration for $\tilde{D}_{12}$.

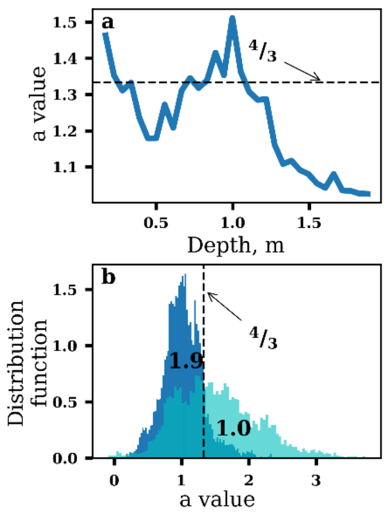

Figure 2. a - dependence of isotropy parameter a on depth. b - distribution function for a, depth 1.0 m and 1.9 m

On the other hand, assuming local isotropy, these values are readily represented (Monin and Yaglom, 1971) through the values of ordinary longitudinal D_{LL} and transverse D_{NN} structural functions with proper arguments. So, an explicit expression for transverse structural functions is derived, providing the opportunity to check the classical relation $a \equiv D_{NN} / D_{LL} = 4/3$.

The mentioned relationship between the generalized and ordinary structural functions may also be used to derive missing expressions for Reynolds stress components, after a proper choice of the pairs of points. In particular, the pairs (A, E) and (E, B) suit to calculating the component $\langle b_1 b_2 \rangle$.

Results and discussion

We applied the described methods, based on the inter-beams velocity correlations to derive some additional information on turbulence structure of the convectively mixed layer, which develops in shallow ice-covered lakes in the late spring as a result of inhomogeneous heating of water by solar radiation.

The field experiment was carried out in the central deep-water part of Lake Vendyurskoe, Russia during the spring convection on 8-13April 2016. The 2 MHz HR Aquadopp profiler in the pulse-to-pulse coherent mode scanned a 2-m thick layer with the blind zone of the first 15 cm from the device head.

We revealed that signals from different beams were not independent and velocity covariance was not vanishing, thus allowing to estimate Reynolds stresses and to check the local isotropy by the described method. In particular, we calculated parameter *a*; Figure 1a presents the values of *a* (averaged over the entire period of measurements) for different depths. For the upper part of the convective layer (from 0.23 to 1.22 m) *a* is close to Kolmogorov value 4/3: $a = 1.22 \pm 0.14$, but decreases sufficiently with further increase of depth. The variations of this parameter with time are rather high, as a histogram (Fig. 1b) illustrates. The study was supported by RFBR (project 16-05-00436_a).

REFERENCES

Howarth,M.J., A.J. Souza A.J. (2005), Reynolds stress observations in continental shelf seas. Deep Sea Res II, 52, 1075–1086.

Guerra M., Thomson (2017), Turbulence Measurements from Five-Beam Acoustic Doppler Current Profilers. J. Atmos. Oceanic Technol., **34**, 1267–1284,https://doi.org/10.1175/JTECH-D-16-0148.1

Lorke A. and Wüest A. (2005), Application of Coherent ADCP for Turbulence Measurements in the Bottom Boundary Layer. J. Atmos. Oceanic Technol., 22, 1821–1828.

Kirincich, A.R., Rosman J.H.(2011), A Comparison of Methods for Estimating Reynolds Stress from ADCP Measurements in Wavy Environments. J. Atmos. Oceanic Technol., 28, 1539–1553.

Lucas N.S., Simpson J.H., Rippeth T.P., Old C.P. (2014), Measuring Turbulent Dissipation Using a Tethered ADCP. J. Atmos. Oceanic Technol., 31, 1826–1837. ,

Monin A.S. and Yaglom A.M. (1971), Statistical fluid mechanics, M.I.T. Press, Cambridge, Mass.

Diapycnal leakage in the Atlantic Meridional Overturning Circulation

L. Cimoli[1]*, A. Mashayek[2], H. Johnson[3], D. Marshall[1], C. Whalen[4], M. Alford[5], J. McKinnon[5] and A. Naveira-Garabato[6]

[1] Department of Physics, University of Oxford, UK; [2] Imperial College, London, UK
[3] Department of Earth Science, University of Oxford, UK; [4] Scripps Institution of Oceanography, San Diego, CA; [4] National Oceanography Centre, Southampton, UK

**Corresponding author, e-mail laura.cimoli@physics.ox.ac.uk*

KEYWORDS
Turbulent mixing; tracers; overturning circulation; Atlantic Ocean.

The Atlantic Meridional Overturning Circulation (AMOC) consists of intermediate and deep waters that form at high latitudes in the North Atlantic and flow southward across the equator, where they connect through the Southern Ocean to the circulation in other ocean basins. The AMOC plays a key role in the oceanic uptake, transport, and sequestration of heat and tracers such as carbon, oxygen and nutrients. Therefore, understanding its role in tracer distributions is of significance for understanding the role of oceans in the climate system.

While turbulent mixing across density surfaces (a.k.a. diapycnal mixing) along the path of AMOC is not believed to be of leading order importance for driving the circulation, its impact on tracers carried around by AMOC has not been fully investigated mostly for lack of observational coverage of mixing, which is a sub-meter scale process. In this work we assess the role of diapycnal mixing in the Atlantic ocean on tracer distributions by employing a range of data from major global oceanic observational programs as well recent advancement in theoretical understanding of ocean turbulence.

We show that while tracer mixing is still difficult to accurately quantify, it is certainly of non-negligible significance: tracers can move between abyssal waters coming from Antarctica and southward flowing deep waters, across denser and lighter southward flowing deep waters, and between southward flowing deep waters and overlying northward flowing intermediate waters. Denser southward flowing deep waters upwell in the Southern Ocean and sink again around Antarctica after becoming abyssal waters, carrying tracers with them and implying millennial tracer ventilation timescales. Lighter deep waters, on the other hand, resurface further north and can be transformed into northward flowing lighter waters, with ventilation timescales of several decades to few centuries. Thus, quantification of mixing and understanding its role in tracer redistribution is of leading order importance for our ability to fully grasp global distributions of tracers such as carbon and nutrients, among others, as well as for our ability to simulate such distributions in climate models.

So far such mixing has not been accurately accounted for in climate models affecting not only tracer cycles in them, but also the representation of other processes, such as Southern Ocean dynamics, as they have to compensate for the lacking of the secondary role of diapycnal mixing in driving the AMOC. Our work highlights the need for major investment in observations, understanding and modeling of turbulent mixing in the Atlantic Ocean, specially along ocean boundaries.

Multi-scale processes of rotation modified mode-2 internal waves

D. Deepwell[1]*, M. Stastna[1], and A. Coutino[1]

[1] *Department of Applied Mathematics, University of Waterloo, Waterloo, Canada*

**Corresponding author, e-mail ddeepwel@uwaterloo.ca*

KEYWORDS
Kelvin waves: Poincaré waves; DNS; internal waves; Mode-2 ISW.

Introduction

Internal solitary waves (ISWs) are a natural and prevalent feature in naturally occurring stratified fluids. They are often remotely observed in regions with a vast horizontal extent for which rotation plays a role in adjusting the waves' dynamics. In the sub-domain whose span-wise extent is on the order of the length of the ISW wavefront, the boundaries play a crucial role in conjunction with rotation to dramatically change the wave from being largely two-dimensional to one with three-dimensional structure on both large and small scales.

Though ISWs of the first mode are most common, recent observations of mode-2 ISWs show them to be more prevalent than previously thought (e.g. Ramp et al. (2015)). Experiments on the evolution of mode-2 ISWs in the presence of rotation were initially reported by Maxworthy (1983) but have not been revisited since. We present the first direct numerical simulations to compare with, and expand upon, these results.

Materials and methods

We present high resolution, three-dimensional, direct numerical simulations of rotation modified mode-2 internal solitary waves at various rotation rates. We study the problem on a laboratory scale easily reproducible in experimental facilities such as the Coriolis rotating platform in Grenoble. A mode-2 ISW is generated by the usual lock-release mechanism where a density perturbation is released into the background stratification.

We solve the stratified Navier-Stokes equations under the Boussinesq approximation on an f-plane using the pseudo-spectral code called SPINS. The primary instabilities are shear instabilities which have a length scale considerably larger than the boundary layer thickness, and hence we have utilized free-slip conditions on all boundaries. To a first approximation the choice of boundary condition is unimportant to the results presented.

Results and discussion

In the presence of side walls, such as a lake, rotation is seen to change the internal solitary-like waves observed in the absence of rotation into a leading Kelvin wave followed by Poincaré waves. Internal solitary and Kelvin waves are common occurrences within mid-latitude lakes (Bouffard and Lemmin (2013), Wiegand and Chamberlain (1987), and Münnich et al. (1992)) and the progression from one to the other is nontrivial.

Mass and energy are found to be advected towards the right-most-side wall (for Northern hemisphere rotation), leading to increased amplitude of the leading Kelvin wave and the formation of Kelvin-Helmholtz (K-H) instabilities on the upper and lower edges of the deformed pycnocline. These fundamentally three-dimensional instabilities are localized within a region near the side wall and intensify in vigour with increasing rotation rate. Additionally, the localized instabilities are linked to previous observations of mixing associated with Kelvin waves and may result in transport of boundary-trapped biogeochemical constituents. This would indicate that increased mixing and transport can occur preferentially on one side of a channel.

Furthermore, secondary Kelvin waves form behind the wave either from resonance with radiating Poincaré waves or the remnants of the K-H instability. The first of these mechanisms is in accord with published work on mode-1 Kelvin waves (Sánchez-Garrido and Vlasenko (2009)); the second is, to the best of our knowledge, novel to the present study. Both types of secondary Kelvin waves form on the same side of the channel as the leading Kelvin wave but are neither as energetic as the leading wave nor create additional K-H instabilities. They would, however, further impact transport.

One simulation utilizes an extremely high resolution with which we characterize the turbulent breakdown of the near-wall K-H billows in terms of enstrophy, viscous dissipation and the Q criterion for partitioning the vortical and strain portions of the velocity gradient (see the attached figure for an instantaneous snapshot of the enstrophy).

Lastly, we compare cases with various Schmidt numbers to explore how this affects the shear instabilities. All Schmidt number values tried give similar general features in the structure of the wavefront but deviate in the strength of the K-H instability and the resulting density overturning. This then adjusts the number of branches within the trailing Poincaré wave field. Care should be made when discussing localized mixing events in the context of low Schmidt numbers.

REFERENCES

Ramp S. R., Y. J. Yang, D. B. Reeder, M. C. Buijsman, and F. L. Bahr (2015), The evolution of mode-2 nonlinear internal waves over the northern Heng-Chun Ridge south of Taiwan, *Nonlin. Processes Geophys.*, 22, 413-431.

Maxworthy T. (1983), Experiments on solitary internal Kelvin waves, *J. Fluid Mech.*, 129, 365-383.

Wiegand R. C., and V. Chamberlain (1987), Internal waves of the second vertical mode in a stratified lake, *Limnol. and Oceanogr.*, 32(1), 29-42.

Münnich M., A. Wüest, and D. M. Imboden (1992), Observations of the second vertical mode of the internal seiche in an alpine lake, *Limnol. and Oceanogr.*, 37(8), 1705-1719.

Bouffard D., and U. Lemmin, (2013), Kelvin waves in Lake Geneva, *J. Great Lakes Res.*, 39, 637-645.

Sánchez-Garrido J. C., and V. Vlasenko (2009), Long-term evolution of strongly nonlinear internal solitary waves in a rotating channel, *Nonlin. Processes Geophys.*, 16, 587-598.

Stability of a tropical crater lake as a sentinel for climate change

N. Deering[1]*, B. Gibbes[1], A. Grinham[1], S. Albert[1], C. Lemckert[2] and B. Boehrer[3]

[1] School of Civil Engineering,
The University of Queensland, Brisbane, Australia
[2] School of Engineering, Mathematics and Statistics,
University of Canberra, Canberra Australia
[3] Department for Lake Research – Limnophysics
Helmholtz Centre for Environmental Research, Germany

**Corresponding author, e-mail nathaniel.deering@uq.net.au*

KEYWORDS
Lakes; stratification; climate change.

Introduction

Lakes and reservoirs are vulnerable to increased thermal stratification as climate change intensifies, potentially transitioning some systems to an oligomictic or meromictic state. While previous research in temperate latitudes has addressed long-term lake temperature changes there are a limited number of studies in tropical systems. Field measurements from Lake Barrine, a natural crater lake located in tropical North Queensland, Australia are used to explore changes in thermal stratification stability driven by climate change. Lake Barrine was identified as an ideal pilot site due to the small and isolated nature of the catchment (lake to catchment area ratio of 1.08) which greatly reduces the influence of terrestrial runoff.

Materials and methods

The influence of changes in air temperature on lake stratification was assessed by comparing the current state of the system and with measurements from the 1980's (Walker 1999). Historical and present day data were compared using thermal Schmidt stability, heat content and estimates of water density (Boehrer et al. 2010). A combination of vertical water profiles, bathymetric survey and water chemistry measurements were used to characterise stratification in Lake Barrine. Evaluation of spatial variability used vertical water profiles of a multiparameter water quality sonde (RBR-XRX620, RBR Ltd., Ottawa, Canada) and for temporal changes in water temperature a vertical chain of 19 RBR-Solo temperature sensors located at the primary research site used in Walker (1999). The temperature chain was located at a water depth of 65 m with consistent sensor spacing of 3.5 m from 1.5 m – 62.5 m deep. This site was used for collection of water samples at 5 m intervals with a Niskin sampler, which were analysed for total and dissolved metals, total and dissolved nutrients as well as major cation/anions. Finally a bathymetric map of the lake was developed using a 200 kHz self-logging GPS depth sounder (Lowrance HDS7, Navico, Tulsa, Oklahoma, USA), with georeferenced data points interpolated across Lake Barrine in ArcGIS (Version 10.3, ESRI Inc., Redlands, California, USA) using the inverse distance weighted function.

Total heat content was calculated using equations from Chapra (2008) and thermal stability was calculated in accordance with Idso (1973). Finally, to account for variations due to dissolved substances, data from 1983 was processed through modern density approximation techniques (Boehrer et al. 2010) and compared to present (2018) stability of Lake Barrine.

Results and discussion

Results indicate Lake Barrine has gone through a strengthening of stratification since the 1980's. Thermal stability assessment by Schmidt stability number shows the system increased from 3300 g·cm/cm² (1988) to 4386 g·cm/cm² (2018) driven by an increase in surface water temperature over this period (Fig 1 A). In addition to an increased thermal stability the total heat content of Lake Barrine also increased by 0.5% from 1988 to 2018. This is evident through the water column with bottom waters rising from 19.5 °C to 20.2 °C. Subsequent decreases in bottom water density due to temperature change is partially offset by vertically expanding zone of increased concentrations of iron within the hypolimnion (Fig 1 B).

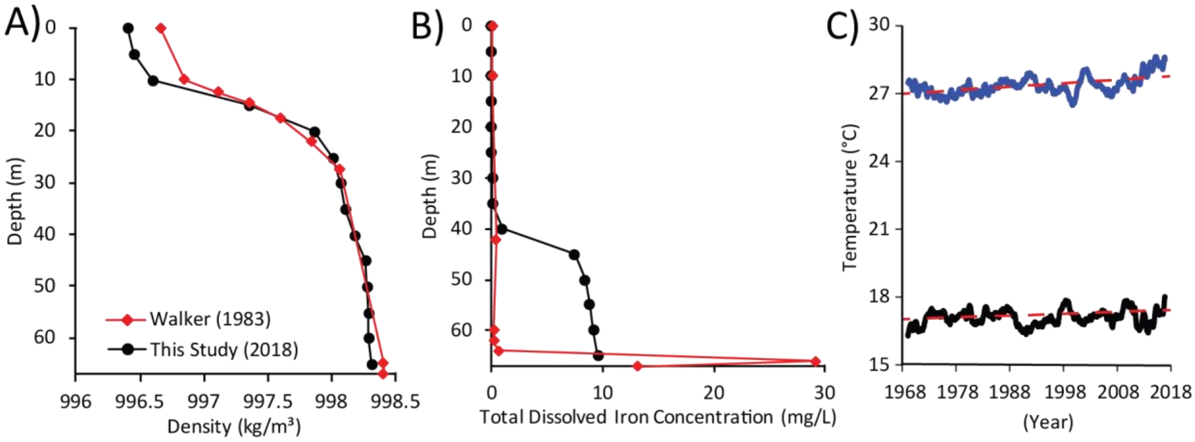

Figure 1. A) Density comparison between Walker's (1999) data from 1983 and current measurements, accounting for dissolved solids. B) Comparison in total dissolved iron throughout the water column of Lake Barrine, indicating mixing is not occurring as frequently as the 1980's. C) Minimum (black) and maximum (blue) air temperature running averages for Walkamin Research Station, 10 km from Lake Barrine. Indication a rising trend (red dashed line) for both sets of observations.

These findings indicate that a rise in Lake Barrine bottom water temperature is consistent with rising air temperature at a nearby Walkamin research station (Fig 1 C). The concurrent increase in dissolved metal concentrations in the hypolimnion suggests a potential to transition to an oligomicitic lake if this trend continues. Future research will establish a long term monitoring program focusing on high frequency temperature and conductivity measurements, providing incite between atmospheric and hypolimnion temperature while monitoring lake stability. This study demonstrates how an oligomictic lake could serve as a climate change temperature sentinel with the hypolimnion warming integrating the inter-annual variability of air temperature.

REFERENCES

Boehrer, B., P. Herzsprung, M. Schultze, and F. Millero (2010), Calculating density of water in geochemical lake stratification models, *Limnol. Oceanogr., Methods* 8, 567-574.

Chapra, S. (2008). *Surface water-quality modeling* (Waveland press).

Idso, B. (1973), On the concept of lake stability, *Limnol. Oceanogr.*, 18, 681-683.

Walker, D. (1999), Some physical and chemical features of two upland crater lakes in tropical north-eastern Australia, *Marine and freshwater research*, 50, 159-177.

GLEON MetOx project: Methane in oxic surface waters

T. DelSontro[1]*, H-P. Grossart[2], D.F. McGinnis[1], Y.T. Prairie[3], M. Koschorreck[4], R. McClure[5], J. Beaulieu[6]

[1]*Department F.-A. Forel for environmental and aquatic sciences*
Faculty of Science, University of Geneva, Geneva, Switzerland
[2]*Experimental Limnology, Leibniz-Institute of Freshwater Ecology and Inland Fisheries, Stechlin, Germany*
[3]*Department of Biological Sciences, University of Quebec at Montreal, Canada*
[4]*Helmholtz Centre for Environmental Research - UFZ, Department Lake Research, Magdeburg, Germany*
[5]*Department of Biological Sciences, Virginia Tech, Blacksburg, VA, USA*
6Office of Research and Development, United States Environmental Protection Agency, Cincinnati, OH, USA

**Corresponding author, e-mail tonya.delsontro@unige.ch*

KEYWORDS
Lakes, methane, advection, stable carbon isotopes

ABSTRACT

The ubiquitous CH_4 oversaturation observed in surface waters, particularly in lakes and reservoirs, remains somewhat of a mystery. The most commonly known methanogenic processes occur in anoxic environments, typically in lake sediments, that can be quite a distance away from surface waters depending on the depth and size of a lake. Yet, most studies find that all lakes, even the largest ones, exhibit oversaturation in their center, leading to what has been termed the 'methane paradox' (e.g., Grossart et al. 2011). Dissolved CH_4 found in the center of a lake has three potential sources: (1) diffusion from sediments and the water column below (Bastviken et al. 2004), (2) dissolving bubbles emanating from sediments below (McGinnis et al. 2006; Varadharajan and Hemond, 2012), and (3) advection from the littoral zone where both diffusion and ebullition from sediments supplies CH_4 to shallow waters (Murase et al. 2003; Wang et al. 2006; Hofmann et al. 2010). However, we also now recognize that CH_4 can be produced in well-mixed, oxic environments (i.e., epilimentic waters), although the exact mechanism by which this occurs is not well constrained (Grossart et al. 2011; Bogard et al. 2014; Yao et al. 206; Wang et al. 2017).

While several studies have known found evidence for CH_4 production in oxic waters, debate remains as to how prevalent of a phenomenon it is globally. A recent study that analyzed surface CH_4 concentrations and stable carbon isotopic signatures in 14 lakes across Quebec and surrounding areas found that 70% of the lakes exhibited the potential for CH_4 production in their oxic surface waters (DelSontro et al. 2017). A recent detailed study of a single Swiss system suggested that ~90% of its total CH_4 emission was due to CH_4 produced under oxic conditions (Donis et al. 2017), while others have found less of a contribution (i.e., 20%; Bogard et al. 2014). To date, studies recognizing the possibility of this methanogenic process and its potential to significantly contribute to total CH_4 emissions from a system have been scarce.

The objective of this project is ultimately to test for the presence of CH_4 production under oxic conditions at a global scale as well as on a temporal scale. We will achieve this by following the sampling regime and modeling techniques outlined in DelSontro et al. (2017) in lakes across GLEON - Global Lakes Ecological Observatory Network. Assuming that vertical diffusion is negligible during stratification (Peeters et al. 1996) and that CH_4 ebullition does not

readily occur in pelagic waters, we will first test the physical transport model that described the spatial heterogeneity of surface CH_4 in lakes of Quebec with data from GLEON lakes. Second, we will use the stable carbon isotopic signature of surface CH_4 in each lake to investigate the presence of CH_4 production relative to CH_4 oxidation in the oxic surface waters of these lakes. We will sample several times over the stratified period to look at any temporal trends in surface CH_4 dynamics during this period.

We currently have 84 collaborators at 66 institutions participating in this project. Collectively, we are sampling 106 water bodies in 26 different countries on 6 continents. We have shipped all sampling kits and northern hemisphere sampling is underway. Southern hemisphere sampling will begin shortly. Samples will be shipped back to Switzerland and analysis should be completed in Spring 2019.

REFERENCES

Grossart, H.-P., Frindte, K., Dziallas, C., Eckert, W. & Tang, K. W. Microbial methane production in oxygenated water column of an oligotrophic lake. *Proceedings of the National Academy of Sciences* **108,** 19657–19661 (2011).

Bastviken, D., Cole, J., Pace, M. & Tranvik, L. Methane emissions from lakes: Dependence of lake characteristics, two regional assessments, and a global estimate. *Global Biogeochemical Cycles* **18,** GB4009 (2004).

McGinnis, D. F., Greinert, J., Artemov, Y., Beaubien, S. E. & Wüest, A. Fate of rising methane bubbles in stratified waters: How much methane reaches the atmosphere? *Journal of Geophysical Research* **111,** C09007 (2006).

Varadharajan, C. & Hemond, H. F. Time-series analysis of high-resolution ebullition fluxes from a stratified, freshwater lake. *Journal of Geophysical Research: Biogeosciences* **117,** G02004 (2012).

Murase, J., Sakai, Y., Sugimoto, A., Okubo, K. & Sakamoto, M. Sources of dissolved methane in Lake Biwa. *Limnology* **4,** 91–99 (2003).

Hofmann, H., Federwisch, L. & Peeters, F. Wave-induced release of methane: Littoral zones as source of methane in lakes. *Limnology and Oceanography* **55,** 1990–2000 (2010).

Wang, H., Wang, W., Yin, C., Wang, Y. & Lu, J. Littoral zones as the ‘hotspots’ of nitrous oxide (N2O) emission in a hyper-eutrophic lake in China. *Atmospheric Environment* **40,** 5522–5527 (2006).

Bogard, M. J. *et al.* Oxic water column methanogenesis as a major component of aquatic CH4 fluxes. *Nature communications* **5,** 5350 (2014).

Yao, M., Henny, C. & Maresca, J. A. Freshwater bacteria release methane as a by-product of phosphorus acquisition. *Applied and Environmental Microbiology* **82,** 6994–7003 (2016).

Wang, Q., Dore, J. E. & Mcdermott, T. R. Methylphosphonate Metabolism by Pseudomonas sp . Populations Contributes to the Methane Oversaturation Paradox in an Oxic Freshwater Lake. *Environmental Microbiology* **19,** 2366–2378 (2017).

DelSontro, T., del Giorgio, P. A. & Prairie, Y. T. No Longer a Paradox: The Interaction Between Physical Transport and Biological Processes Explains the Spatial Distribution of Surface Water Methane Within and Across Lakes. *Ecosystems* doi.org/10.1007/s10021-017-0205-1 ? (2017). doi:10.1007/s10021-017-0205-1

Donis, D. *et al.* Full-scale evaluation of methane production under oxic conditions in a mesotrophic lake. *Nature Communications* **8,** 1661 (2017).

Peeters, F., Wuest, A., Piepke, G. & Imboden, D. M. Horizontal mixing in lakes. *Journal of Geophysical Research* **101,** 18361–18375 (1996).

Impact of the Global Climate Shift of 1976-1978 on the Caspian Sea Thermohaline Circulation

G.S. Diakonov[1,3]*, R.A. Ibrayev[1,2,3]

[1]Shirshov Institute of Oceanology, Russian Academy of Sciences, Moscow, Russian Federation
[2]Marchuk Institute of Numerical Mathematics, Russian Academy of Sciences, Moscow, Russian Federation
[3]Northern Water Problems Institute of Karelian Research Centre Russian Academy of Sciences, Petrozavodsk, Republic of Karelia, Russian Federation

**Corresponding author, e-mail gleb.gosm@gmail.com*

KEYWORDS
Caspian Sea; climate shift; ocean modelling.

Introduction

We investigate the response of the Caspian Sea water masses and thermohaline circulation to the climate shift that occurred in 1976-1978 in the global climate. The main feature of the climatic shift was the transition to a regime of increasing zonal (western) form of atmospheric circulation, cyclonic activity and general hydration in the basin of the Caspian Sea and its catchment area. By the mid-1990s this regime reached saturation and was replaced by a quasi-stationary regime, which is in effect to the present day.

In the Caspian Sea the climatic regime shift of 1976-1978 led to a change in the type of termohaline stratification of waters. With a sharp increase in the influx of fresh water, a transition began from subtropical to moderate type of water stratification. At the same time, the "buoyancy reserve" (the potential energy of water stratification) in the Caspian Sea below 100 m has doubled. Decrease of salinity and increase of winter temperature of surface Caspian waters after 1976-1978 led to a significant decrease of their density and deterioration of the conditions for ventilation of deep waters.

Materials and methods

We aim to quantify these phenomena using a numerical reconstruction of the Caspian Sea circulation in 1960-1990s. By means of numerical computer modeling we reproduce both the sea circulation regime prior to the climatic shift and the transition to the new thermohaline structure of the Caspian Sea. This approach makes it possible to investigate in detail the transition process including the changes of surface and deep currents as well as the distribution of water temperature, salinity and density, and to assess the impact of these changes on the physical processes governing the sea circulation.

For the numerical reconstruction we use a high-resolution (~4 km) 3d-hydrodynamic ocean model forced by ECMWF Era-40 atmospheric reanalysis data and the discharge of five major Caspian rivers. The model reproduces both seasonal and long-term evolution of the Caspian Sea water masses parameters and level height (fig.1). Previously the model was used to investigate and quantify the impact of various natural and anthropogenic factors on the sea water balance (Dyakonov and Ibrayev, 2018). Now we attempt to reproduce the response of the sea to global climate change and to determine whether the signal, related to such change, can be distinguished from background fluctuations and model errors.

Results and discussion

First, we analyze the reconstructed sea surface height (SSH), which is an integral indicator of the model quality, as it depends on the sea surface temperatures, that reflect the thermohaline circulation of the entire sea. From fig.1 one can conclude that the model reproduces the quasi-stationary circulation regime prior to 1976 quite well, yielding after the climate shift of 1978 a slight SSH downtrend (relative observations) due to error accumulation. In 1978-1995 both the observed and the reconstructed SSH exhibit a rapid rise, associated with the transition to a new quasi-stationary regime.

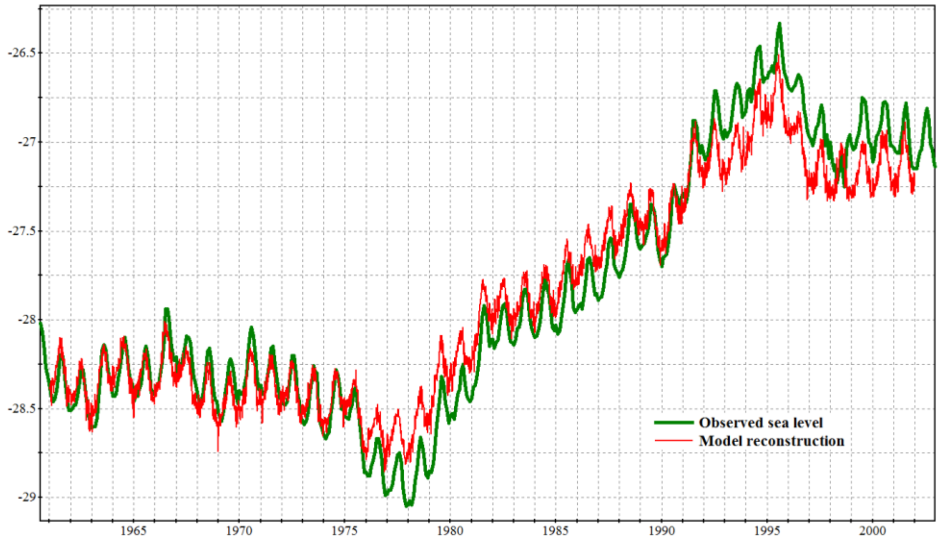

Fig.1. Evolution of the Caspian Sea surface height (m, relative Mean Sea Level): observations and model reconstruction.

The analysis of the thermohaline circulation is performed for each of the three Caspian basins (northern, central and southern) separately, because being partly isolated from one another these basins have very different thermohaline regimes. In the central Caspian basin, the regime transition is most distinct, which can be seen in the salinity evolution (fig.2). After four years of model spin-up, required to adjust salinity distribution to river discharge, the reconstructed sea circulation reaches a quasi-stationary regime, that continues until 1978 (regime-1 on fig. 2). In correlation with the SSH evolution (fig.1) a thermohaline regime shift is obtained during 1978-1995. The shift is characterised by salinity downtrends in the entire upper 150 m sea layer, associated with the intensification of river discharge and the increase of air humidity in the Caspian region. The temperatures of the upper layer increase by ~1 °C (not presented on the figures) which is a result of air humidification, causing lower latent heat losses. In the mid-1990's, after the saturation of the climate shift in the atmosphere a new quasi-stationary regime is reached, and both the SSH on fig.1 and the salinities on fig.2 stabilize (regime-2 on fig. 2). Eventually the sea salinity decreased by ~1 psu in the Northern Caspian and by 0.2-0.4 psu in the upper 150 m layer of the central and southern basins. In the deeper waters the effect on temperature and salinity is indistinguishable from systematic model errors.

Overall one can note a clear correlation between the Caspian Sea level and salinity in its upper layer – both related to the increased river discharge and the evaporation weakening, caused by global climate change. The presented results suggest, that the Caspian Sea is rather sensitive to such climatic shifts and that the associated signal in its circulation patterns can be adequately reproduced by modern 3d hydrodynamic models.

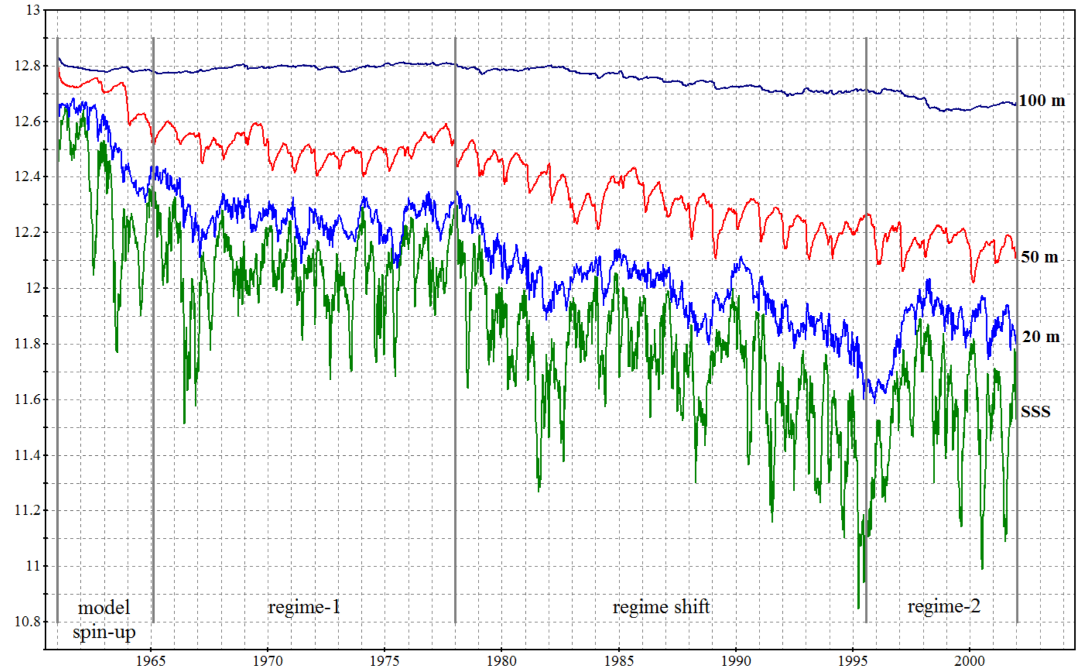

Fig.2. Model reconstruction of the salinity evolution (psu) in the central basin of the Caspian Sea at different depths: 100 m, 50 m, 20 m and at the surface (SSS).

REFERENCES

Dyakonov, G.S. and R.A. Ibrayev (2018), Reproduction of interannual variability of the Caspian Sea level in a high-resolution hydrodynamic model, *Oceanology, 58(1)*, 8-18, doi: 10.1134/S0001437018010046.

Buoyancy-driven cross-shore flows in lakes induced by night-time cooling: field observations

T. Doda[1,2*], H. N. Ulloa[2], A. Wüest[1,2] and D. Bouffard[1]

[1] *Eawag, Swiss Federal Institute of Aquatic Science and Technology, Surface Waters - Research and Management, Kastanienbaum, Switzerland*
[2] *Physics of Aquatic Systems Laboratory, École Polytechnique Fédérale de Lausanne, Lausanne, Switzerland*

**Corresponding author, e-mail tomy.doda@eawag.ch*

KEYWORDS
Cross-shore buoyancy-driven flows; differential cooling; horizontal transport; convection.

Introduction

Cross-shore flows in lakes connect the littoral to the pelagic zones and can have major biogeochemical implications by transporting nutrients, dissolved gases, particles and organisms (e.g., MacIntyre & Melack, 1995). One type of horizontal transport, referred to as “thermal syphon”, is driven by horizontal temperature gradients associated with differential cooling/heating (Monismith, Imberger, & Morison, 1990). In this study, we investigate the cooling-driven thermal syphon. This occurs during night-time, in the nearshore region of lakes or in side-arms. If the heat flux is uniform over the lake surface, shallower regions cool faster than deeper regions: nearshore water become negatively buoyant and start to plunge creating a cold density current into the pelagic zone. At the surface, a return flow forms from the baroclinic response. Three regions can be distinguished along the cross-shore direction (Mao, Lei, & Patterson, 2010): a nearshore region dominated by conduction (vertical isotherms), a transitional region corresponding to the development of the density current and an offshore region composed of two processes: penetrative convection near the surface and the density current near the bottom.

Cross-shore buoyancy-driven flows have been well-studied both via laboratory experiments (e.g., Sturman, Oldham, & Ivey, 1999) and by numerical modelling (e.g., Mao et al., 2010). However, field observations are limited and most of them focused on the side-arm effect (e.g., Monismith et al., 1990) or on winter cooling (e.g., Fer, Lemmin, & Thorpe, 2002). High-resolution measurements are lacking to better understand and quantify the thermal syphon and its consequence in the mass exchange and the ventilation processes in lakes. The temporal and spatial variabilities of the thermal syphon still need to be determined.

The present study aims at filling these gaps by extensively monitoring both penetrative convection and cross-shore flow in an alpine lake over several months.

Materials and methods

Lake Cadagno (46.55°N, 8.71°E) is a small meromictic lake located at 1920 m above sea level, in the Piora valley (Ticino, Switzerland). Due to its location, the lake is relatively wind sheltered and experiences strong night-time cooling, which makes it a potential site to study thermal syphons. It has a surface area of 0.26 km^2 and it reaches 21 m at the deepest point (Del Don, Hanselmann, Peduzzi, & Bachofen, 2001).

Measurements consist of both mooring data and microstructure profiles. Three vertical moorings are installed along a cross-shore transect from June to September 2018. The location of the transect was chosen according to the presence of a shallow region nearshore that is expected to drive cross-shore flows. The first mooring M1 (depth of 4.5 m) is installed in this region where the density current is initiated. The two other moorings M2 (depth of 7.5 m) and M3 (depth of 18 m) are located in the steeper region offshore, above and below the August thermocline, respectively.

Thermistors chains continuously measure the lake temperature at these three locations, from surface to bottom. A one-meter vertical resolution is used, except in the top first meter and in the bottom two meters where the resolution is increased up to 4 sensors/m to capture the penetrative convection and density currents respectively. Current velocity is also sampled at the three moorings, using pulse-coherent Acoustic Doppler Current Profilers (ADCP). Conductivity is measured at M1 and M2 to get information on the possible influence of subaquatic springs. Additionally, Photosynthetically Active Radiation (PAR), dissolved oxygen concentration and turbidity are monitored at different depths along M3.

Two other moorings M4 and M5 are installed at the lake bottom to measure water temperature 30 cm above the sediment over the entire summer. M4 is parallel to the transect M1-M3 and allows increasing the spatial resolution in the cross-shore direction. M5 is deployed along the 8.5 m isobath and collects information on the structure of the flow in the alongshore direction.

To study the development and decline of the thermal syphon over one night (6:00 pm – 10:00 am), microstructure profiles are taken along the cross-shore and alongshore directions, using the PME SCAMP microprofiler (downward mode). The obtained high-resolution temperature data can be used to estimate the turbulence intensity across the water column, related to the combined effects of the density current and penetrative convection.

The transition between penetrative convection (night) and stable stratification (day) leads to the inhibition of the cross-shore flow. This process is monitored by taking microstructure profiles in the early morning (5:00 am – 8:00 am) from a platform located in the deepest region of the lake. High-resolution temperature data from the very top layers is obtained by using the microprofiler in upward mode. The onset of light penetration through the water column is determined by a temporary mooring composed of three PAR sensors.

Finally, a small meteorological station provides air temperature, wind and solar radiation data.

Preliminary results will be presented and discussed.

REFERENCES

Del Don, C., Hanselmann, K. W., Peduzzi, R., & Bachofen, R. (2001). The meromictic alpine Lake Cadagno: orographical and biogeochemical description. *Aquatic Sciences*, *63*(1), 70–90.

Fer, I., Lemmin, U., & Thorpe, S. (2002). Winter cascading of cold water in Lake Geneva. *Journal of Geophysical Research: Oceans*, *107*(C6).

MacIntyre, S., & Melack, J. M. (1995). Vertical and horizontal transport in lakes: linking littoral, benthic, and pelagic habitats. *Journal of the North American Benthological Society*, *14*(4), 599–615.

Mao, Y., Lei, C., & Patterson, J. C. (2010). Unsteady near-shore natural convection induced by surface cooling. *Journal of Fluid Mechanics*, *642*, 213–233.

Monismith, S. G., Imberger, J., & Morison, M. L. (1990). Convective motions in the sidearm of a small reservoir. *Limnology and Oceanography*, *35*(8), 1676–1702.

Sturman, J., Oldham, C. E., & Ivey, G. N. (1999). Steady convective exchange flows down slopes. *Aquatic Sciences*, *61*(3), 260–278.

Diurnal Cycling of Convective Plume Formation

Alexander Forrest[1,2,]*, Hugo Ulloa[3] and Bernard Laval[4]

[1] Civil & Environmental Engineering, University of California – Davis, Davis, CA, USA
[2] Tahoe Environmental Research Center, University of California – Davis, Incline Village, NV, USA
[3] EPFL, Physics of Aquatic Systems Laboratory – Margaretha Kamprad Chair, Lausanne, Switzerland
[4] Civil Engineering, University of British Columbia, Vancouver, BC, Canada

**Corresponding and presenting author, e-mail alforrest@ucdavis.edu*

KEYWORDS
Nearshore heating, penetrative convection, convective cells, autonomous underwater vehicles, Pavilion Lake

ABSTRACT

Penetrative convection through surface cooling and buoyant plume formation through daytime heating of the lakebed are both processes that are well known to drive vertical mixing in the water column in the nearshore. The nature of the formed convective plumes during both of these phases and how they interact with the lake boundaries remains a source of limited field observations. Negatively buoyant, falling plumes are formed during cooling periods (during the night) and positively buoyant, rising plumes are formed during heating periods (during the day). These plumes have been studied experimentally and scaled analytically but there is limited data examining lateral scales and horizontal variability. This lack of knowledge results from the challenges of making robust lateral observations in near-shore regions or having sufficient resolution in numerical models to resolve these features. In August 2007, an Autonomous Underwater Vehicle (AUV) was run at ~1.7 m/s along repeat 500 m, constant depth (2.5 m) transects from the nearshore (~5 m water depth) to the pelagic (~60 m water depth) in Pavilion Lake, BC, Canada in the middle of the convective layer making 16 Hz Conductivity-Temperature-Depth measurements (~6-8 cm sample spacing). These runs were made continuously for three hours just after sunset during the onset of penetrative convection and three hours just after sunrise during the formation of positively buoyant plumes. Minimal winds (< 0.2 m/s) during this time period resulted in ideal conditions to examine the lateral variability of these plumes. Constructed wavenumber spectra allowed the dominant plume widths (10-25 m) to be determined. These plume widths were relatively constant during the initial onset of both processes but then along lake bed currents began to form. Characterizing the nature of these plumes during both the heating and cooling phase of the diurnal cycle allows nearshore water entrainment to be better understood.

Simulating Panarea's offshore CO_2 seeps as a natural proxy for potential leakage from sub-seabed CO_2 storage

J. Gros,* S. Sommer, A. Dale, M. Schmidt

GEOMAR Helmholtz-Zentrum für Ozeanforschung, Kiel, 24148, Germany.

**Corresponding author, e-mail jogros@geomar.de*

ABSTRACT

Natural subsea gas venting offshore Panarea Island (Aeolian Islands, Italy) is known since historical times. >95%-pure CO_2 is vented into the sea at water depths extending up to ~100 m. The numerous venting sites range from individual bubble streams to more vigorous releases which generate upward bubble plumes. The past and future anthropic production of CO_2 raises high climatic concerns. Undergroung CO_2 storage is considered as a mitigation option, already implemented at a few pioneering facilities. As a consequence, the scientific interest is on the rise for natural proxies to potential undesired leaks from subseabed CO_2 storage facilities. The gas venting site offshore Panarea Island was therefore visited during *R/V Poseidon* cruise POS469 in May 2014. Several venting sites have been characterized by a variety of instrumental techniques. This dataset is used to develop a model of aqueous dissolution and further tracking of dissolved carbon dioxide species. The model builds on the existing bubble and plume model TAMOC, previously validated to 64 laboratory datasets for bubbly jets and bubble plumes in quiescent conditions, stratified stagnant conditions, and crossflow conditions, as well as field data from the 2010 *Deepwater Horizon* oil spill and the *DeepSpill* field experiment. The TAMOC model is used to simulate the bubble dynamics including (rapid) mass transfers, three-dimensional movement, and the possible development of a bubble plume. The TAMOC model is coupled to a second model tracking the displacement of dissolved CO_2 and the resulting impact on the carbonate system. Better understanding of the dynamics in play offshore Panarea Island will ultimately provide insights about the expected risks resulting from the possible failures of existing and upcoming offshore, subseabed CO_2 storage facilities.

Interactions between physical and biogeochemical controls on lake carbon gas emissions in spring

J. Jansen*, B. Thornton, M. Wik, and P. Crill

Department of Geological Sciences and Bolin Centre for Climate Research, Stockholm University, Stochkholm, Swedent

**Corresponding author, e-mail joachim.jansen@geo.su.se*

ABSTRACT

Northern lakes are an important source to the atmosphere of the climate forcing trace gases methane (CH_4) and carbon dioxide (CO_2). Emissions are predicted to increase in a warmer climate because of the strong temperature-dependency of ecosystem-level fluxes and longer ice-free seasons. A significant portion of the annual emissions — up to 60% for CH_4 and 30% for CO_2 — takes place in spring, after prolonged ice cover. However, while current Arctic climate change primarily affects the winter season, comparatively little remains known of the physical and biogeochemical drivers of under-ice accumulation and ice-out efflux of carbon gas. Here we present a detailed, multi-year budget of CH_4 and CO_2 for three subarctic lakes in northern Sweden that covers both the ice-covered (2015–2018) and open water seasons (2009–2017). We include measurements of dissolved oxygen, CH_4 stable isotopes and the lake thermal structure. We find that summer CO_2 fluxes depended on catchment C inputs, while CH_4 emissions were a strong function of water temperature. Seasonal redox regime shifts regulated carbon gas storage in winter: pCO_2 increased until all available oxygen was depleted, after which an absence of aerobic methanotrophy facilitated CH_4 accumulation at rates higher than the summer flux. More CH_4 accumulated in years with a longer ice-cover period. However, not all this CH_4 may reach the atmosphere in spring, due to re-oxygenation of the water column associated with snowmelt runoff entering the lake and buoyancy-driven convection. We computed the turbulence-driven diffusive CH_4 fluxes with a surface renewal model and then used an isotope fractionation model to assess the importance microbial oxidation in summer and in spring. Results indicate that the 64–98% of stored CH_4 reaches the atmosphere. Our findings question the assumption that a longer ice-free season will categorically increase annual CH_4 emissions from northern lakes.

Physical, chemical, and biological effects of changing stratification in deep lakes. Can mixing regimes qualify as alternative stable states?

J.P. Mesman[1,2,3]*, S. Goyette[2,3], J. Kasparian[2,3] and B.W. Ibelings[1,3]

[1] Department F.-A. Forel for Environmental and Aquatic Sciences
Faculty of Science, University of Geneva, Geneva, Switzerland
[2] Group of Applied Physics, University of Geneva, Geneva, Switzerland
[3] Institute for Environmental Sciences, University of Geneva, Geneva, Switzerland

**Corresponding author, e-mail Jorrit.Mesman@unige.ch*

KEYWORDS
Deep lakes; climate change; stratification; mixing regimes; alternative stable states.

Introduction

One of the major consequences of climate warming in deep lakes is enhanced thermal stratification. Rising surface water temperatures, reduced ice cover, longer summer stratification, and steeper thermoclines are being observed and this trend is predicted to continue (Shimoda et al., 2011). In deep lakes, thermal stratification greatly controls the spatial distribution of dissolved substances and living organisms. The stronger separation between epilimnion and hypolimnion that results from climate warming promotes increased vertical heterogeneity in oxygen and nutrient concentrations in the water column. In turn, this affects phytoplankton, zooplankton, and fish – both in terms of biomass and species composition (Ficke et al., 2007; Winder & Sommer, 2012).

A potential step-change in the relation between climate warming and thermal stratification in a lake, is when a shift in mixing regime occurs. A mixing regime is defined by the frequency and extent of physical mixing. The strengthening of thermal stratification is altering these regimes in many lakes (Livingstone, 2008). Polymictic lakes of intermediate depth (5-10 m average depth) stratify for longer periods in summer and especially in combination with a reduction in transparency this can evolve into seasonal stratification (Kirillin, 2010; Shatwell et al., 2016). The disappearance of ice cover in some temperate deep lakes removes or shortens the period with inversed stratification, gradually turning dimictic into monomictic lakes (Ficker et al., 2017). As the climate warms, winter periods more frequently fail to cause sufficient convective mixing to mix the entire lake, which promotes a shift from holomixis to meromixis (Schwefel et al., 2016). If incomplete mixing prevails long enough for a chemically-different and denser layer to form near the sediment, this meromixis might even become permanent (Matzinger et al., 2007).

Seasonal mixing regimes differ from each other in several physical, chemical, and biological aspects. In this study we investigate if these different regimes can qualify as alternative stable states, like the well-known clear vs. turbid states in shallow lakes (Scheffer, 1998). Alternative stable states possess feedbacks that maintain the existing situation, providing resilience against regime shifts. This resilience applies to both the pristine and disturbed state, causing hysteresis in lake restoration efforts (Ibelings et al., 2007). To assess the potential alternative stability of mixing regimes, we first reviewed the existing literature on the physical, chemical, and biological effects of increased stratification in deep lakes. We put a particular focus on possible feedback loops that could help stabilise a certain mixing regime. After this review, we list the changes that can be expected around mixing regime shifts and then discuss if mixing regimes could indeed be seen as alternative stable states.

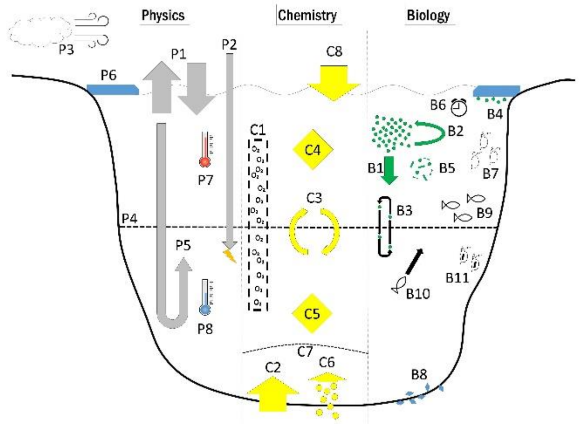

Figure 1: Schematic overview of the physical, chemical and biological processes discussed during the review.

P1: Surface heat flux
P2: Light penetration
P3: Wind
P4: Thermocline depth and strength
P5: Deep-water mixing
P6: Ice cover
P7: Epilimnetic temperature
P8: Hypolimnetic temperature

C1: Oxygen concentration
C2: Internal loading of nutrients & other chemicals
C3: Exchange of substances between epi- and hypolimnion
C4: Epilimnion nutrient concentration
C5: Hypolimnion nutrient concentration
C6: Greenhouse gas emissions
C7: Permanent meromixis
C8: External loading of nutrients

B1: Phytoplankton sinking rates
B2: Phytoplankton biomass and growth
B3: Phytoplankton buoyancy-regulation
B4: Effect of ice on phytoplankton
B5: Phytoplankton species composition
B6: Timing spring blooms phytoplankton & zooplankton
B7: Zooplankton
B8: Benthos
B9: Fish productivity
B10: Thermal oxygen-squeeze
B11: Parasitism

Physical, chemical, and biological effects of changing stratification (Figure 1)

Climate warming is causing a clear rise in epilimnetic temperatures, while diverging hypolimnetic temperature trends can be explained by mixing regime, lake morphology and local factors such as wind speed and water transparency. Summer stratification will lengthen and become more stable, with reversed trends in winter stratification, promoting a shift from dimictic to monomictic behaviour in lakes that are likely to experience years without ice cover. Reduced complete mixing events imply a shift from holomictic to more meromictic behaviour. A clear climatic trend in thermocline depth is lacking so far, but this presumably seems to be more strongly affected by wind speed and transparency than by temperature (Shimoda et al., 2011; Kraemer et al., 2015; Magee & Wu, 2017).

Anoxia in deep lakes is becoming more likely as a result of stronger stratification and changes in mixing regimes. This can enhance internal nutrient loading, but the stronger separation between hypolimnion and epilimnion might cause surface nutrient concentrations to decline in lakes where internal loading is the main source of nutrients. However, there is an increased risk of nutrient peaks after deep mixing events. The possibility of climate-induced formation of permanent meromixis by internal loading is not yet well covered by the existing literature (Sahoo et al., 2013; Lehmann et al., 2015; Schwefel et al., 2016).

Rising water temperatures, stronger stratification, increased risk on anoxia, and a more heterogeneous distribution of nutrients will alter phytoplankton communities. Depending on trophic status, phytoplankton biomass can both increase (in eutrophic systems) or decrease (oligotrophic) with climate change. Small and buoyancy-regulating species are likely to benefit most from the trend of increasing stratification. The earlier melting of ice and onset of stratification can cause shifts in the spring blooms of phytoplankton and zooplankton and a longer growing season. Habitat of fish species is affected by rising temperatures, posing a potential risk for coldwater adapted fish in temperate lakes if this is combined with anoxia (Ficke et al., 2007; Winder & Sommer, 2012; Kraemer et al., 2017).

Mixing regimes as alternative stable states?

Here we assess the different regime shifts and whether or not they can be seen as shifts in alternative stable states. During a period with warm and calm weather, stratification can form in polymictic lakes, which reduces oxygen concentrations near the sediment (Wilhelm & Adrian, 2008). If this episode lasts long enough for anoxia to form, phosphorus mobilization can stimulate algal growth and therefore reduce transparency, which further restricts heating to the upper layer and reinforces the stratified state. A shift from dimictic to holomictic is almost exclusively determined by atmospheric conditions, so there is little influence of previous year's ice cover and therefore a lack of hysteresis. A model study by Sugiyama et al. (2017) suggests that the ice-albedo feedback can be relevant for heating of large and deep lakes, but this hasn't yet been shown in observational data. Reduced frequency of complete mixing, so the shift from holomixis to meromixis, shows something that could be described as “reversed hysteresis”. Incomplete mixing stimulates heating of the hypolimnion, which facilitates complete mixing in subsequent years (Livingstone, 1997). So, continuation of the current state is hampered. The exception can be formation of permanent meromixis, where water density near the sediment increases as caused by build-up of salts. This layer can resist to further mixing and allow for an alternatively stable mixing regime to form. However, it should be noted that permanent meromixis cannot form in shallow lakes or basins that are prone to strong seiching.

This study showcases the importance of changes in thermal stratification, in line with other reviews (Gerten & Adrian, 2002; Shimoda et al., 2011; Winder & Sommer, 2012), yet zooms in on the mixing regime shifts in particular. These transitions are becoming more likely under the influence of a warming climate. Mixing regimes may differ in several aspects, but may generally not be seen as alternative stable states, unless anoxia in a polymictic lake triggers further stratification, or if permanent meromixis is induced. Therefore shifts from dimictic to monomictic and from holomictic to meromictic are unlikely to be abrupt and irreversible, but seasonal stratification in formerly polymictic lakes and permanent meromixis can exhibit resilience to perturbations.

REFERENCES

Ficke, A. D., Myrick, C. A., & Hansen, L. J. (2007). Potential impacts of global climate change on freshwater fisheries. *Reviews in Fish Biology and Fisheries, 17*(4), 581-613. doi:10.1007/s11160-007-9059-5

Ficker, H., Luger, M., & Gassner, H. (2017). From dimictic to monomictic: Empirical evidence of thermal regime transitions in three deep alpine lakes in Austria induced by climate change. *Freshwater Biology, 62*(8), 1335-1345. doi:10.1111/fwb.12946

Gerten, D., & Adrian, R. (2002). Effects of climate warming, North Atlantic Oscillation, and El Nino-Southern Oscillation on thermal conditions and plankton dynamics in northern hemispheric lakes. *The Scientific World Journal, 2*, 586-606. doi:10.1100/tsw.2002.141

Ibelings, B. W., Portielje, R., Lammens, E. H. R. R., Noordhuis, R., van den Berg, M. S., Joosse, W., & Meijer, M. L. (2007). Resilience of Alternative Stable States during the Recovery of Shallow Lakes from Eutrophication: Lake Veluwe as a Case Study. *Ecosystems, 10*(1), 4-16. doi:10.1007/s10021-006-9009-4

Kirillin, G. (2010). Modeling the impact of global warming on water temperature and seasonal mixing regimes in small temperate lakes. *Boreal environment research, 15*(2), 279-293.

Kraemer, B. M., Anneville, O., Chandra, S., Dix, M., Kuusisto, E., Livingstone, D. M., . . . Sitoki, L. M. (2015). Morphometry and average temperature affect lake stratification responses to climate change. *Geophysical Research Letters, 42*(12), 4981-4988.

Kraemer, B. M., Mehner, T., & Adrian, R. (2017). Reconciling the opposing effects of warming on phytoplankton biomass in 188 large lakes. *Scientific Reports, 7*(1), 10762. doi:10.1038/s41598-017-11167-3

Lehmann, M. F., Simona, M., Wyss, S., Blees, J., Frame, C. H., Niemann, H., . . . Zopfi, J. (2015). Powering up the “biogeochemical engine”: the impact of exceptional ventilation of a deep meromictic lake on the lacustrine redox, nutrient, and methane balances. *Frontiers in Earth Science, 3*. doi:10.3389/feart.2015.00045

Livingstone, D. M. (1997). An example of the simultaneous occurrence of climate-driven “sawtooth” deep-water warming/cooling episodes in several Swiss lakes. *Internationale Vereinigung für theoretische und angewandte Limnologie: Verhandlungen, 26*(2), 822-828.

Livingstone, D. M. (2008). A change of climate provokes a change of paradigm: taking leave of two tacit assumptions about physical lake forcing. *International Review of Hydrobiology, 93(4‐ 5)*, 404-414.

Magee, M. R., & Wu, C. H. (2017). Response of water temperatures and stratification to changing climate in three lakes with different morphometry. *Hydrology and Earth System Sciences, 21*(12), 6253-6274. doi:10.5194/hess-21-6253-2017

Matzinger, A., Schmid, M., Veljanoska-Sarafiloska, E., Patceva, S., Guseska, D., Wagner, B., . . . Wüest, A. (2007). Eutrophication of ancient Lake Ohrid: Global warming amplifies detrimental effects of increased nutrient inputs. *Limnology and Oceanography, 52*(1), 338-353.

Sahoo, G., Schladow, S., Reuter, J., Coats, R., Dettinger, M., Riverson, J., . . . Costa-Cabral, M. (2013). The response of Lake Tahoe to climate change. *Climatic Change, 116*(1), 71-95.

Scheffer, M. (1998). *Ecology of Shallow Lakes*. London: Chapman & Hall.

Schwefel, R., Gaudard, A., Wüest, A., & Bouffard, D. (2016). Effects of climate change on deep‐ water oxygen and winter mixing in a deep lake (Lake Geneva)–Comparing observational findings and modeling. *Water Resources Research*.

Shatwell, T., Adrian, R., & Kirillin, G. (2016). Planktonic events may cause polymictic-dimictic regime shifts in temperate lakes. *Scientific Reports*, *6*, 24361. doi:10.1038/srep24361
Shimoda, Y., Azim, M. E., Perhar, G., Ramin, M., Kenney, M. A., Sadraddini, S., Gudimov, A., Arhonditsis, G. B. (2011). Our current understanding of lake ecosystem response to climate change: What have we really learned from the north temperate deep lakes? *Journal of Great Lakes Research*, *37*(1), 173-193.
Sugiyama, N., Kravtsov, S., & Roebber, P. (2017). Multiple climate regimes in an idealized lake–ice–atmosphere model. *Climate Dynamics, 50*(1-2), 655-676. doi:10.1007/s00382-017-3633-x
Wilhelm, S., & Adrian, R. (2008). Impact of summer warming on the thermal characteristics of a polymictic lake and consequences for oxygen, nutrients and phytoplankton. *Freshwater Biology*, *53*(2), 226-237.
Winder, M., & Sommer, U. (2012). Phytoplankton response to a changing climate. *Hydrobiologia*, *698*(1), 5-16. doi:10.1007/s10750-012-1149-2

Assessing the optimal input data frequency for the GOTM Lake Physical Model

Tadhg Moore[1]*, Karsten Bolding[2], Jorn Bruggeman[2], Raoul-Marie Couture[3], Mary Dillane[4], Moshe Estroti[5], Elvira de Eyto[4], Gideon Gal[5], Jose-Luis Guerrero[3], Eleanor Jennings[1], Eric Jeppesen[6], Anders Nielsen[6], Denis Trolle[6], and Don Pierson[7]

[1] Centre for Freshwater and Environmental Studies, Dundalk Institute of Technology, Dundalk, Co. Louth, Ireland
[2] Bolding & Bruggeman ApS
[3] NIVA, Oslo, Norway
[4]Marine Institute, Newport, Co. Mayo, Ireland
[5]Kinneret Limnological Laboratory, Kinneret, Israel
[6]Aarhus University, Silkeborg, Denmark

**Corresponding author, e-mail tadhg.moore@dkit.ie*

KEYWORDS
Lakes; environment; water quality; modelling; high frequency monitoring.

Introduction

Lake water quality is increasingly under pressure due to anthropogenic activities including directional climate change and for example intensification of agriculture. Lake models have been developed to gain a greater understanding of the processes that govern lake water quality and to develop methods to simulate water quality. However, modelling water quality requires a modelling framework that includes models of lake physics, biogeochemical models and catchment models. The General Ocean Turbulence Model (GOTM) was developed to model hydrodynamics in 1-dimension in the oceans. It has been adapted for use in lake and reservoirs. The current study is linked to the PROGNOS project (Predicting in lake responses to change using near real time models) (http://prognoswater.org/) a Water JPI funded project which aims to develop a modelling framework that can predict changes in the water quality of lakes and reservoirs in the short-term i.e. 5-7 days. Threats such as algal blooms and increasing levels of dissolved organic matter (DOM) impact lakes as they can affect water aesthetics, recreational use, water treatment processes and drinking water quality (Delpla et al., 2009; Whitehead et al., 2009). The modelling framework adopted within PROGNOS includes coupling a lake physical model with a lake biogeochemical model and using local meteorological forecast data to drive the model. For a model to be used in a water management framework it is critical that to increase monitoring efficiencies there is a need to know at what frequency lake water temperature profile data needs to be collected at to calibrate the lake model and if freely available gridded weather data products can be used to run the model rather than locally measured meteorological.

Materials and methods

Water temperature profile data were subsampled at increasing time steps and the resulting datasets were used to calibrate the model. Additionally, model performance was assessed using five different meteorological datasets: local measured data and four different gridded datasets were used. These assessments were carried out for three different lakes: Feeagh (Ireland), Erken (Sweden) and Langtjern (Norway) which are of varying size and various mixing regimes. Modelled water temperature was then compared to observed water temperature from the HFM systems on each of the three sites for both time periods using several comparison metrics. For this comparison, each dataset was assessed over seven distinct periods: 1) the calibration, 2) validation, 3) isothermal, 4) inverse stratification (only for Langtjern), 5) stratification, 6) mixing events and 7) warming events. The metrics included direct comparison of water temperatures, temperature at the top 5m and the bottom 5m, as well as the derived functions Schmidt stability (Schmidt, 1928), and mixed layer depth.

Results and discussion

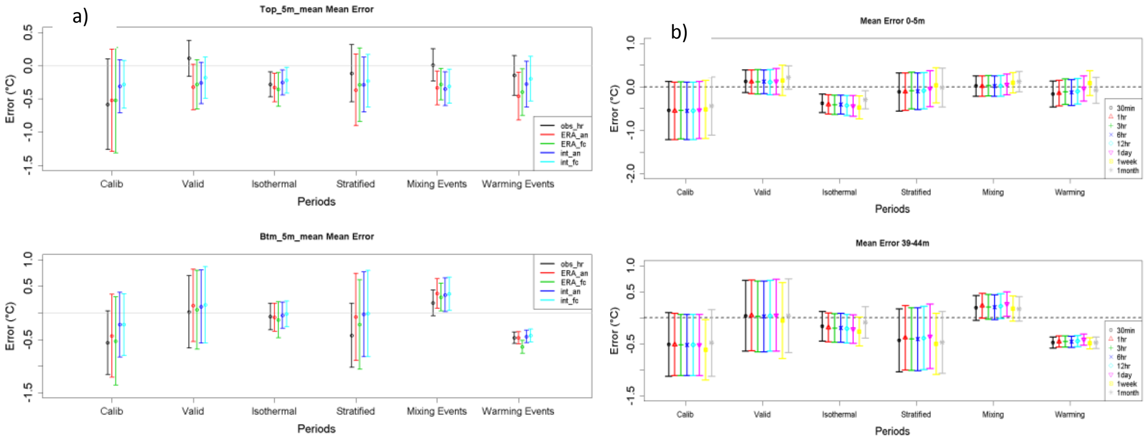

Fig 1. a) Mean error and standard deviation for the top 5m and bottom 5m for each meteorological dataset for Feeagh. b) Mean error and standard deviation for the top 5m and bottom 5m for each temporal frequency.

Despite there being differences between the locally observed meteorological data and the gridded ECMWF data, this did not result in there being a large difference between the model performance with the different meteorological datasets. The calibration of the lake model with the different meteorological datasets (ECMWF Interim and ECMWF ERA5) allowed the model to reproduce similar lake temperature profiles across all three lakes. The modelling experiment to investigate the effect of changing the temporal frequency of the calibration data on model performance showed that even the use of relatively low-resolution data (e.g. at weekly or monthly time intervals) simulated water temperature data with a high degree of accuracy.

This work showed that gridded meteorological datasets, which are freely obtainable on-line, could be used to run GOTM and replicate observed water temperature profiles to a high degree of accuracy. The use of gridded data offers many benefits for lake modellers as it allows the GOTM model to be set up on lakes where there is little to no local meteorological data collected on site or for when equipment malfunctions and creates gaps in the dataset. The results from this investigation imply that the model can be used with confidence even for lakes which have low frequency monitoring data. This would be an important benefit for water managers as they could save in terms of human resources, time and budget if the frequency at which monitoring was undertaken could be reduced.

REFERENCES

Delpla, I., Jung, A. V., Baures, E., Clement, M., & Thomas, O. (2009). Impacts of climate change on surface water quality in relation to drinking water production. *Environment International*, *35*(8), 1225–1233. https://doi.org/10.1016/j.envint.2009.07.001

Whitehead, P. G., Wilby, R. L., Battarbee, R. W., Kernan, M., & Wade, A. J. (2009). A review of the potential impacts of climate change on surface water quality. *Hydrological Sciences Journal*, *54*(1), 101–121. https://doi.org/10.1623/hysj.54.1.101

Evaluation of historical patterns of thermal structure of Lake Erken using hydrodynamic model

S. Moras*, A. Ayala-Zamora, D. Pierson

Department of Ecology and Evolution, Faculty of Science and Technology, Uppsala University, Uppsala, Sweden

**Corresponding author, e-mail simonemoras93@gmail.com*

ABSTRACT

The thermal structure of lakes is strictly related to climate and the variability of thermal and mixing dynamics. In this study, we used a hydrodynamic model (GOTM) to simulate hourly time-step water temperature of lake Erken (Sweden) over the period 1961-2016, using seven climatic parameters as forcing data: wind speed, air temperature, atmospheric pressure, relative humidity, cloud cover, precipitation and shortwave radiation. From the long-term simulations of water temperature, this study focuses on detecting possible trends on water temperature at different depths. Moreover, the analysis of the simulated temperature will assess whether changes in the phenology of thermal stratification, such as changes in the timing and depth of stratification have occurred over the 56-years period of study. Providing a complete dataset of hourly water temperature over the last 56 years from lake Erken will also be a valuable resource of information for future research that involves, for example, experiments on regime shift, phytoplankton production, nutrient load, gas ebullition etc.

Climatic forcing data were retrieved from a weather station located on a small island in the lake where automated high frequency data have been collected since 1988. During the period 1961-1988, climate data were retrieved from paper records collected from the same station and from weather stations in the vicinity of the lake. The simulated water temperature has been calibrated with real water temperature data measured over the study period.

Preliminary results have shown that the modelled surface temperature is well predicted and show a rise in the mean surface water temperature during summer. Surface water temperatures were mostly below 20 °C during the period 1961-1970, as confirmed by manual measurements from that time period. More recent periods reveal that surface temperature in summer is usually over 20° C, suggesting that climate change could have an effect on surface water temperature.

Convection near the Temperature of Maximum Density

Jason Olsthoorn*, Edmund Tedford and Gregory Lawrence

Department of Civil Engineering, University of British Columbia, BC, Canada

**Corresponding author, e-mail Jason.Olsthoorn@ubc.ca*

KEYWORDS
Lakes; Numerical Modelling; Equation of State; Under-Ice Convection; Mixing;

Introduction

Fresh water has the property that it's temperature of maximum density (T_{MD}) is above its freezing point. This feature allows for the possibility of forming a 'reverse stratification' in northern lakes, where the water is colder at the surface than it is at depth. The formation of this reverse stratification has been observed in a number of different lake volumes and geometries (see Farmer and Carmack (1981) and Kirillin *et al.* (2012)).

In this paper, we examine the convection of waters near T_{MD}. As a simplification of the problem of a surface cooled water body, we study the classic 'Rayleigh-Taylor' problem where we prescribe a non-linear equation of state for the fluid density as a function of temperature. We are particularly interested in how this additional nonlinearity alters the evolution of the density field.

Materials and methods

Chen and Millero (1984) performed a comprehensive evaluation of the equation of state of fresh water. From their results, it can be shown that, for shallow bodies of water (where the hydrostatic pressure variation is negligible in the equation of state), the equation of state is nearly quadratic about T_{MD}. Thus, near T_{MD}, the equation of state is essentially nonlinear. However, for fluid temperatures much greater than T_{MD}, a local linear approximation is appropriate. Thus, in this paper, we will consider two equations of state, given:

$$\rho_{lin} = -T, \qquad \rho_{quad} = -T^2.$$

Here, ρ is the nondimensionalized fluid density, and T is the fluid temperature.

The classic Rayleigh-Taylor problem is defined by the evolution of an initially unstable two-layer stratification, in which a more dense fluid layer is located above a less dense fluid layer. The density interface between the two layers is unstable to a range of wavenumber perturbations, which grow to finite amplitude and subsequently lead to an overturning of the density field. As we are interested in this problem where it applies to lake water near the temperature of maximum density, we will prescribe a density difference of $\Delta\rho \setminus \rho_0 = 1.3 \times 10^{-4}$, where ρ_0 is a reference density for water. This density difference corresponds, to the density jump between water of $8°C$ to $4°C$.

In order to assess the dependency of the convection on the equation of state, we will perform two-dimensional numerical simulations of the Navier-Stokes equations under the Boussinesq approximation. Particularly noteworthy is that, due to certain numerical constraints, these simulations will be performed assuming a constant volume. However, this constant volume approximation, when considering a nonlinear equation of state, implies that there is a violation of the conservation of mass within the system. Due to the limited density variations in the numerical simulations, we do not believe that this will have a significant effect on our results.

Results and discussion

Figure 2 is a plot of the density field at a particular output time for ρ_{lin}(a) and ρ_{quad} (b). This figure highlights that the nonlinearity of the equation of state alters the symmetry of the problem. In particular, the quadratic equation of state results in the upward propagating bubbles being retarded and smaller than in the corresponding linear case. Conversely, in the lower layer, the downward propagating plumes impact the bottom boundary first and are larger in extent for a nonlinear equation of state.

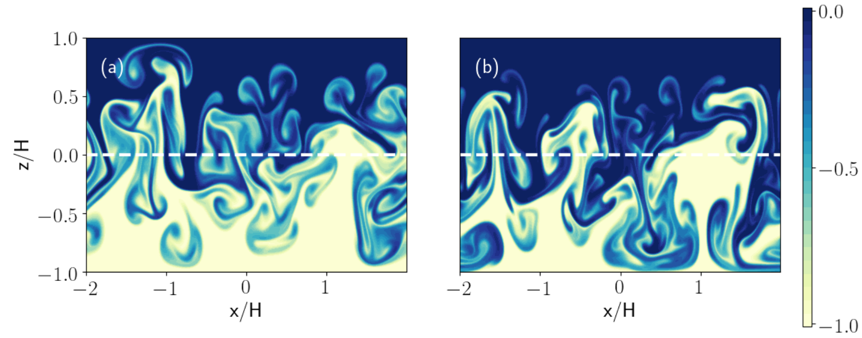

Figure 2 Comparison of the horizontally averaged density field as a function of time for ρ_{lin} (a) and ρ_{quad} (b). Contours of the 5% and 95% density isopycnals have also

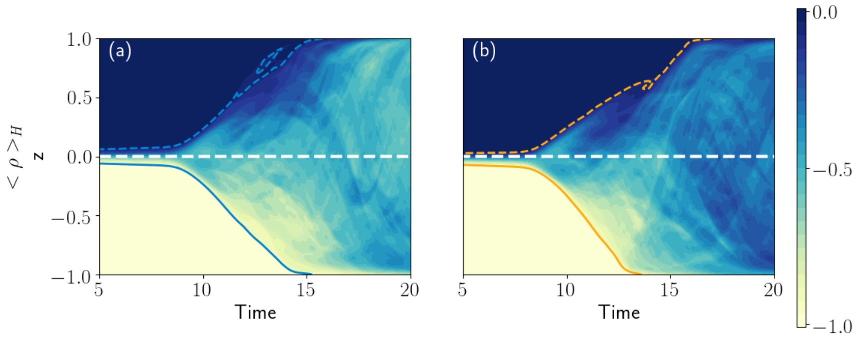

We reiterate this point in Figure 1, which is a plot of the horizontally averaged density field profiles as a function of time for ρ_{lin}(a) and ρ_{quad} (b). In addition, we have included the 5% and 95% isopycnal contours. By comparing the two contours, it becomes apparent that in an averaged sense, the mixing region grows symmetrically for a linear equation of state, while there is an asymmetry to that region when the equation of state is nonlinear.

This work highlights that the nonlinearity of the equation of state near the temperature of maximum density of lake water can affect the structure of the convection. This may prove to be a significant feature when considering the lake turnover and subsequent establishment and break down of the reverse-stratification in lakes. More work, including laboratory studies, are currently underway to understand this phenomenon.

REFERENCES

Chen, C. T. A., & Millero, F. J. (1986). Precise Thermodynamic Properties For Natural-Waters Covering Only The Limnological Range. Limnology And Oceanography, 31(3), 657–662.

Farmer, D. M., & Carmack, E. (1981). Wind mixing and restratification in a lake near the temperature of maximum density. Journal of Physical Oceanography, 11,1516-1533.

Kirillin, G., Leppäranta, M., Terzhevik, A., Granin, N., Bernhardt, J., Engelhardt, C., … Zdorovennov, R. (2012). Physics of seasonally ice-covered lakes: A review. Aquatic Sciences, 74(4), 659–682.

Multi-lake Swiss Survey: hydrodynamic response to climate forcing

C. Ordóñez[1]*, T. Langenegger[1], T. DelSontro[1], S. Flury[2], K. W. Tang[3] and D. F. McGinnis[1]

[1] Department F.-A. Forel for environmental and aquatic sciences
Faculty of Science, University of Geneva, Geneva, Switzerland
[2] Stream Biofilm and Ecosystem Research Laboratory, Institute of Environmental Engineering, School of Architecture, Civil and Environmental Engineering, Ecole Polytechnique Fédérale de Lausanne, Lausanne, Switzerland
[3] Department of Biosciences, Swansea University, Swansea SA2 8PP, United Kingdom

**Corresponding author, e-mail cesar.ordonez@unige.ch*

KEYWORDS
Lakes; climate change; water quality.

ABSTRACT

The changes of lakes are often a reflection of changing climate forcing or alterations on the surrounding land use. Meteorological processes impact the lake's internal heating, cooling and mixing, while an increase in agriculture or urban development can increase the loading of nutrients on the lake, thereby impacting the trophic state. To understand these changes, we chose seven Swiss Lakes for intense monitoring in 2018 with the goal to assess the overall 'health' of the lakes with an emphasis on climate effects, hydrodynamics, greenhouse gases (methane and carbon dioxide) and ecology. We selected two sets of lakes with identical climate forcing, three in the Swiss Plateau and four in the Pre-Alpine region. Each group consists of lakes that are geographically close but have different water quality characteristics. Two campaigns of measurements (June-July and September) are planned, where CTD profiles (temperature, salinity, Chlorophyll a, oxygen, pH, PAR and conductivity), and water column concentrations and emission of methane and carbon dioxide were measured. Water samples for nutrients and algae were also obtained. In addition, a mooring with light, oxygen, temperature and water level loggers were deployed in each lake with 1 minute sampling resolution for the duration of the summer. Finally, in each region a weather station was installed to measure basic meteorological parameters every 10 minutes.

With this database, we will determine how hydrodynamics of the lakes respond differently to the same climatic conditions due to varying water quality (i.e. light dynamics). We will then compare the two sets of lakes from the different zones to investigate the role of the varying climate settings. Moreover, these data will provide a key benchmark for future studies, and allow us to create lake-wide budgets relating environmental variables to lake health. In this poster presentation, we will present our preliminary results.

Effect of meso-scale surface water temperature heterogeneity on surface cooling estimates of a large lake: Airborne remote sensing results from Lake Geneva

A. Irani Rahaghi[1]*, U. Lemmin[1], D.A. Barry[1]

[1] *Ecological Engineering Laboratory (ECOL), Environmental Engineering Institute (IIE), Faculty of Architecture, Civil and Environmental Engineering (ENAC), Ecole Polytechnique Fédérale de Lausanne (EPFL), 1015 Lausanne, Switzerland*

**Corresponding author, e-mail abolfazl.iranirahaghi@epfl.ch*

KEYWORDS
Surface water temperature, surface cooling, remote sensing, Lake Geneva, atmospheric boundary layer stability.

Introduction

Lake Surface Water Temperature (LSWT) is one of the main parameters for the estimation of surface cooling in lakes. Surface cooling estimates, including long-wave radiation and the surface turbulent heat fluxes, may be sensitive to space and time averaging of the input variables including LSWT. A small (~ 1°C) variation in the LSWT, particularly under near-neutral Atmospheric Boundary Layer (ABL) stability conditions, may result in a significant modification of surface cooling of a water body. To estimate the surface heat fluxes over water bodies, in situ point measurements or satellite surface temperature data are most often used. Satellite thermal images are representative for a surface area with typical pixel resolution of O(1 km). Thus far, however, little attention has been given to LSWT spatial heterogeneity at sub-pixel satellite resolution. In the present case study, we assess the effect of LSWT meso-scale variation on the surface cooling distribution and its area-averaged estimate.

Materials and methods

A measurement platform comprising (i) an airborne balloon for thermal imagery (called BLIMP), and (ii) an autonomous catamaran (called ZiviCat) are used to resolve the LSWT at meso-scales. The BLIMP was attached to a small balloon tethered to a winch on a boat, from which its height is controlled. It carried a thermal imagery package suspended beneath it. Simultaneous ground-truthing of the BLIMP data was achieved using the ZiviCat which measures in situ near-surface water temperatures as well as other meteorological parameters.

This study was carried out over Lake Geneva (Fig. 1). Four field measurement data sets were selected for this study that their locations and dates are indicated in Fig. 1. The calibrated Monin-Obukhov similarity concept and the Stefan- Boltzmann law with a surface water emissivity of 0.97 were employed to estimate the turbulent heat fluxes and long-wave back radiation, respectively.

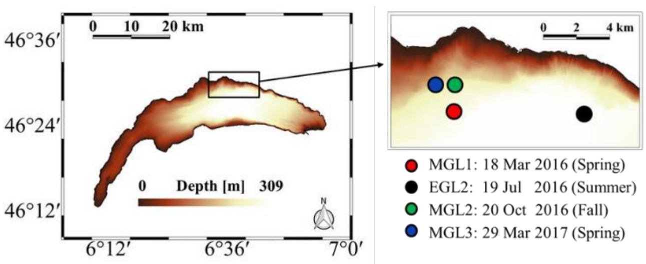

Fig. 1. Location and bathymetry of Lake Geneva. The inset shows the area of the selected missions.

Results and discussion

The registered thermal images for all selected missions are presented in Fig. 2. It shows various cold-warm patches and streak-like structures on the lake surface. It indicates that the LSWT spatial variability within a typical satellite pixel can be significant. The spatial variability is more pronounced during the MGL1 and EGL2 missions with an LSWT spatial range of > 2 and > 3.5°C, respectively, over an area covering less than 1 km^2. MGL2 is a representative case for the cold season, when the spatial variability of LSWT at meso-scales is negligible (< 0.1°C). Except for MGL2, the remaining selected LSWT patterns show a negatively skewed distribution (top panels in Fig. 3).

We used the calibrated bulk formulas together with the obtained LSWT spatial maps (Fig. 2) and the area-averaged meteorological data to compute the lake surface cooling (Q_c) patterns. The results showed a spatial surface cooling range of > 20 Wm^{-2} and > 40 Wm^{-2} for MGL1 and EGL2 missions, respectively. Due to the nonlinear relationship between turbulent surface heat fluxes and LSWT, the negatively skewed LSWT distributions resulted in both negatively and positively skewed surface cooling patterns, respectively, under very stable or predominantly unstable ABL conditions, and predominantly stable ABL conditions (bottom panels in Fig. 3). Implementing a mean spatial filter, the effect of area-averaged LSWT on the surface cooling estimation of a typical satellite pixel was assessed. The effect of the averaging filter size on the mean spatial surface cooling values was negligible, except for predominantly stable ABL conditions when a reduction of ~3.5 Wm^{-2} from high O(1 m) to low O(1 km) pixel resolution was obtained.

REFERENCES

Brodeau, L., B. Barnier, S. K. Gulev, and C. Woods. 2017. Climatologically significant effects of some approximations in the bulk parameterizations of turbulent air-sea fluxes. J. Phys. Oceanogr. **47:** 5-28. doi: 10.1175/Jpo-D-16-0169.1.

Hughes, P. J., M. A. Bourassa, J. J. Rolph, and S. R. Smith. 2012. Averaging-related biases in monthly latent heat fluxes. J. Atmos. Oceanic Technol. **29:** 974-986. doi: 10.1175/Jtech-D-11-00184.1.

Mahrt, L., and T. Hristov. 2017. Is the influence of stability on the sea surface seat flux important? J. Phys. Oceanogr. **47:** 689-699. doi: 10.1175/Jpo-D-16-0228.1.

Mahrt, L., and D. Khelif. 2010. Heat fluxes over weak SST heterogeneity. J. Geophys. Res.: Atmos. **115:** D11103. doi: 10.1029/2009jd013161.

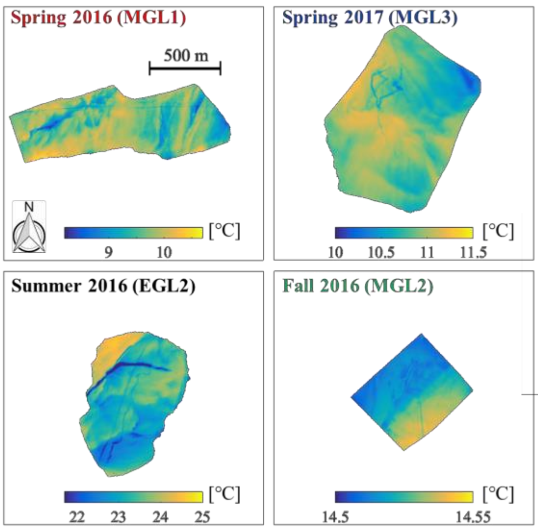

Fig. 2. Meso-scale lake surface water temperature patterns for all selected field missions. Note that the temperature range of the legends is different in each panel, and all panels cover an approximately 1.8 km × 1.8 km area.

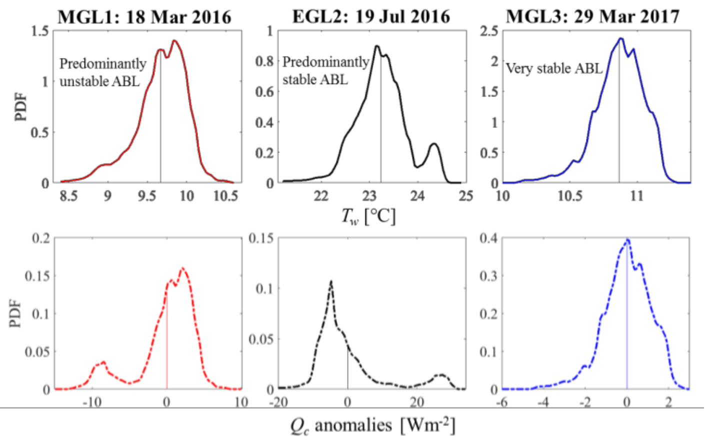

Fig. 3. Probability distribution function (PDF) of the three selected field missions for LSWT (top panels) and the corresponding surface cooling anomalies (bottom panels). The thin vertical lines indicate the mean value for each distribution. Note that the range of abscissa is different in each panel.

Differential cooling and near-shore dynamics in a large lake

R. S. Reiß[1]*, U. Lemmin[1], D. A. Barry[1]

[1] *Ecological Engineering Laboratory (ECOL), Environmental Engineering Institute (IIE), Faculty of Architecture, Civil and Environmental Engineering (ENAC), Ecole Polytechnique Fédérale de Lausanne (EPFL), 1015 Lausanne, Switzerland*

**Corresponding author: rafael.reiss@epfl.ch*

KEYWORDS
Lake Geneva; differential cooling; density current; fiber-optic distributed temperature sensing

Introduction

Density currents generated by differential cooling in lakes with shallow shore regions or side basins are associated with increased vertical mixing, deep water renewal and cross-shore transport of nutrients and other substances. Previous field experiments in Lake Geneva, the largest lake in Western Europe, showed that such cold-water density currents are a common phenomenon during winter, frequently reaching the thermocline at O(100 m) depth (Fer, Lemmin, and Thorpe 2002). As part of a project investigating large-scale interbasin exchange in Lake Geneva, we examined near-shore wintertime density currents in order to better understand cold-water formation.

Materials and methods

The study is based on field observations taken on the northern shore of Lake Geneva near Buchillon, 20 km west of Lausanne, in the winters of 2016-2018. Bottom temperatures are inferred from a fiber-optic Distributed Temperature Sensing (DTS) system, laid down on the lateral slope starting at the shore, with a spatial and temporal resolution of O(1 m) and O(0.1°C), respectively. Temperature and current velocities in the water column were recorded by ADCP and thermistor chain moorings. The time-series data are complemented by several CTD profiles taken along transects normal to the shoreline near the moorings. Data from a nearby meteorological mast were used to select calm days favoring convective cooling. Figure 1 shows the mooring locations and the bathymetry at the study site.

Earlier studies focused on the steady-state dynamics along one transect. Our goal is to investigate the generation of density currents and the effect of different shore geometries.

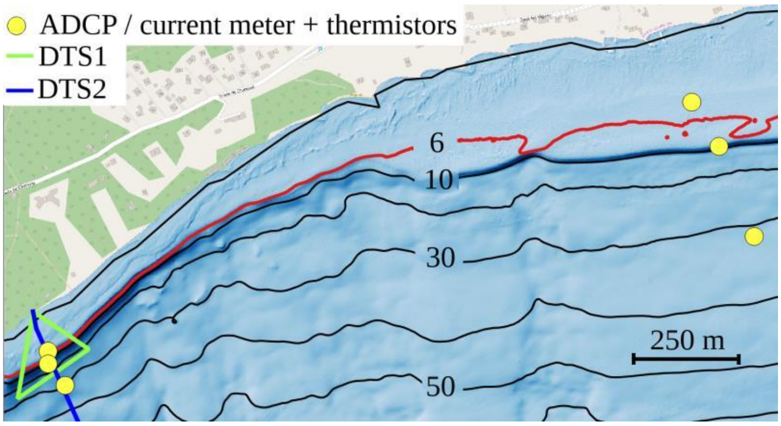

Figure 1: Mooring locations and bathymetry. The red line marks the 6-m depth isobaths.

Preliminary results and discussion

During periods of surface heat loss, i.e., positive surface buoyancy flux B_0, DTS bottom temperatures show cold fronts progressing downslope with the coldest temperatures in the near-shore part, illustrating differential cooling (Figure 2a,b). However, our observations indicate that even during periods with low wind and strong cooling, currents on the shallow shelf have a dominant alongshore component (not shown). This suggests that local wind stress and possibly the large-scale circulation might have to be taken into account when investigating nearshore cold-water formation and cooling dynamics in Lake Geneva.

Figure 2c shows the near-bottom temperature recorded at the two 10-m depth moorings at the wide (eastern) and narrow (western) shelf, respectively. The wide and narrow parts of the shelf show significantly different responses to surface cooling. Starting with similar temperatures the wide shelf cooled down by 0.5°C whereas only minor temperature fluctuations were observed at the narrow shelf. At the wide shelf a cold bottom layer of up to 10-m thickness was visible in the CTD transect until the thermocline at 100-m depth (not shown).

To further elucidate the effect of the shallow shelf width on the generation of cold-water density currents as well as the contribution of both surface heat loss and wind stress a numerical modeling study is planned.

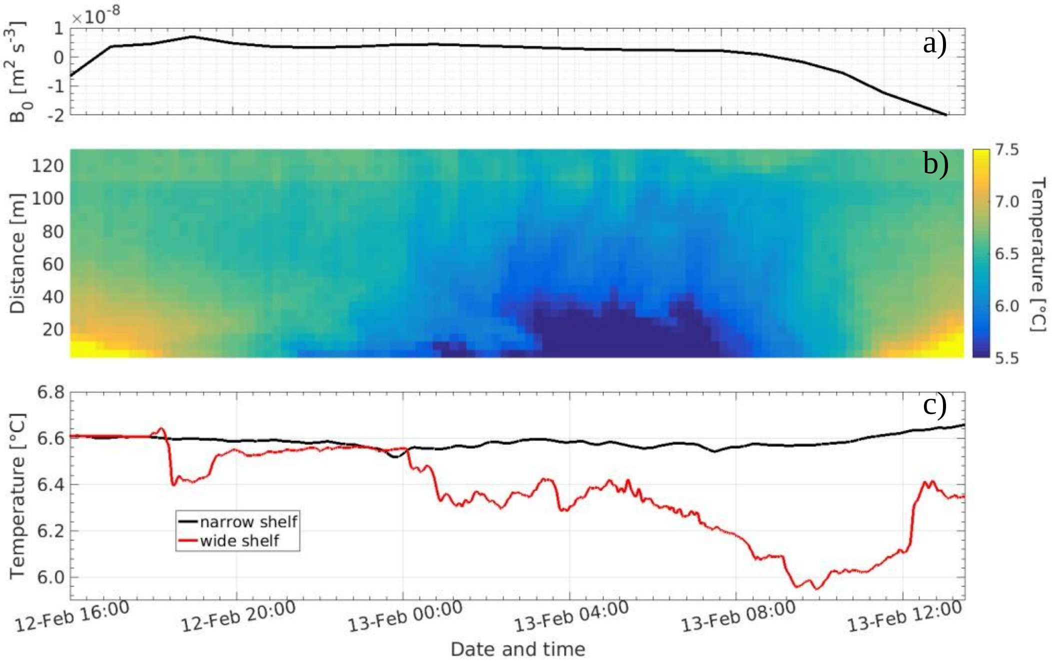

Figure 2: Time series of a) surface buoyancy flux B_0, b) DTS bottom temperatures as a function of distance from the shore and c) thermistor near-bottom temperature at the 10-m depth moorings at both the narrow and wide shelf from 12 to 13 February 2018

REFERENCES

Fer, I., Lemmin, U., and Thorpe, S. A. 2002. "Winter Cascading of Cold Water in Lake Geneva." *Journal of Geophysical Research* 107 (C6). https://doi.org/10.1029/2001JC000828.

Optical characteristics of Aral Sea waters obtained by above water measurements with passive optical complex EMMA

V. Rostovtseva and I. Goncharenko*

P.P. Shirshov Institute of Oceanology RAS, Moscow, Russia

**Corresponding author, email goncharenko@ocean.ru*

ABSTRACT

Studying of the water content and distribution of water main natural constituents over the lakes and marine coastal zones is efficient with the help of satellite passive optical remote sensing methods. However, all of them need ground truth measurements. We held such measurements with our semiautomatic passive optical complex EMMA (Ecological Monitoring of Marine Aquatoria) from board a small motorboat in the salty waters of Eastern Aral Sea in October 2017. Using the new method of signals processing [1], developed and tested by us in the Black Sea and at the Brazilian Coast, we got the spectra of water absorption indices. That enabled us to estimate concentrations of the pigments, “yellow substance” and suspended matter on the route of the boat motion. We compared the obtained estimates with the averaged data of the previous years researches in this region and with some satellite data got in the same period of 2017. Then the remote sensing reflectance spectra of the Aral, derived from EMMA measurements, are collated with the OWT (Optical Water Types) classification [2] suggested for the great amount of freshwater lakes and also with the Black Sea reflectance spectra: their discrepancies are discussed.

REFERENCES

Rostovtseva V.V. Method for sea water absorption spectra estimation on the basis of shipboard passive remote sensing data and pure sea water properties. - *Atmospheric and Oceanic Optics,* 2016, 29(2), 162-170

M. A. Eleveld, A. B. Ruescas, A. Hommersom, T. S. Moore, S. W. M. Peters, C. Brockmann. An optical classification tool for global lake waters. – *Remote sensing, 2017, 9, 420;* doi:10.3390/rs9050420

Local hydrodynamics in fragmented seagrass canopies

Teresa Serra[1,*],Jordi Colomer[1], Marianna Soler[1], Xavier Casamitjana[1] and Carolyn Oldham[2]

[1] *Department of Physics, University of Girona, 17071, Girona, Spain*

[2] *Department of Civil, Environmental and Mining Engineering, The University of Western Australia, Perth WA 6009 Australia,*

**Corresponding author, email teresa.serra@udg.edu*

ABSTRACT

Vegetated systems cover less than 0.5% of the sea bed but account for up to 70% of the carbon storage in ocean sediment. The potential for seagrass to store carbon is partially attributed to erosion protection and sediment stabilization afforded by seagrass meadows. Therefore, aquatic plants play a critical role in protecting coastal areas however there are knowledge gaps surrounding the conditions that optimize this function. The systematic creation of gaps within canopies results in fragmentation and the architecture of fragmented canopies differs substantially from non-fragmented canopies. Canopy fragmentation leads to spatial heterogeneity in hydrodynamics and therefore heterogeneity in the sheltering of canopy communities. Identifying the level of instability due to canopy fragmentation is important for canopies in coastal areas impacted by human activities and indeed, climate change. The gap orientation relative to the wave direction is expected to play an important role in determining wave attenuation and sheltering. Initially we investigated the effect of a single transversal gap within a canopy (i.e. a gap oriented perpendicular to the wave direction) on hydrodynamics, which was compared to fully vegetated canopies (i.e. no gaps) and also to bare sediment. The wave velocity increased with gap width for the two canopy densities studied (2.5% and 10% solid plant fraction) reaching wave velocities found over bare sediments. The turbulent kinetic energy (TKE) within the gap also increased, but was more attenuated by the adjacent vegetation than the wave velocity. As expected, denser canopies produced a greater attenuation of both the wave velocity and the turbulent kinetic energy within an adjacent gap, compared to sparse canopies. Using non-dimensional analysis and our experimental data, a parameterization for predicting TKE in a canopy gap was formulated, as a function of easily measured variables. A fragmented canopy model was then developed to determine the overall mixing level in such canopies. The model revealed that canopies with large gaps present more mixing than canopies with small gaps despite having the same total gap area in the canopy. Furthermore, for the same total gap area, dense fragmented canopies provide more shelter than sparse fragmented canopies.

Effect of temperature on zooplankton vertical migration

S. Simoncelli[1,2]*, D. J. Wain[2] and S. J. Thackeray[3]

[1] *Leibniz Institute of Freshwater Ecology and Inland Fisheries (IGB), Berlin, Germany*
[2] *Department of Architecture and Civil Environmental, University of Bath, Bath, United Kingdom*
[3] *Centre for Ecology and Hydrology, Lancaster Environment Centre Lancaster, United Kingdom*

**Corresponding author, e-mail simoncelli@igb-berlin.de*

KEYWORDS
zooplankton; *Daphnia*; bulk velocity; Diel Vertical Migration.

Introduction

Zooplankton diel vertical migration (DVM) is an ecologically important process, affecting nutrient transport and trophic interactions in lakes and oceans. Several laboratory and field observations suggest that the speed at which zooplankton migrate is influenced by the drivers affecting the DVM. Variations in this velocity can be used as a proxy to infer possible reactions and behavioural changes in zooplankton population. However, available measurements of zooplankton displacement velocity during the DVM in the field are rare, therefore it is not known which factors are key in driving this velocity.

In this study, we continuously measured the displacement velocity (DV) of the migrating layer at sunset and sunrise in the field , along with the DVM drivers. We quantified v_{up} as the bulk velocity at dusk, when zooplankton actively swim to reach the surface, and employed a correlative approach to infer the dependence of v_{up} upon the DVM drivers. At sunrise, when organisms usually sink towards the aphotic lake layer, the mean DV is referred as v_{down}. This velocity was instead modelled and correlated with zooplankton density and size measured in the laboratory to verify whether organisms sank.

Materials and methods

Data were measured during summer 2015 and 2016 in a small and deep (40m) oligotrophic lake, located in southwest UK and mostly populated by *Daphnia*. We employed a bottom-mounted Acoustic-Doppler current profiler (ADCP) to measure the volume backscatter strength (VBS), a proxy for zooplankton concentration and position in the water column. The zooplankton displacement velocity DV was estimated from temporal variations of VBS during the DVMs with a custom image-processing algorithm. We inferred the upwards displacement velocity (v_{up}) for the sunset migration and the sinking velocity (v_{down}) for the downwards movement at sunrise.

We collected time series of temperature data, chlorophyll-a concentration with a fluorometer, and zooplankton vertical concentration before the DVM with a zooplankton net. Solar radiation data were used to infer the relative increase in light intensity when the DVM began, coupled with transparency measurements from Secchi disk and PAR profiles.

We also modelled the *Daphnia* sinking rate with a custom Stokes-like equation using information about zooplankton density, body length and width, and appendages length measured in the laboratory from organisms collected in the field. *Daphnia* was assumed to behave like a sinking ellipsis with the antennae modelled as small cylinders.

Results and discussion

The upwards bulk velocity v_{up} (Fig 1, positive values) exhibited an increasing pattern over time ranging between 2 and 5 mm/s. v_{up} was strongly correlated with the water temperature in the zooplankton migrating layer (Fig 2a). Based upon our analysis, chlorophyll concentration, relative change of light intensity, and zooplankton concentration and size during the DVM did not seem to play an important role in affecting v_{up}. This suggests that temperature may be a key mechanical factor controlling swimming activity. Temperature can increase metabolic rates and zooplankton require less effort to propel themselves in a less viscous fluid.

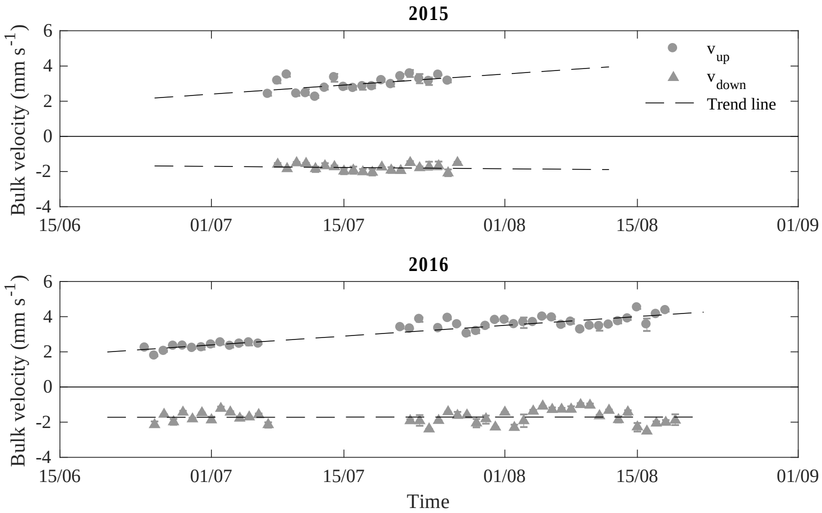

Figure 1: Time series of bulk velocity v_{up} at sunset (grey dots, positive values) and v_{down} at sunrise (grey triangles, negative values) in 2015 and 2016. The black dashed lines show instead the trend lines fitted to the points.

v_{down} (Fig 1, negative values) was instead constant ranging between 1 and 2 mm/s for both years. Modelling *Daphnia* as sinking ellipsis shows that their sinking rates from our model (Fig 2b, blue curve) are within the observed range in the field (Fig. 2b, grey rectangle) and are not affected by the water temperature during the DVM. The good agreement between the model and the field data strongly indicates that organisms sank during the DVM because organism's buoyancy and gravity are the only governing parameters of the reverse DVM.

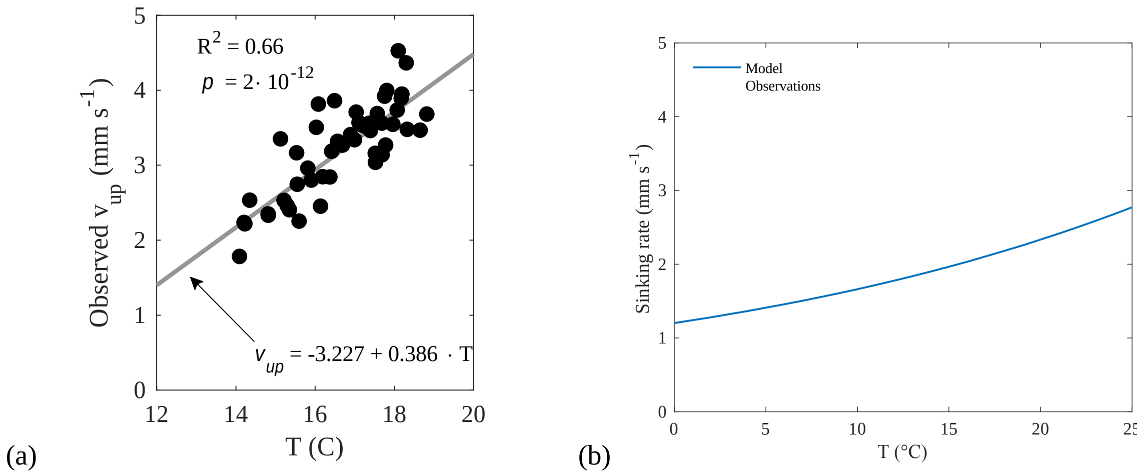

Figure 2: panel (a) shows the correlation between the water temperature T in the migrating layer and the observed upwards velocity. The grey line represents the fitted model to the regression dataset whose equation is reported in the bottom right corner. Panel (b) reports the sinking rates of *Daphnia* (thick line) as a function of the temperature T with the 95% confidence interval (shaded area). Grey area shows the observed range of v_{down}.

Hydrodynamics and sediment transport in the near-field region of the Rhône plume in Lake Geneva (France/Switzerland): Measurements and 3D modelling

F. Soulignac[1]*, U. Lemmin[1], D. A. Barry[1]

[1] *Ecological Engineering Laboratory (ECOL), Environmental Engineering Institute (IIE), Faculty of Architecture, Civil and Environmental Engineering (ENAC), Ecole Polytechnique Fédérale de Lausanne (EPFL), Switzerland*

**Corresponding author: frederic.soulignac@epfl.ch*

KEYWORDS
Lake; river plume, hydrodynamics; sediment transport, measurements, 3D modelling

Introduction

Past studies of the mixing of Rhône River in Lake Geneva concentrated on mid and far-field regions and were based mainly on point measurements of few variables. Giovanoli (1990) showed the seasonal variability of the Rhône interflow spreading. Halder et al. (2013) inferred the paths and the mixing of Rhône River in Lake Geneva from the stable isotope composition of water. Based on three-dimensional (3D) hydrodynamic simulations, Lemmin (2016) also suggested the most likely trajectories taken by the Rhône discharge in Lake Geneva in connection with two predominant gyres and small ones located in front of the river inflow. However, the development of the river plume is strongly dictated by the flow characteristics in the near-field region where the concentration of suspended particles may not be negligible.

In this context, the objective of this study is to develop a data collection strategy to characterize the hydrodynamics and the fate of suspended particles in the near-field region of the Rhône plume in Lake Geneva. A parallel objective is the development of a 3D hydrodynamic and sediment transport model.

Materials and methods

The study site is the eastern part of Lake Geneva where the Rhône River enters the lake. The Rhône accounts for approximately 75% of the total inflow and the majority of suspended sediment in the lake.

During periods of suspended sediment discharge, we consider monitoring the river plume along a circular arc centred on the river inflow using an echo sounder (Echologger EU400). In situ (from a boat) measurements of the plume are assisted by an automated data acquisition system that provides the GPS coordinates for measurements and tracks the sampling trajectory, thereby creating a precise step-by-step characterization of the plume after data fitting over the plume path.

The following measuring instruments are used: i) an acoustic Doppler current profiler with bottom tracking (ADCP-Teledyne Marine Workhorse Sentinel) mounted on a small catamaran towed by the boat, ii) a conventional CTD probe (Meerestechnik Elektronik) and iii) an optical instrument for in situ observations of the particle-size distribution and volume concentration (Sequoia LISST-100X).

The 3D model set up is built using the Delft3D suite software. The grid size varies from 100 m in the area around the river mouth to 500 m for the rest of the lake.

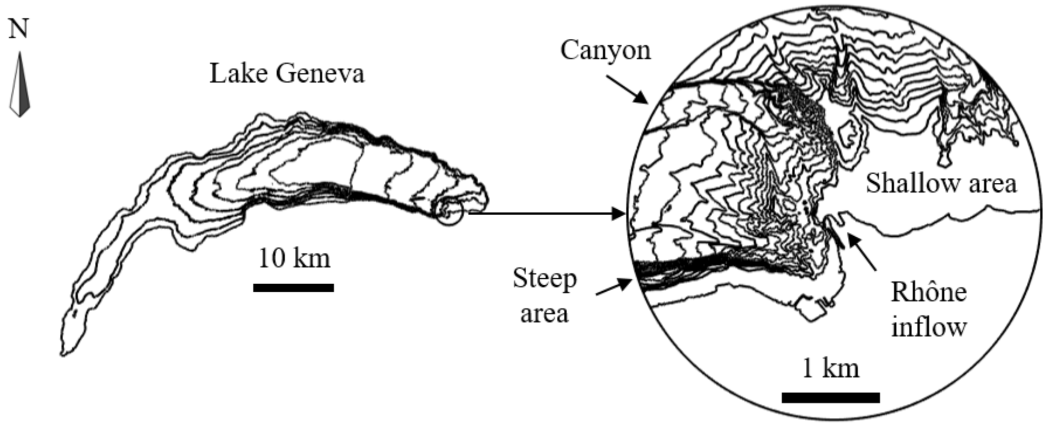

Fig. 1: Study site.

Preliminary results

Preliminary tests on another tributary of Lake Geneva, the Aubonne River, show that the automated procedure for river plume characterization is reliable. On 19 April 2018, the plume was in the form of an overflow because the river temperature was higher than the lake surface temperature (not shown). The field measurement campaign starting June 2018 will sample Rhône interflow in a similar fashion.

The 3D numerical simulations show that the main hydrodynamic patterns observed during earlier hydrodynamic campaigns in 2016 and 2017 (data from ADCP profiles in the Rhône canyon) are well reproduced by the model (not shown). This model will subsequently be used to investigate the interaction of suspended sediment transport/deposition, and physical mixing processes. In particular, mixing is generated by gyres located in the region of the river inflow (Fig. 2).

The measurements of the field campaigns will be used to better calibrate/validate the 3D model in the vicinity of river inflow. This work should help to better understand the mixing of the Rhône River water in Lake Geneva.

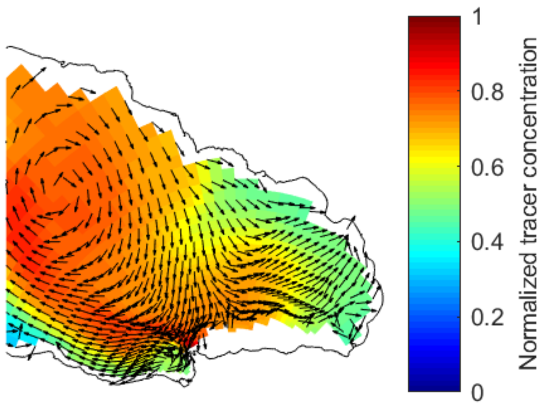

Fig. 2: Simulation results on 9 July 2016, at 15-m depth

REFERENCES

Giovanoli, F. (1990), Horizontal Transport and Sedimentation by Interflows and Turbidity Currents in Lake Geneva, In: Tilzer M.M., Serruya C. (eds) Large Lakes. Brock/Springer Series in Contemporary Bioscience. Springer, Berlin, Heidelberg.

Halder, J., L. Decrouy, T. W. Vennemann (2013) Mixing of Rhône River water in Lake Geneva (Switzerland-France) inferred from stable hydrogen and oxygen isotope profiles, Journal of Hydrology, 477, 152-164.

Lemmin, U. (2016), Mouvement des masses d'eau, In: Lemmin U. (eds) Dans les abysses du Léman. Presses polytechnniques et universitaires romandes, Lausanne, Switzerland.

Micrometeorological and hydro-chemical measurements of mass and energy exchange between atmosphere and water surfaces using a floating platform

U. Spank[1*], M. Hehn[1], P. S. Keller[2], M. Koschorreck[2] und C. Bernhofer[1]

[1] *Technische Universität Dresden, Institute of Hydrology and Meteorology, Chair of Meteorology, Germany*
[2] *Helmholtz Centre for Environmental Research - UFZ, Department of Lake Research, Germany*

**Corresponding author, Uwe.Spank@tu-dresden.de*

KEYWORDS
Eddy covariance measurements; evaporation; floating observation platform; mass and energy exchange; methane and carbon dioxide fluxes; sensible and latent heat flux.

Introduction

The emissions of carbon dioxide (CO_2) and methane (CH_4) from inland waters are an important but a currently inadequately considered component of global greenhouse gas (GHG) balance. Reservoirs are thereby particular hot spots of GHG release as organic material is increasingly sedimented here. The emissions of reservoirs are thereby highly variable in time and space as well as spatial and temporal characteristics of release are significantly different for CO_2 and CH_4. At present, little is known about the actual emissions from reservoirs in the temperate climate zone and processes controlling the GHG emissions are only partly understood.

In our project –TREGATA–, launched last year, we investigate the CO_2 and CH_4 emissions from two German reservoirs, the mesotrophic Rappbode reservoir in the Harz Mountains and the eutrophic Bautzen reservoir in Lusatia. The research focuses on developing a basic understanding of the processes that control the release of CO_2 and CH_4. We want to investigate how changes of water depths, trophic level and meteorological variables affect the GHG emissions. However, measurement and analysis of energy exchange between atmosphere and water surface, and the exact quantification of evaporation are also important components of our research.

Materials and methods

The monitoring programme has focus on a continuous observation of mass- and energy exchange between reservoir and atmosphere. For this purpose, a floating observation platform is applied, which is equipped with a combination of micrometeorological and hydro-chemical measurements systems. The platform was first set up in 2017 at the Rappbode reservoir and put into operation. This platform is also operated this year with an identical setup of sensors and measurement devices but with improved of remote control systems on the Bautzen reservoir **(Figure 1)**.

Figure 1: Floating observation platform installed on the Bautzen reservoir and equipped with micrometeorological and hydro-chemical measurement systems for continuous monitoring of mass- and energy exchange between water surface and atmosphere

Eddy covariance (EC-) measurements are the core of the micrometeorological monitoring programme. The EC technique can be assessed to be the state-of-the-art monitoring method for the spatially integrated observation of mass and energy flux exchange between ground and atmosphere in high temporal resolution. Thus, EC measurements provide an excellent tool to observe water vapour fluxes (evaporation, E), carbon dioxide fluxes (F_{CO2}), methane fluxes (F_{CH4}), as well as sensible heat flux (H) and latent heat flux (LE) resulting from energy equivalent of E. Despite the frequent and successful application of the EC method in numerous projects investigating mass and energy exchange of forests, croplands, grasslands and other types of land surfaces, its application over water surfaces is rare. Only few publications report on EC measurements above water surfaces such as lakes and reservoirs. However, it is to emphasise that EC measurements on floating platforms are not a standard task but imply several serious technical and scientific challenges. Notwithstanding that the concept of a floating platform is an elegant opportunity for EC measurements which are largely unaffected by surrounding land surfaces.

Continuous hydro-chemical observations of dissolved oxygen, CO_2 and CH_4 and continuous measurements of radiation balance (R_n; individual measurement of all four components), meteorological standard variables (i.e., air temperature, air humidity, wind speed, and wind direction), wave height, water surface temperature and water temperature profile (20 layers) complement the EC measurements. Additionally, the spatial variability of F_{CO2} and F_{CH4} is investigated within the complete reservoir by regularly executed chamber measurements and analyses of dissolved CO_2 and CH_4 in surface water. The heat storage in the reservoir and heat storage change (ΔS) are determined from measured water temperatures. Thus, all four components of energy balance, i.e., R_n, H, LE, and ΔS are provided by independent measurements, and the reliability and fidelity of measured energy fluxes (i.e., H and LE) can be assessed from imbalance or closure gap of energy balance equation.

Results and discussion

For an example, we would like to present the mean diurnal cycles of H, LE, F_{CO2} and F_{CH4} derived from EC measurements on Bautzen reservoir for May 2018 in **Figure 2**. The temporal course of energy fluxes (i.e., H and LE) and F_{CO2} show clear diurnal patterns being consequence mainly of day time characteristic of solar radiation, air temperature, water surface temperature, air humidity and wind speed. The characteristic of F_{CO2} is also confirmed by hydro-chemical measurements of dissolved CO_2 in surface water. So a clear undersaturation of CO2 caused by photosynthetic activity of alga were observed at daytime; however, water was nearly saturated at night.

Such diurnal characteristic was not detected for F_{CH4}. It can be assumed that diurnal variations of meteorological drivers have less effect on F_{CH4} release as CH_4 is mainly produced in anoxic parts of sediments on the ground and it emits mainly in term of ebullition. Thus, CH_4 production and CH_4 release are widely decoupled from daytime characteristic of meteorological variations. On our point of view, CH_4 emissions are controlled by meteorological drives on a larger scale of time. So we hypothesise that meteorological situations altering the hydro-chemical environment on ground, variables that do not have a clear diurnal cycle, e.g. air pressure, and parameters interrelate with seiches and internal waves are most important what we want to prove with our measurements in Bautzen.

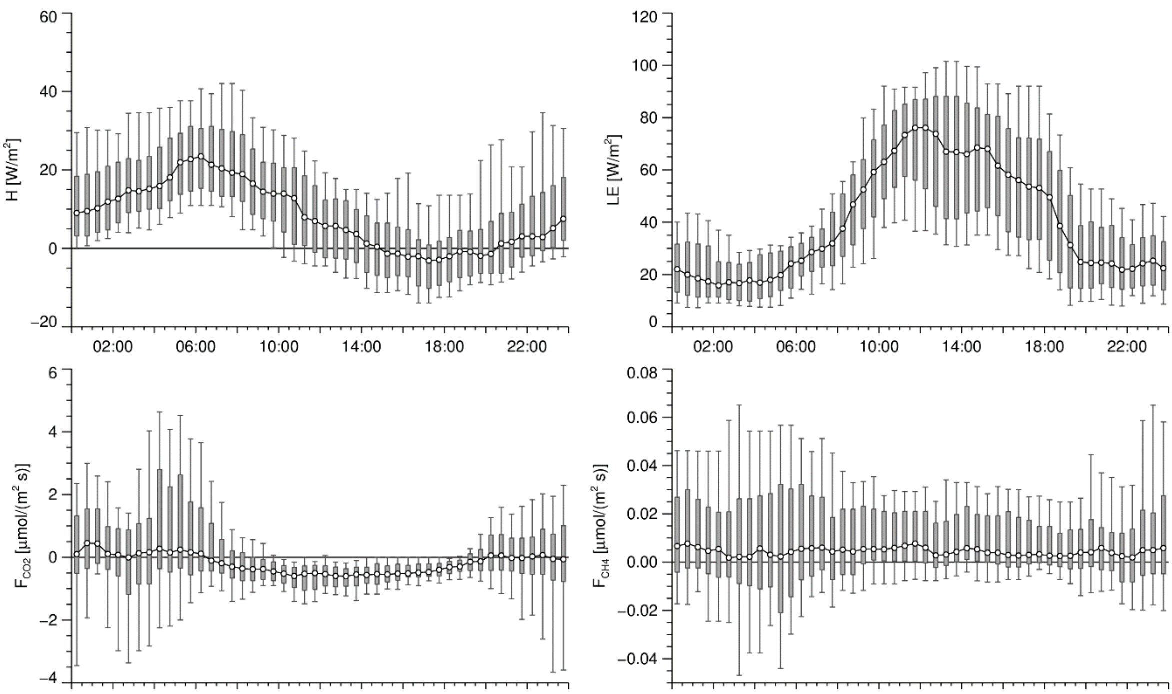

Figure 2: Mean diurnal cycles of sensible heat flux (H), latent heat flux (LE), carbon dioxide flux (F_{CO2}) and methane flux (F_{CH4}) derived from EC measurements on Bautzen reservoir for May 2018. Boxplots presents 10%, 25%, 50%, 75%, and 90% percentiles.

Lake Kivu: Development of a 3D model as framework for management of methane extraction in Lake Kivu

Meinard Tiessen[1]*, Augusta Umutoni[2], Gaetan Sakindi[2], Damien Bouffard[3], Rob Uittenbogaard[1] and Reimer de Graaff[1]

[1] *Deltares, P.O. Box 177, 2600 MH Delft, The Netherlands*
[2] *Lake Kivu Monitoring Program / Rwanda Energy Group (REG) KN82 Street 3 Nyarugenge district, Kigali City, Rwanda*
[3] *Eawag, Swiss Federal Institute of Aquatic Science and Technology, Surface Waters - Research and Management, Kastanienbaum, Switzerland*
**Corresponding author, e-mail: meinard.tiessen@deltares.nl*

KEYWORDS
Lakes; salinity stratification; methane entrapment, methane extraction; 3D model; internal waves.

Introduction

Lake Kivu is located on the border between the Republic of Rwanda and the Democratic Republic of Congo in the tectonically and volcanically active East African rift valley system. The lake is 485 m deep and unique in the world due to its stable water column stratification that traps CH_4 and CO_2 in the deepest layers (> 280m). Rwanda plans to exploit the large amount of trapped CH_4 (ca. 55 km3) to generate electrical power. After methane extraction, the pumped-up water will be re-injected in the lake (Wuest et al, 2012).

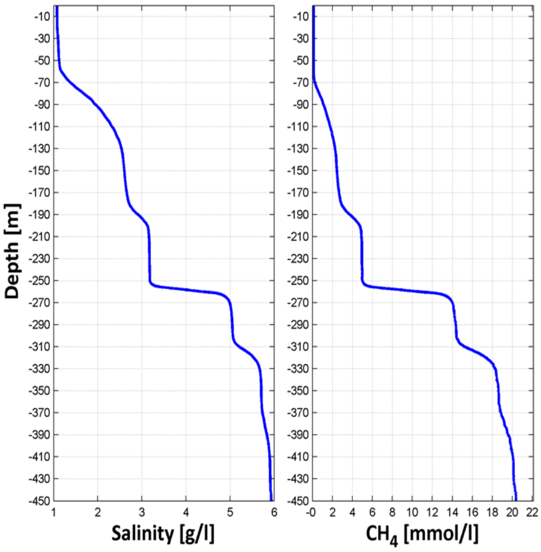

Figure 3 Salinity and methane profile over depth of Lake Kivu (Schmid et al, 2005)

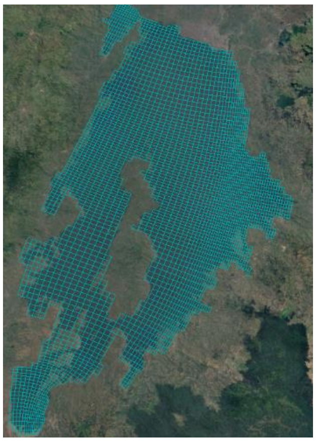

Figure 4 Model grid (coarsened).

Materials and methods

This three-year project has multiple aims: Using a 3D hydrodynamic model and field measurements of current profiles over the entire depth of the lake, the first aim of this study is to gain valuable knowledge on the horizontal circulation and mixing processes. The model will additionally provide a better understanding of the effects of deep water extractions and re-injection upon the lake structure (e.g. stratification) in the deep layers (around 240 m) and in the biozone (around 0-70 m) as well the horizontal circulation patterns that may affect other methane extraction locations Finally, the 3D model will act as a framework representing present and future scientific findings and can be used to test and validate new ideas and future plans for the lake.

Results and discussion

At the moment, a model based on the z-layer version of the orthogonal curvilinear hydrostatic code DelftD-FLOW with k-ε turbulence model including buoyancy terms is being developed with up to 500 vertical layers to accurately account for the strong vertical density profile though excluding double-diffusion staircases. In addition, spatially variable wind patterns (from the 2.5 km COSMO-model, Thiery et al, 2015) have been applied to study the impact of daily and seasonal meteorological patterns on circulation and bio-zone mixing. Furthermore, river inflows, outflows and most importantly sub-aquatic discharges have been included. The latter are the primary source of stratification and CO_2 and CH_4 entrapment. The density effect of these gasses is also implemented in the model. Our year-long simulations agree with the observations of stable stratification. In addition, the simulations suggest that daily wind-driven patterns create diurnal internal seiches as suggested in Tietze (1978) (model results shown in 3). However, at the moment current velocity data over depth (via multiple ADCPs) are still being collected that will be used to check this model-hypothesis.

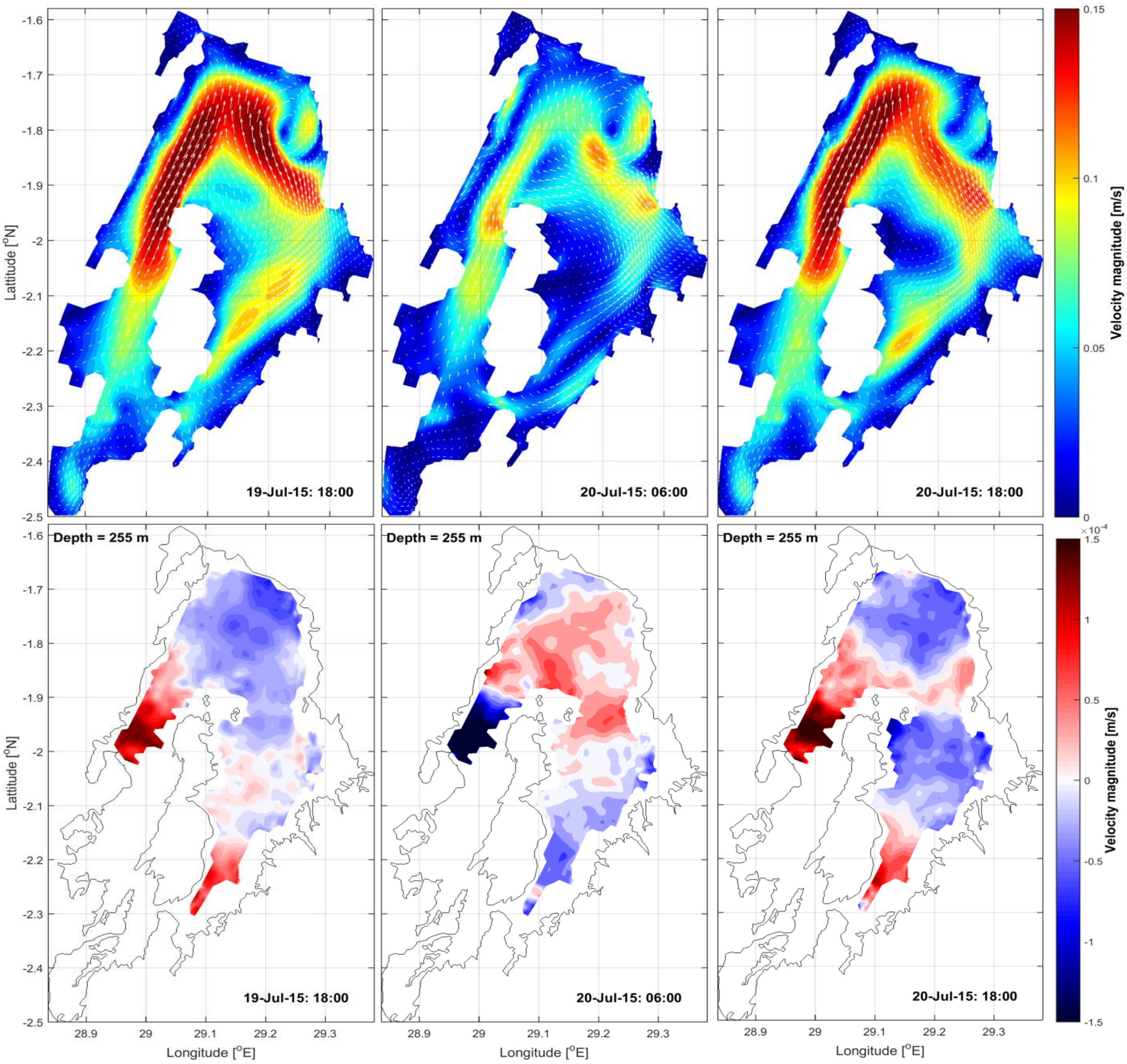

Figure 3. Model results using the coarsened model (100 depth layers): Daily wind patterns result in recurring horizontal motions at the surface (top), and vertical motions at the pycnocline (bottom).

REFERENCES

Schmid M, Halbwachs M, Wehrli B, Wüest A. (2005) Weak mixing in Lake Kivu: new insights indicate increasing risk of uncontrolled gas eruption. Geochem Geophys Geosyst 6:Q07009. doi: 10.1029/2004GC000892.

Thiery W, Davin EL, Panitz HJ, Demuzere M, Lhermitte S, van Lipzig N. (2015). The impact of the African Great Lakes on the regional climate. Journal of Climate, 28(10), 4061-4085.

Tietze, K. (1978), Geophysikalische Untersuchung des Kivusees und seiner ungewöhnlichen Methangaslagerstätte - Schichtung, Dynamik und Gasgehalt des Seewassers, PhD Thesis, Christian-Albrechts-Universität, Kiel, Germany.

Wüest A, Jarc L, Bürgmann H, Pasche N, Schmid M.(2012) Methane formation and future extraction in lake Kivu. In: Descy JP, Darchambeau F, Schmid M, editors, Lake Kivu: Limnology and biogeochemistry of a tropical great lake, Springer; 2012. pp. 13–29.

Temporal variability in thermally-driven cross-shore exchange: The role of the M_2 tide

Hugo N. Ulloa[1]*, Kristen A. Davis[2], Stephen G. Monismith[3] and Geno Pawlak[4]

[1] *Physics of Aquatic Systems Laboratory (APHYS), École Polytechnique Fédéral de Lausanne, Switzerland.*
[2] *Civil and Environmental Engineering, University of California, Irvine, California, USA.*
[3] *Environmental Fluid Mechanics Laboratory, Stanford University, Stanford, California, USA.*
[4] *Mechanical and Aerospace Engineering, University of California, San Diego, California, USA.*

**Corresponding author, e-mail hugo.ulloa@epfl.ch*

KEYWORDS
Fringing reef system; buoyancy-driven cross-shore flows; tidally-driven alongshore flows.

ABSTRACT

Cross-shore exchange in coastal regions is a fundamental process that modulates mass and heat transport between the nearshore and the adjoining ocean, and can regulate complex ecosystems such as coral reefs. Although various mechanisms can provide intermittent perturbations to the cross-shore exchange, persistent forcing mechanisms, such as diurnal winds and tidally-driven currents, can lead to systematic variability in the regular cross-shore exchange pattern.
We examine temporal variability of baroclinic cross-shore exchange in the context of a tropical fringing reef system focusing on the role of tidally driven along shore flow. Ensemble diurnal phase averaging of cross-shore flow at the Kilo Nalu Observatory (KNO) in Oahu, Hawaii shows a robust diurnal signal associated with an unsteady buoyancy/diffusive dynamic balance, although significant variability is observed at sub-diurnal time scales. In particular, persistent fortnightly variability in the diurnal flow patterns is consistent with modulation by the semidiurnal alongshore tidal flow. The alongshore flow plays a direct a role in the cross-shore exchange momentum balance via Coriolis acceleration but also affects the cross-shore circulation indirectly via its influence on vertical turbulent diffusion. An idealized linear theoretical model for thermally driven cross-shore flow is formulated using the long-term time-averaged diurnal dynamic balance at KNO as a baseline. The model is driven at leading order by the surface heat flux, with contributions from the alongshore flow and cross-shore wind appearing as linear perturbations. Superposition of the idealized solutions for Coriolis and time-varying eddy viscosity perturbations are able to reproduce key aspects of the fortnightly variability. Modifying the model to consider a more realistic along-shore flow and considering effects of nightly convection lead to further improvements in comparisons with KNO observations. The ability of the theoretical approach to reproduce the fortnightly patterns indicates that semi-diurnal variations in the alongshore flow are effective in modulating the cross-shore flow via Coriolis and vertical turbulent transport mechanisms.

Stable isotopes in water indicate sources of nutrients that drive algal blooms in the tributary bay of a subtropical reservoir

Zhengjian Yang[1], Bao Cheng[1], Yaqian Xu[1], Defu Liu[1, 2]*, Jun Ma[1], Daobin Ji[2]

[1] *Hubei Key Laboratory of Ecological Restoration of River-lakes and Algal Utilization, Hubei University of Technology, Wuhan, Hubei Province, China;*
[2] *Engineering Research Center of Eco-Environment in TGR Region, Ministry of Education, China Three Gorges University, Yichang, Hubei Province, China.*

**Corresponding author, e-mail dfliu@189.cn*

KEYWORDS
Nutrient source; hydrogen and oxygen isotopes; hydrodynamics; algal blooms; Three Gorges Reservoir (TGR).

Introduction

Algal blooms have become one of the most important ecological problems in the tributary bays of the Three Gorges Reservoir (TGR) (Stone, 2008; Zhou et al., 2009). Generally, regional nutrient enrichment is an essential factor leading to eutrophication and algal blooms. It was suggested that nutrients could not be the limiting factor for algal blooms in the TGR, and the driving factors for eutrophication were directly attributed to the slower flow caused by the Three Gorges Dam (TGD) (Fu et al., 2010; Xu et al., 2010). In fact, although there were no algal blooms in the Yangtze River (YR), the water was rich in nutrients before and after the completion of the TGD (Huang et al., 2014; Lou and Yin, 2016; Ran et al., 2017). However, the driving mechanism underlying nutrient enrichment in the tributary bays, especially the identity of the main source, is still a controversial issue.

Materials and methods

2.1 Research area and sampling sites

The Xiangxi River (XXR) is the largest tributary in the region near the TGD (Fig. 1, a). This river originates from Shennongjia Mountain and flows into the main stream of the TGR in Guojiaba (GJB). The average annual temperature is approximately 16.6 °C. The average annual rainfall and river discharge are, respectively, 1015.6 mm and 40.18 $m^3 \cdot s^{-1}$. When the TGR is operated at a water level of 175 m, a covered reach (XXB), caused by the TGR's backwater, is approximately 40 km from the estuary to the Zhaojun Town.

From January, 2010 to December, 2011, eleven sampling sites (at intervals of approximately 3 km) were set to monitor the temporal and spatial variations of environmental parameters in the XXB, which are represented as XX00-XX10 in succession from the estuary to the end of the backwater (Fig. 1, b). One other site (abbreviated as GJB) was located at the main stream of the TGR. There was also a site in the upstream natural inflow river of XXB, represented as "Inflow".

2.2 Monitoring and testing methods

Two 350 ml bottles of water were collected using a water sampler (QCC15-2.5, Beijing, China) at depths of 0.5 m and 2 m and then at 10 m intervals to the bottom. One was sent to a local laboratory to measure the TN, NO^-_3-N, TP, PO^-_4-P and Si concentrations according to a national standard (China, 1995; Wei, 2002). The other bottle was filtered through a Whatman GF/C filter. Then, both the water and filter were stored in a cold box (< 5 °C) and transported back to the laboratory. The water was used to measured δD and $\delta^{18}O$ using a laser absorption water isotope spectrometer analyzer (LWIA V2, Liquid Water Isotope Analyzer; LRG

Company, USA) relative to Vienna Standard Mean Ocean Water (VSMOW) (Graig, 1961). The measurement precision of δD and δ^{18}O were 0.19‰ and 0.06‰, respectively. WT and Turb. were measured using a Hydrolab DS5X multiprobe sensor (Hydrolab, USA) from the river surface to the bottom at 1-m intervals.

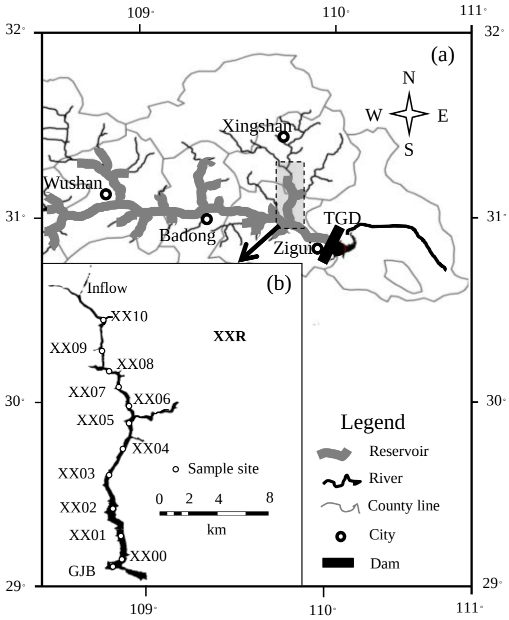

Figure 1. (a) Location of the XXR in the TGR. (b) Locations of the sampling sites in XXB.

Results and discussion

Hydrodynamic changes

The longitudinal profiles of water FV from the estuary to the end of the backwater in XXB were shown in Fig. 2. On January 16, all of the water flowed toward the estuary from the end of the bay, without any layered bidirectional density current (Fig. 2a). However, on February 18, in the area around the estuary, water from the YR intruded into XXB though the bottom layer (white vectors in Fig. 2b), which took the form of a wedge. On March 29, there was a marked level of water flowing into the XXB through the bottom layer from the YR (white vectors in Fig. 2c), while water from XXB flowed toward the YR through the upper layer (black vectors in Fig. 2c). On July 4, 2010, it was very interesting that water from the YR intruded into XXB through the middle layer (white vectors in Fig. 2d), and water in XXB flowed to the estuary both through surface and bottom layers (black vectors in Fig. 2d). However, on October 3, the hydrodynamics showed a completely opposite trend compared to those shown in Fig. 2c; water from the YR intruded into the bay though the surface layer, while the bottom layer of water flowed into the the YR in the opposite direction.

Nutrient and water exchanges between GJB and XXB

Generally, the spatial distribution of δ^{18}O and δD in precipitation is affected by latitude, altitude and distance from the ocean (Bowen and Wilkinson, 2002; Dansgaard, 1964). Based on this, δ^{18}O and δD composition is usually used as natural conservative tracer to identify water sources (Bogaard et al., 2007); specifically, the more similar the δ^{18}O and δD

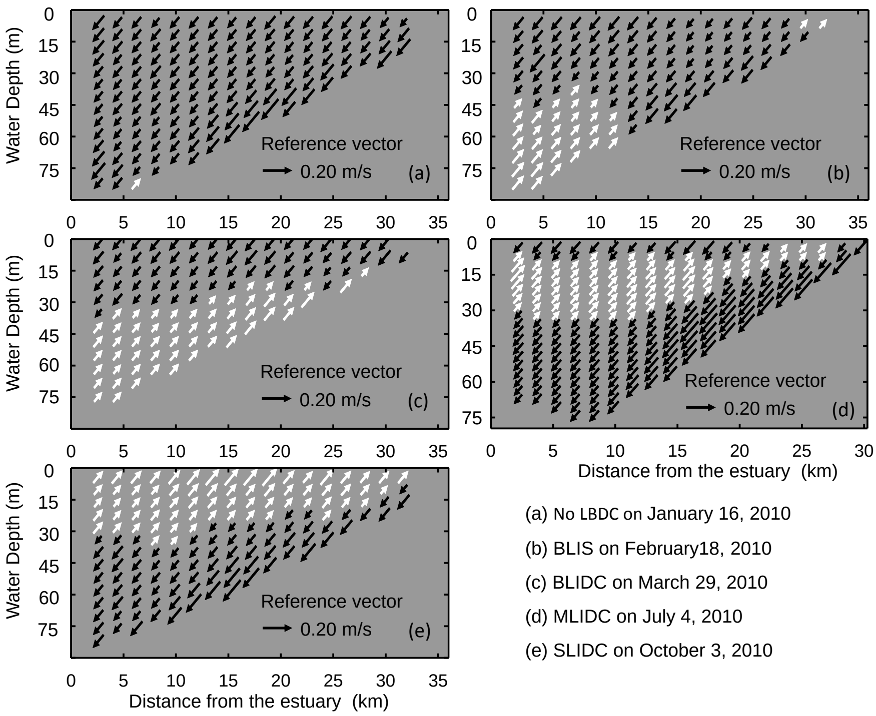

Figure 2. The characteristics for no LBDC (a), BLS (b), BLIDC (c), MLIDC (d) and SLIDC (e) in XXB. The white vector group represents the water flowing toward the upstream region of XXB, and the black vector group represents the opposite condition; the distance value “0” on the horizontal axis represents the site of GJB.

composition in a source of water is to the body of water it flows into, the greater the volume of water that comes from that source. In the YR basin, the $\delta^{18}O$ and δD compositions in the precipitation decrease gradually from east to west (Liu et al., 2009) . In the YR basin runoff water is mainly from the precipitation, and therefore, the $\delta^{18}O$ and δD values in the western region should be both less than those in the eastern region (Ding et al., 2013). In the runoff upstream of XXB (Inflow), the variation in $\delta^{18}O$ and δD ranged from -8‰ to -9‰ and -50‰ to -60‰, respectively; but at GJB, values ranged from -13‰ to -11‰ and -81‰ to -91% respectively. As these represent significant differences between GJB and Inflow, the $\delta^{18}O$ and δD compositions could be used to indicate the exchange of nutrients and water between GJB and XXB (Yang et al., 2015).

Changes in the $\delta^{18}O$ and δD composition, nutrients, and estimated nutrient contribution rates into XXB, according to the hydrodynamics, are shown in Tab. 2. . In stage I, the hydrodynamic corresponded to that shown in Fig. 2a and b. As the water discharge, both at Inflow and the YR, were very low in this period (Cui et al., 2011), and there was no LBDC (Fig. 2a), at best, a BLIS was present (Fig.2, b) in XXB; therefore, water from Inflow and GJB likely had a slight effect on the water in XXB. However, the $\delta^{18}O$ and δD compositions in XXB were shown to be more similar to those at GJB (Fig. 3a).The mostly likely reason for this is that water in XXB, at that time, was mainly water that came from GJB during the impounding period of the TGR last year. This is also the reason why there were high N and Si and low P contents at XX06, because N and Si contents at GJB were relatively high and P contents were low in stage I.

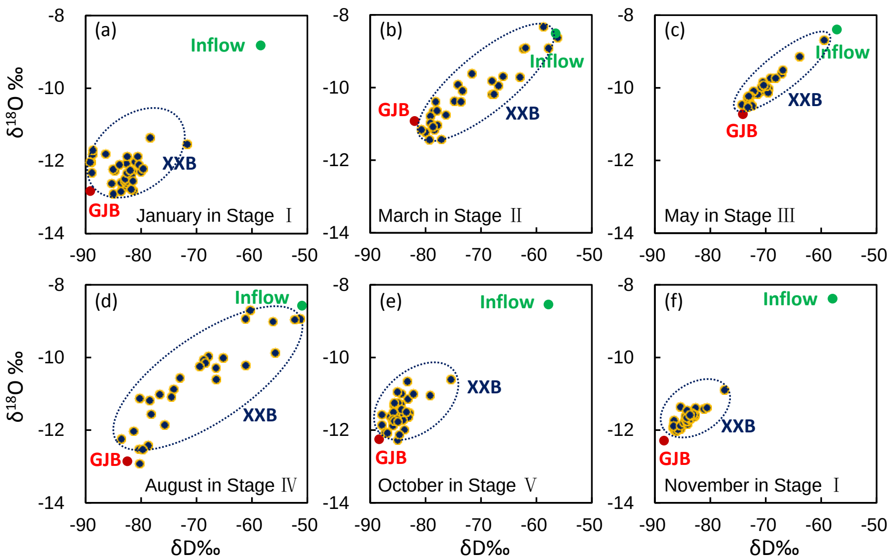

Figure 3. Spatial and temporal distributions of the $\delta^{18}O$ and δD composition in XXB, GJB and the inflow site over the five stages in 2012. The blue points with yellow circles represent the $\delta^{18}O$ and δD compositions at different sites and depths in XXB.

ACKNOWLEDGEMENTS

This work was supported by the National Natural Science Foundation of China (Grant No. 51509086 and 91647207), the Natural Science and Technology Major Special Program of China (Grant No. 2014ZX07104-005), and the National Key Project R & D of China (2016YFC0402204 and 2016YFC0401702).

REFERENCES

Bogaard T, Guglielmi Y, Marc V, Emblanch C. Hydrogeochemistry in landslide research: a review. Bull. Soc. géol. Fr 2007; 178: 113-126.
Bowen G J, Wilkinson B. Spatial distribution of δ18O in meteoric precipitation. Geology 2002; 30: 315-318.
MWR of China. Determination of silica (dissolved). SL 91.1-1994. Beijing, 1995.
Cui Y, Liu D, Song L, Xiao S. Application of Digital Filtering Theory in Baseflow Separation in Xiangxi River Watershed of Three Gorges Reservoir Area. Journal of China Hydrology 2011; 31: 18-23. (in Chinese)
Dansgaard W. Stable istopes in precipitation. Tellus 1964; 16: 436-468.
Ding T, Gao J, Shi G, Chen F. Spacial and temporal variations of H and O isotope compositions of the Yangtze River water and their environmental implication. Acta Geologica Sinica 2013; 84: 661-676. (in Chinese)
Fu B, Wu B, Lv Y, Xu Z. Three Gorges Project: Efforts and challenges for the environment. Progress in Physical Geography 2010; 34: 1-14.
Graig H. Standard for Reporting Concentrations of Deuterium and Oxygen-18 in Natural Waters. Science 1961; 133: 1833-1834.
Huang Y, Zhang P, Liu D, Yang Z, Ji D. Nutrient spatial pattern of the upstream, mainstream and tributaries of the Three Gorges Reservoir in China. Environ Monit Assess 2014; 186.
Liu Z, Tian L, Yao T, Chai X. Spatial distribution of δ18O in precipitation over China. Chinese Sci Bull 2009; 56: 804-811. (in Chinese)
Lou B, Yin S. Spatial and seasonal distribution of phosphorus in the mainstem within the Three Gorges Reservoir before and after impoundment. Water Science & Technology 2016; 73: 636-642.
Ran X, Lex B, Yu Z, Beusen A. Nitrogen transport, transformation, and retention in the Three Gorges Reservoir: A mass balance approach. Limnology and Oceanography 2017; 62: 2323-2337.
Stone R. Three Gorges Dam:Into the Unknown. Science 2008; 321: 628.
Wei F. Water and wastewater monitoring and analysis methods(4th ed). Beijing: China Environmental Science Press, 2002. (in Chinese)
Xu Y, Cai Q, Han X, Shao M, Liu R. Factors regulating trophic status in a large subtropical reservoir, China. Environ Monit Assess 2010; 169: 237-248.
Yang L, Liu D, Huang Y, Yang Z. Isotope analysis of the nutrient supply in Xiangxi Bay of the Three Gorges Reservoir Ecological Engineering 2015; 77: 65-73.
Zhou G, Bi Y, Zhao X, Hu Z. Algal growth potential and nutrient limitation in spring in Three-Gorges Reservior, China. Fresenius Environmental Bulletin 2009; 18: 1642-1647.

Simulation of lake surface temperature and ice cover with 1-D model

Xin Zhang[1,2*] , Bertram Boehrer[2] , Kaicun Wang[1]
1. College of Global Climate and Earth System Science, Beijing Normal University, 100875, Beijing, China
2. Helmholtz Centre for Environmental Research - UFZ, Department Lake Research, Brückstrasse 3a, D-39114 Magdeburg, Germany

*Corresponding author, email: xzhang0828@mail.bnu.edu.cn

KEYWORDS:
Lakes surface temperature; ice phenology; modeling; MODIS; ARC-Lake

Water temperature and ice phenology are sensitive to climate warming and can alter the structure and function of aquatic ecosystems. They are good indicators of climate variability and climate change. The performance of lake surface temperature and ice phenology in China would be limited because of the limited long-term observation. For this purpose, we investigated the characteristic the pattern of lake temperature and ice in Lake Chaohu, Lake Hulun and Lake Namco, which are three typical lakes located in different climate zones in China. Lake surface temperature and ice cover phenology were simulated on Lake Namco, Lake Hulun and Lake Chaohu in China, using the 1-D hydrodynamic model, General Lake Model (GLM), from 2000 to 2016, forcing with data from weather stations and re-analysis datasets. The validation data of the lake surface temperature could be mainly derived from satellite data, Moderated Resolution Imaging Spectroradiometer (MODIS) Land Surface Temperature products and ARC-Lake (ATSER Reprocessing for Climate: Lake Surface Temperature &Ice Cover) , and combined with one-year in-situ temperature measurement. The in-situ temperature measurement was also used to validate the accuracy of satellite data. For ice phenology validation, we extracted the ice-state period by counting the coverage of ice for whole lake from the two satellite results.
The MODIS-derive LWST showed a systematical cool bias and ARC-lake-derived LWST fitted a good agreement (Fig.1), compared with in situ measurement. The lake model GLM could successfully reproduce the features of surface temperature during open-water period. The overall agreement between simulation and remote sensing data and in-situ results during the open water and were good. For ice-cover periods, GLM could simulate the ice-on and ice-off date when the lake becomes fully covered or not. Because of missing observational data, a comparison was not possible, Hence, the ice information from MODIS and ARC-lake show a good agreement with GLM ice simulation. The simulation results also demonstrate that climate warming could have a significant impact on lakes temperature and ice-covered period. Remote sensing data is a promising data source for model validation when in-situ data is rarely obtained.

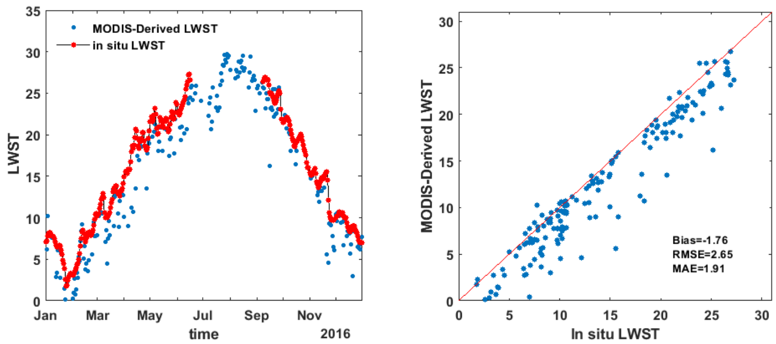

Fig.1 A comparison of the lake water surface temperature(LWST) from MODIS-Derived against in situ Measurement from 1st January 2016 to 31st December 2016 in Lake Chaohu

Methane Emissions during Lake Overturn: A Tug-of-War between Physical Mixing and Methanotrophs

M. Zimmermann[1,2]*, M. J. Mayr[1,2], D. Bouffard[1], W. Eugster[2], B. Wehrli[1,2], H. Bürgmann[1] and A. Brand[1]

[1] *Eawag, Swiss Federal Institute of Aquatic Science and Technology, Surface Waters - Research and Management, Kastanienbaum, Switzerland*
[2] *Departement of Environmental Systems Science, ETH Zürich, Switzerland*

**Corresponding author, e-mail matthias.zimmermann@eawag.ch*

KEYWORDS
Methane emissions; microbial methane oxidation; lake overturn; modelling.

Introduction

Stratified lakes with anoxic bottom waters are potentially important sources of methane emissions to the atmosphere (Bastviken *et al.*, 2011, 2004). During the stratified season, methane produced in the sediments accumulates in the anoxic hypolimnion. Methane oxidizing bacteria (MOB) largely prevent the emission of this methane by oxidizing up to 74-88% of the diffusive methane flux at the oxic-anoxic interface (Utsumi *et al.*, 1998; Kankaala *et al.*, 2006). In contrast, little is known about the fate of methane during the annual autumn overturn. During this period, large amounts of methane are mixed into the oxygen-rich epilimnion, potentially creating favourable conditions for MOB. However, the transfer of methane to the atmosphere could happen too rapidly for MOB to oxidize a substantial amount of methane before it escapes to the atmosphere. Here, we investigate to which extent MOB are able to reduce methane emission during the autumn overturn.

Materials and methods

The fate of methane during the autumn overturn (October to January) was determined by taking profiles of methane concentrations (gas chromatography) and MOB abundance (FISH & epifluorescence microscopy) in a small (surface area: 0.46 km^2; depth: 16 m), eutrophic lake (Lake Rotsee) during 10 field campaigns in 2016/1017. The methane emissions during the autumn overturn in 2016 were quantified with eddy-covariance flux measurements. The temperature evolution of the water column was continuously measured with a thermistor string (RBRconcerto T24, RBR).

The interplay of the three main processes controlling methane emissions (physical mixing, equilibration with the atmosphere and microbial methane oxidation) was studied by combining a physical model of the mixed layer with a growth model for MOB. The mixed layer was modelled as a single box with expanding box size (thermocline deepening). Assuming that convection is the dominant mixing process, the velocity of the thermocline deepening was formulated according to Zilitinkevich (1991). The heat flux at the surface of the lake was parameterized as described in Goudsmit (2002). The emission of methane to the atmosphere was formulated according to the boundary layer model of Liss and Slater (Liss and Slater, 1974) combined with the surface renewal model where the gas transfer coefficient (k) is calculated based on the dissipation of wind shear (ε_P) and buoyancy (ε_B) (MacIntyre *et al.*, 2010; Read *et al.*, 2012; Soloviev *et al.*, 2007). Assuming that methane is the main limiting nutrient and assuming that only a fraction of the oxidized methane is incorporated into MOB biomass (Leak and Dalton, 1986a, 1986b), we formulated the growth of MOB based on a Monod-type methane oxidation kinetics multiplied by the growth yield.

Results and discussion

From October to November only 4% of the methane released to the water column were emitted to the atmosphere and biomass of MOB in the mixed layer increased by a factor of 12. Despite the simplicity of the model, it reproduces the evolution of the mixed layer (Pearson's $r=0.96$, $p < 0.01$) as well as the cumulative methane emissions (model: 0.456 Mg (C), measured: 0.461 Mg (C)) very well. Compared to the total amount of methane supplied to the mixed layer (model: 11.3 Mg (C)) the model also predicts that only 4% are emitted to the atmosphere.

The model results suggest that convection and wind take on different roles during the autumn overturn. At the mixed layer depth, the dissipation of buoyancy is about one order of magnitude higher (0.5×10^{-8} W kg^{-1}) than the dissipation of wind shear (10^{-9} W kg^{-1}). In contrast, the gas transfer coefficient is dominated by the wind component (80±12 %). This implies that wind mainly transfers methane from the top few meters of the water column to the atmosphere while convection drives the deepening of the thermocline and the supply of methane to the mixed layer.

Interestingly, the comparison of the timescales at which the three processes operate shows that the transfer of methane to the atmosphere is about two orders of magnitudes slower (10 d μM^{-1}) than the supply of methane to the water column (2.4 h μM^{-1}), leaving enough time for MOB to oxidize about 76% of the methane. At the onset of the autumn overturn, the capacity of MOB to oxidize the methane is of the same order of magnitude as the supply of methane. The capacity strongly increases with increasing biomass and even exceeds the supply of methane towards the end of the autumn overturn.

In general, these results suggest that MOB substantially reduce the potential methane emissions to the atmosphere also during the autumn overturn. Furthermore, we show that a comparably simple model is able to reproduce the behaviour of this complex interplay.

REFERENCES

Bastviken D, Cole J, Pace M, Tranvik L. (2004). Methane emissions from lakes: Dependence of lake characteristics, two regional assessments, and a global estimate. *Global Biogeochem Cycles* **18**: 1–12.

Bastviken D, Tranvik LJ, Downing JA, Crill PM, Enrich-Prast A. (2011). Freshwater Methane Emissions Offset the Continental Carbon Sink. *Science (80-)* **331**: 50.

Goudsmit G-H. (2002). Application of k-ε turbulence models to enclosed basins: The role of internal seiches. *J Geophys Res* **107**: 3230.

Kankaala P, Huotari J, Peltomaa E, Saloranta T, Ojala A. (2006). Methanotrophic activity in relation to methane efflux and total heterotrophic bacterial production in a stratified, humic, boreal lake. *Limnol Oceanogr* **51**: 1195–1204.

Leak DJ, Dalton H. (1986a). Growth yields of methanotrophs - 1. Effect of copper on the energetics of methane oxidation. *Appl Microbiol Biotechnol* **23**: 470–476.

Leak DJ, Dalton H. (1986b). Growth yields of methanotrophs - 2. A theoretical analysis. *Appl Microbiol Biotechnol* **23**: 477–481.

Liss PS, Slater PG. (1974). Flux of Gases across the Air-Sea Interface. *Nature* **247**: 181–184.

MacIntyre S, Jonsson A, Jansson M, Aberg J, Turney DE, Miller SD. (2010). Buoyancy flux, turbulence, and the gas transfer coefficient in a stratified lake. *Geophys Res Lett* **37**: 2–6.

Read JS, Hamilton DP, Desai AR, Rose KC, MacIntyre S, Lenters JD, *et al.* (2012). Lake-size dependency of wind shear and convection as controls on gas exchange. *Geophys Res Lett* **39**: 1–5.

Soloviev A, Donelan M, Graber H, Haus B, Schlüssel P. (2007). An approach to estimation of near-surface turbulence and CO 2 transfer velocity from remote sensing data. **66**: 182–194.

Utsumi M, Nojiri Y, Nakamura T, Nozawa T, Otsuki A, Seki H. (1998). Oxidation of dissolved methane in a eutrophic, shallow lake: Lake Kasumigaura, Japan. *Limnol Oceanogr* **43**: 471–480.

Zilitinkevich. (1991). Turbulent Penetrative Convection. Avebury Technical.

Limnology Center
EPFL
ÉCOLE POLYTECHNIQUE FÉDÉRALE DE LAUSANNE

UNIVERSITÉ DE GENÈVE
FACULTÉ DES SCIENCES
Section des sciences de la Terre et de l'environnement

NORTEK

PICARRO

ROCKLAND SCIENTIFIC

terra 4
Gesellschaft für Geosystemanalyse mbH

JURA TROIS-LACS DREI-SEEN-LAND
SOLOTHURN

SOLOTHURN
services | meetings | events